

Over-the-Air Federated Learning and Optimization

Jingyang Zhu, *Graduate Student Member, IEEE*, Yuanming Shi, *Senior Member, IEEE*,
Yong Zhou, *Senior Member, IEEE*, Chunxiao Jiang, *Senior Member, IEEE*, Wei Chen, *Senior Member, IEEE*,
and Khaled B. Letaief, *Fellow, IEEE*

Abstract—Federated learning (FL), as an emerging distributed machine learning paradigm, allows a mass of edge devices to collaboratively train a global model while preserving privacy. In this tutorial, we focus on FL via over-the-air computation (AirComp), which is proposed to reduce the communication overhead for FL over wireless networks at the cost of compromising in the learning performance due to model aggregation error arising from channel fading and noise. We first provide a comprehensive study on the convergence of AirComp-based FEDAVG (AIRFEDAVG) algorithms under both strongly convex and non-convex settings with constant and diminishing learning rates in the presence of data heterogeneity. Through convergence and asymptotic analysis, we characterize the impact of aggregation error on the convergence bound and provide insights for system design with convergence guarantees. Then we derive convergence rates for AIRFEDAVG algorithms for strongly convex and non-convex objectives. For different types of local updates that can be transmitted by edge devices (i.e., local model, gradient, and model difference), we reveal that transmitting local model in AIRFEDAVG may cause divergence in the training procedure. In addition, we consider more practical signal processing schemes to improve the communication efficiency and further extend the convergence analysis to different forms of model aggregation error caused by these signal processing schemes. Extensive simulation results under different settings of objective functions, transmitted local information, and communication schemes verify the theoretical conclusions.

Index Terms—Federated learning, over-the-air computation, convergence analysis, and optimization.

I. INTRODUCTION

With the ever-growing communication, computation, and caching capabilities of various edge devices (e.g., smart phones, sensors, and Internet of Things (IoT) devices), the sixth generation (6G) wireless communication system is undergoing a paradigm transformation from connected everything to connected intelligence, thereby envisioning to support ubiquitous artificial intelligence (AI) services and applications (e.g., immersive extended reality, holographic communication, sensory interconnectivity, and digital twins) [1]–[3]. A large amount of data collected and generated by edge devices together with their sensing, computation, and communication

capabilities have opened up bright avenues for training machine learning (ML) models at the network edge [4]. However, in conventional distributed ML for cloud AI, cloud servers need to gather raw data from all devices, resulting in excessive communication overhead and severe privacy concern. To this end, federated edge learning (FL) [5]–[7], as an emerging distributed ML framework, has been proposed to enable many edge devices to train an ML model under the coordination of an edge server without sharing their local data. Although promising, supporting FL over wireless networks still encounters multi-faceted determining factors, including transmission schemes, networking, and resource optimization [8].

To mitigate the communication bottleneck problem, it is essential to design efficient model transmission schemes. The existing studies can be divided into two categories, i.e., digital modulation based FL (digital FL) and over-the-air computation (AirComp)-based FL (AirFL). The existing studies on digital FL [9]–[21] typically adopted the orthogonal multiple access (OMA) scheme to transmit local models, where the frequency and time blocks are orthogonally divided. In this case, the transmission latency of digital FL will be proportional to the number of edge devices [22], leading to high transmission delay of FL over large-scale wireless networks. To overcome this challenge, AirComp, as a promising task-oriented scheme that leverages the waveform superposition property of wireless multiple-access channel (MAC) [23], was proposed to enable concurrent model transmission over the same time-frequency channel [24], thus considerably reducing the communication delay [25]–[27]. Motivated by this advantage, AirFL was proposed to achieve fast analog model aggregation [28], where multiple edge devices transmit their local information concurrently, and the edge server directly obtains the aggregated local information from the superimposed signal. Substantial progress has recently been made in the area of AirFL [22], [28]–[73], including tackling the learning performance degradation caused by the channel fading and the receiver noise in each model aggregation.

The underlying network architecture is an essential factor that affects both the communication efficiency and the convergence rate of FL systems. From the perspective of network architectures, existing studies on digital FL cover client-server FL [9]–[17] and hierarchical FL [18]–[21]. In addition to the client-server network architecture, AirFL has also been studied in diverse network architectures. To fully utilize the diversified communication links and geographically dispersed computing resources, device-edge-cloud collaboration has been investigated from a variety of perspectives such as decentralized AirFL by exploiting device-to-device links [29]–[32], multi-cell AirFL with inter-cell interference

Jingyang Zhu, Yuanming Shi, and Yong Zhou are with the School of Information Science and Technology, ShanghaiTech University, Shanghai 201210, China (e-mail: {zhujy2, shiyym, zhoyouyong}@shanghaitech.edu.cn).

Chunxiao Jiang is with the Tsinghua Space Center, Tsinghua University, Beijing, 100084, China. (e-mail: jchx@tsinghua.edu.cn).

Wei Chen is with the Department of Electronic Engineering and the Beijing National Research Center for Information Science and Technology, Tsinghua University, Beijing 100084, China (e-mail: wchen@tsinghua.edu.cn).

Khaled B. Letaief is with the Department of Electronic and Computer Engineering, Hong Kong University of Science and Technology, Clear Water Bay, Hong Kong, and also with Peng Cheng Laboratory, Shenzhen 518066, China (e-mail: eekhaled@ust.hk).

management [33], and hierarchical AirFL for alleviating communication costs and accelerating convergence [34], [35]. Besides, space-air-ground integration (e.g., reconfigurable intelligent surface (RIS)-assisted AirFL [36]–[40], unmanned aerial vehicle (UAV)-assisted AirFL [41], and satellite-assisted AirFL [42]) provides an integrated information platform that can serve different learning algorithms and topologies in order to establish seamless communication and services between ground facilities and the airspace.

To support communication-efficient FL with limited radio resources, wireless resource management and optimization is essential. In particular, there have been comprehensive studies on digital FL focusing on communication system design and wireless resource allocation, covering different types of objective functions (e.g., training loss function [9]–[11], latency [12]–[14], and energy consumption [15], [16]). Furthermore, the literature investigating resource optimization in AirFL include transceiver design [28], [43]–[53], [55], [56] (e.g., beamforming design [28], [43], power control [44]–[51], precoding and denoising factor design [53], [54], and hyperparameter optimization [52], [55]), device selection [28], [37], [43], [50], [63]–[65], and privacy protection by utilizing the inherent channel noise [46], [69], [70]. To address the practical challenges for implementing AirFL, some attempts focus on developing synchronization techniques [71] and digital modulation schemes for deployment in off-the-shelf communication systems (e.g., LTE, Wi-Fi 6, and 5G) [72], [73].

As the communication system design for AirFL highly depends on characterizing the impact of the channel fading and receiver noise on the convergence of the AirFL algorithms, it is important to conduct explicit convergence analysis. The key factors that affect the convergence analysis can be summarized as follows: the impact of the receiver noise on the convergence bound, the type of local updates (i.e., local model, local gradient, or model difference), the property of the objective functions (e.g., strongly convex or non-convex), the choice of the learning rates (i.e., diminishing or constant), the characterization of data heterogeneity, and the choice of the number of local updates. These issues arising from the communication systems and learning algorithms are strongly coupled in AirFL. For instance, the choice of the learning rate relies on the objective functions and the number of local updates, and it also affects the optimality of the objective function. As another example, in the error-free case, transmitting different types of local updates leads to different model aggregation steps, which are mathematically equivalent. However, such an equivalence is no longer valid in AirFL. The inequivalence is clearly demonstrated in the following two aspects. First, due to different numbers of local updates, transmitting different types of local updates may lead to different convergence rates and robustness to data heterogeneity, which need to be thoroughly investigated and discussed. Second, different types of transmit signals together with the corresponding model aggregation steps have different robustness to the receiver noise, affecting the convergence performance as well. Hence, the coupling between the number of local updates and the type of transmit signals presents a

new challenge for designing AirFL algorithms and analyzing their convergence, which needs to be revealed.

Despite prior works have achieved encouraging results of analyzing AirComp-based federated stochastic gradient descent (FEDSGD) and federated averaging (FEDAVG) [5] algorithms, a comprehensive understanding of these issues is still lacking, which motivates this comprehensive tutorial on the convergence of AirFL.

A. Main Contributions

In this paper, we provide a comprehensive understanding of AirComp-based FEDAVG (AIRFEDAVG) algorithms. We first provide convergence analysis with respect to the model aggregation error caused by receiver noise for benchmark algorithm AIRFEDAVG-MULTIPLE (AIRFEDAVG-M, i.e., the model difference is transmitted by an edge device after several local updates in AIRFEDAVG) with a diminishing learning rate in the strongly convex settings. Then we provide asymptotic analysis for the upper bound to characterize the impact of noise by the mean square error (MSE) of the model aggregation, and further arrive at some insightful conclusions for AIRFEDAVG-M by the case study of denoising factor. Following the same principle, we extend the asymptotic analysis and case study to the non-convex settings. We then extend our analysis to variant algorithms: AIRFEDAVG-SINGLE (AIRFEDAVG-S, i.e., edge devices transmit their local gradients after a single local update) and AIRFEDMODEL (i.e., edge devices transmit their local models). We also figure out the influence of the number of local updates by analyzing the convergence results for AIRFEDAVG-M and make comparisons between AIRFEDAVG-M and AIRFEDAVG-S. In summary, from a systematic perspective, we provide a detailed taxonomy of the AIRFEDAVG algorithms based on the type of model aggregation error (i.e., unbiased and biased), the transmitted signal (i.e., model difference, local gradient, or local model), the number of local updates (i.e., multiple or single), objective functions (i.e., strongly convex or non-convex), and learning rates (i.e., diminishing or constant), as shown in Fig. 1. Our main contributions can be summarized as follows.

- We present a novel convergence analysis framework for AIRFEDAVG with respect to the model aggregation error at the edge server, regardless of whether the transmitted signal can be unbiased estimated by the edge server or not. We first provide convergence and asymptotic analysis for AIRFEDAVG-M to characterize the impact of the MSE and then apply the analysis to AIRFEDAVG-S and AIRFEDMODEL.
- In terms of the type of local updates, we reveal that the convergence of the AIRFEDAVG-M and AIRFEDAVG-S algorithms (i.e., transmitting model difference or local gradient) can be guaranteed, while transmitting local model may cause the divergence in the training procedure based on the convergence results.
- To elaborate the convergence results of the learning algorithms (i.e., AIRFEDAVG-M and AIRFEDAVG-S) in different scenarios, we provide convergence results for

both strongly convex and non-convex objective function under non-IID dataset with different learning rates. The details of the convergence results are listed in Table I.

- We provide a case study and demonstrate the optimality gap for strongly convex case and error bound for non-convex case, and characterize the impact of the signal-to-noise ratio (SNR) on the convergence rate. We also derive the maximum number of local updates required for AIRFEDAVG-M to preserve convergence for both cases and verify that AIRFEDAVG-M can achieve linear speedup with respect to the number of local updates and the number of edge devices.

We conduct substantial simulations to evaluate the performance of the proposed AIRFEDAVG-M, AIRFEDAVG-S, and AIRFEDMODEL under different system designs, i.e., precoding factors and SNRs. Results confirm that assisted by AirComp, transmitting local model is not a good choice. Besides, simulations also indicate that AIRFEDAVG-M can achieve linear speedup, but may suffer from highly non-IID data, and AIRFEDAVG-S is more robust to the channel noise and non-IID data despite linear slower convergence compared with AIRFEDAVG-M.

B. Organization and Notation

The rest of this paper is organized as follows. Section II provides some preliminaries for learning and optimization theory. Section III describes the AirFL system model and AIRFEDAVG-M algorithm. Convergence analysis, case study and insights of AIRFEDAVG-M are given in Section IV. The convergence results of different variants, i.e., AIRFEDAVG-S and AIRFEDMODEL, are provided in Section V. Further discussions are given in VI. Numerical results are presented in Section VII to verify the theoretical findings. In Section VIII, we draw our conclusions.

Notation: The operators $\|\cdot\|_2$, $(\cdot)^T$, $(\cdot)^H$, $\langle \cdot, \cdot \rangle$, and $|\cdot|$ denote ℓ_2 -norm, transpose, Hermitian, inner product, and modulus, respectively. $\mathbb{E}[\cdot]$ denotes the expectation over a random variable. For a function f , ∇f is its gradient. $[T]$ denotes the set $\{0, 1, \dots, T-1\}$. $\mathcal{O}(\cdot)$ is the big-O notation, which stands for the order of arithmetic operations. The notations N , E , T , t , μ , and L denote the number of edge devices, the number of local updates, the number of communication rounds, each communication round, μ strong convexity, and L -smoothness, respectively.

II. PRELIMINARIES

Before diving into the discussion on FL, we start by introducing some preliminaries of learning and optimization theory [74], [75] to facilitate better understanding of our analysis.

A. Learning and Optimization Theory

We consider the following general empirical risk minimization problem

$$\underset{\mathbf{x} \in \mathbb{R}^d}{\text{minimize}} \quad f(\mathbf{x}) := \frac{1}{m} \sum_{i=1}^m f_i(\mathbf{x}), \quad (1)$$

where d is the dimension of vector \mathbf{x} , the objective function $f : \mathbb{R}^d \rightarrow \mathbb{R}$ is continuously differentiable, m is the number of data samples, and $f_i : \mathbb{R}^d \rightarrow \mathbb{R}, i = 0, 1, \dots, m$ is the sample-wise loss function. The optimal solution to problem (1) is denoted by $\mathbf{x}^* := \arg \min_{\mathbf{x} \in \mathbb{R}^d} f(\mathbf{x})$.

1) *Objective Function:* For the objective function, we have the following definition and assumption.

Definition 1 (*L-Smoothness*). *The objective function $f : \mathbb{R}^d \rightarrow \mathbb{R}$ is continuously differentiable and its gradient, i.e., $\nabla f : \mathbb{R}^d \rightarrow \mathbb{R}^d$, is Lipschitz continuous with constant $L > 0$ if the following inequality holds*

$$\|\nabla f(\mathbf{x}) - \nabla f(\mathbf{y})\|_2 \leq L \|\mathbf{x} - \mathbf{y}\|_2, \quad \forall \mathbf{x}, \mathbf{y} \in \mathbb{R}^d. \quad (2)$$

We can equivalently rewrite (2) as

$$f(\mathbf{x}) \leq f(\mathbf{y}) + (\mathbf{x} - \mathbf{y})^T \nabla f(\mathbf{y}) + \frac{L}{2} \|\mathbf{x} - \mathbf{y}\|_2^2, \quad \forall \mathbf{x}, \mathbf{y} \in \mathbb{R}^d.$$

Assumption 1. *The objective function f is lower bounded by a scalar f^{inf} , i.e., $f(\mathbf{x}) \geq f^{\text{inf}} > -\infty$.*

To solve problem (1), the dominant methodology is the vanilla stochastic gradient descent (SGD), which applies the following iterative update rule

$$\mathbf{x}^{t+1} = \mathbf{x}^t - \eta^t \mathbf{g}(\mathbf{x}^t, \boldsymbol{\xi}^t), \quad (3)$$

where η^t is the learning rate or step size in iteration t , $\boldsymbol{\xi}^t$ is a random variable indicating the selection of data samples, and $\mathbf{g}(\mathbf{x}^t, \boldsymbol{\xi}^t)$ is the output of the stochastic first-order oracle that is a noisy version of gradient $\nabla f(\mathbf{x}^t)$. The following assumption is made for the stochastic gradient estimation.

Assumption 2. *The stochastic gradient estimation $\mathbf{g}(\mathbf{x}^t, \boldsymbol{\xi}^t)$ is unbiased and has a bounded variance in each iteration:*

$$\begin{aligned} \mathbb{E}[\mathbf{g}(\mathbf{x}^t, \boldsymbol{\xi}^t)] &= \nabla f(\mathbf{x}^t), \\ \mathbb{E}[\|\mathbf{g}(\mathbf{x}^t, \boldsymbol{\xi}^t) - \nabla f(\mathbf{x}^t)\|_2^2] &\leq \sigma^2, \end{aligned}$$

where constant parameter $\sigma^2 \geq 0$ and the expectation is taken with respect to the distribution of random variable $\boldsymbol{\xi}^t$.

If the objective function is strongly convex, then we have the following definition.

Definition 2 (*Strong Convexity*). *The objective function $f : \mathbb{R}^d \rightarrow \mathbb{R}$ is strongly convex if there exists a constant $\mu > 0$ such that*

$$f(\mathbf{x}) \geq f(\mathbf{y}) + (\mathbf{x} - \mathbf{y})^T \nabla f(\mathbf{y}) + \frac{\mu}{2} \|\mathbf{x} - \mathbf{y}\|_2^2, \quad \forall \mathbf{x}, \mathbf{y} \in \mathbb{R}^d.$$

For strongly convex objectives, the convergence performance can be evaluated by the optimality gap, which is defined as

$$\text{Gap}^t := f(\mathbf{x}^t) - f(\mathbf{x}^*)$$

in iteration t . To attain a given accuracy ϵ within T iterations, the optimality gap is expected to satisfy $\mathbb{E}[\text{Gap}^T] \leq \epsilon$, where the expectation is taken over $\boldsymbol{\xi}^t, t = 0, 1, \dots, T$. However, to train deep neural networks (DNN) and convolutional neural networks (CNN), the objective function f is likely to be smooth but non-convex. For non-convex objectives, it is

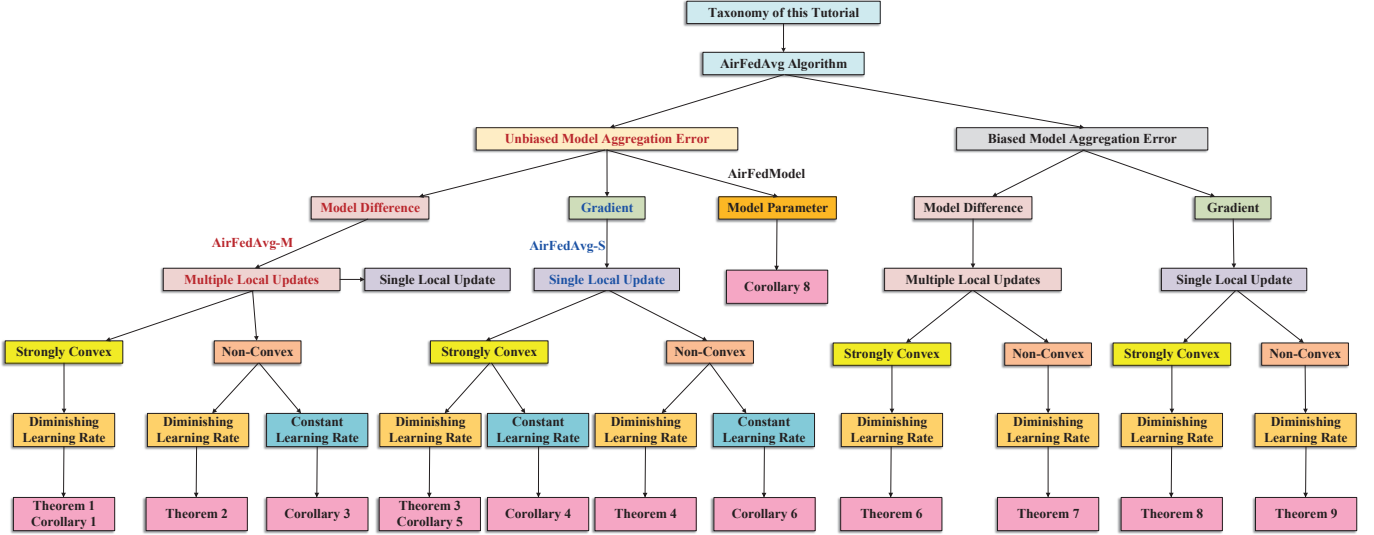


Fig. 1. Taxonomy of this tutorial.

TABLE I

MAIN CONVERGENCE RESULTS OF AIRFEDAVG ALGORITHMS IN THIS TUTORIAL, FROM THE PERSPECTIVES OF STRONGLY CONVEX (SC) AND NON-CONVEX (NC) OBJECTIVES, LOCAL INFORMATION (LI) TO TRANSMIT, MODEL AGGREGATION ERROR (MAE), LOCAL UPDATE (LU), LEARNING RATE (LR), CONVERGENCE RATE (CR), AND DOMINANT VARIABLE (DV).

Location	Result	Algorithm	Objective	LI	MAE	LU	LR	CR	DV
Section IV	Theorem 1	AIRFEDAVG-M	SC	Difference	Unbiased	E	Diminishing	-	MSE
	Corollary 1	AIRFEDAVG-M	SC	Difference	Unbiased	E	$\mathcal{O}(1/t)$	$\mathcal{O}(\frac{1}{NET})$	SNR
	Theorem 2	AIRFEDAVG-M	NC	Difference	Unbiased	E	Diminishing	-	MSE
	Corollary 3	AIRFEDAVG-M	NC	Difference	Unbiased	E	$\mathcal{O}(\sqrt{\frac{N}{ET}})$	$\mathcal{O}(\frac{1}{\sqrt{NET}})$	SNR
Section V	Theorem 3	AIRFEDAVG-S	SC	Gradient	Unbiased	1	Diminishing	-	MSE
	Corollary 4	AIRFEDAVG-S	SC	Gradient	Unbiased	1	Constant	$\mathcal{O}((1 - \frac{\mu}{L})^T)$	MSE
	Corollary 5	AIRFEDAVG-S	SC	Gradient	Unbiased	1	$\mathcal{O}(1/t)$	$\mathcal{O}(\frac{1}{NT})$	SNR
	Theorem 4	AIRFEDAVG-S	NC	Gradient	Unbiased	1	Diminishing	-	MSE
	Corollary 6	AIRFEDAVG-S	NC	Gradient	Unbiased	1	$\mathcal{O}(\sqrt{\frac{N}{T}})$	$\mathcal{O}(\frac{1}{\sqrt{NT}})$	SNR
	Corollary 8	AIRFEDMODEL	SC	Model	Unbiased	1	Diminishing	-	MSE
Section VI	Theorem 6	AIRFEDAVG-M	SC	Difference	Biased	E	Diminishing	-	MSE, Bias
	Theorem 7	AIRFEDAVG-M	NC	Difference	Biased	E	Diminishing	-	MSE, Bias
	Theorem 8	AIRFEDAVG-S	SC	Gradient	Biased	1	Diminishing	-	Bias
	Theorem 9	AIRFEDAVG-S	NC	Gradient	Biased	1	Diminishing	-	Bias

common to consider an upper bound on the weighted average norm of the gradient of the objective function, i.e.,

$$\frac{1}{\sum_{t=0}^{T-1} \eta^t} \sum_{t=0}^{T-1} \eta^t \mathbb{E} \left[\|\nabla f(\mathbf{x}^t)\|_2^2 \right],$$

for the first T iterations. If the learning rate is a constant, i.e., $\eta^t = \eta, \forall t$, then it reduces to $\frac{1}{T} \sum_{t=0}^{T-1} \mathbb{E} \left[\|\nabla f(\mathbf{x}^t)\|_2^2 \right]$. Furthermore, we say that solution \mathbf{x}^t is an ϵ -stationary point if $\|\nabla f(\mathbf{x}^t)\|_2^2 \leq \epsilon$.

In addition, some objective functions meet the Polyak-Lojasiewicz (PL) condition, which is defined as follows.

Definition 3 (PL Condition). *The objective function $f : \mathbb{R}^d \rightarrow \mathbb{R}$ satisfies the PL condition with constant μ , i.e.,*

$$\|\nabla f(\mathbf{x}^t)\|_2^2 \geq 2\mu[f(\mathbf{x}^t) - f(\mathbf{x}^*)].$$

Note that the PL condition is weaker than strong convexity, and usually considered in the analysis of non-convex cases.

TABLE II
CONVERGENCE RESULTS FOR STRONGLY CONVEX (SC) AND NON-CONVEX (NC) OBJECTIVES

	Learning Rate	Convergence Gap	Convergence Rate
SC	$\mathcal{O}(1)$	non-diminishing	$\mathcal{O}(\rho^T), \rho \in (0, 1)$
	$\mathcal{O}(1/t)$	diminishing	$\mathcal{O}(1/T)$
NC	$\mathcal{O}(1/\sqrt{T})$	non-diminishing	$\mathcal{O}(1/\sqrt{T})$
	$\mathcal{O}(1/t)$	diminishing	-

2) *Convergence Properties under Different Learning Rates:* To solve problem (1) with SGD, the choice of learning rate is crucial for the convergence gap and convergence rate¹. To be specific, for strongly convex objectives with a constant learning rate, the expected objective function linearly converges to the neighborhood of the optimal value, but with

¹In this tutorial, convergence gap refers to the optimality gap in the strongly convex case and the upper bound on the weighted average norm of the gradient of the objective function in the non-convex case. Convergence rate is a measure of how fast the difference between the objective function value of the solution and its estimates goes to zero.

TABLE III
OVERVIEW OF LOCAL SGD AND FEDAVG ALGORITHMS

Algorithm	Objective	BG	BGD	Local Update	Learning Rate	Convergence Rate
FEDAVG [76]	SC	✓	✗	$\mathcal{O}(1)$	$\mathcal{O}(1/t)$	$\mathcal{O}(1/NT)$
Local SGD [77]	SC	✓	✗	$\mathcal{O}(T^{1/2}N^{-1/2})$	$\mathcal{O}(1/t)$	$\mathcal{O}(1/NT)$
FEDAVG [78]	NC+PL	✗	✓	$\mathcal{O}(T^{2/3}N^{-1/3})$	$\mathcal{O}(1/t)$	$\mathcal{O}(1/NT)$
Local SGD [76]	NC+PL	✗	✗	$\mathcal{O}(T^{2/3}N^{-1/3})$	$\mathcal{O}(1/t)$	$\mathcal{O}(1/NT)$
FEDAVG [78]	NC	✗	✓	$\mathcal{O}(T^{1/2}N^{-3/2})$	$\mathcal{O}(N^{1/2}T^{-1/2})$	$\mathcal{O}(1/\sqrt{NT})$
Local SGD [79]	NC	✓	✗	$\mathcal{O}(T^{1/4}N^{-3/4})$	$\mathcal{O}(N^{1/2}T^{-1/2})$	$\mathcal{O}(1/\sqrt{NT})$
Local SGD [80]	NC	✗	✗	$\mathcal{O}(T^{1/2}N^{-3/2})$	$\mathcal{O}(N^{1/2}T^{-1/2})$	$\mathcal{O}(1/\sqrt{NT})$
Local SGD with Momentum [81]	NC	✗	✗	$\mathcal{O}(T^{1/2}N^{-3/2})$	$\mathcal{O}(N^{1/2}T^{-1/2})$	$\mathcal{O}(1/\sqrt{NT})$
	NC	✗	✓	$\mathcal{O}(T^{1/4}N^{-3/4})$	$\mathcal{O}(N^{1/2}T^{-1/2})$	$\mathcal{O}(1/\sqrt{NT})$
VRL-SGD [82]	NC	✗	✗	$\mathcal{O}(T^{1/2}N^{-3/2})$	$\mathcal{O}(N^{1/2}T^{-1/2})$	$\mathcal{O}(1/\sqrt{NT})$

a non-diminishing optimality gap due to the noisy gradient estimation [75]. In contrast, using a decaying learning rate leads to a diminishing optimality gap at the cost of achieving a sublinear convergence rate², where the learning rate satisfies the following conditions:

$$\sum_{t=0}^{\infty} \eta^t = \infty, \quad \sum_{t=0}^{\infty} (\eta^t)^2 < \infty. \quad (4)$$

Similarly, for non-convex objectives with a constant learning rate, the error bound on the average of squared gradients is non-diminishing as well [75]. In addition, using a diminishing learning rate leads to the following result:

$$\liminf_{t \rightarrow \infty} \mathbb{E} \left[\|\nabla f(\mathbf{x}^t)\|_2^2 \right] = 0. \quad (5)$$

More precisely, (5) can be written as

$$\frac{1}{\sum_{t=0}^{T-1} \eta^t} \sum_{t=0}^{T-1} \eta^t \mathbb{E} \left[\|\nabla f(\mathbf{x}^t)\|_2^2 \right] \xrightarrow{T \rightarrow \infty} 0. \quad (6)$$

Table II gives more detailed information about the above statements.

B. Federated Learning

With the capability of enhancing the data privacy and reducing the communication overhead, FL becomes a research hotspot, where N workers collaboratively train a global model without sharing private data. The objective function can be written as

$$\underset{\mathbf{x} \in \mathbb{R}^d}{\text{minimize}} \quad F(\mathbf{x}) := \frac{1}{N} \sum_{n=1}^N F_n(\mathbf{x}), \quad (7)$$

where F_n of each worker n can be viewed as f in (1). To solve this problem, various algorithms, including vanilla distributed SGD, paralleled SGD, Local SGD, and FEDAVG algorithms, have been proposed in [5], [76]–[87] to achieve linear speed-up in model training with respect to the number of workers. Specifically, Local SGD is fully-synchronized, where the model averaging step, i.e., taking an average over all workers' local model parameters, is performed once each worker finishes one local update [80]. To reduce the communication overhead, Local SGD with periodic averaging and FEDAVG

were proposed, where the frequency of the model averaging step can be chosen [77]. The difference in nomenclature is that Local SGD usually refers to distributed settings with homogeneous data, while FEDAVG is used in FL with heterogeneous data [88]. The detailed comparison of these algorithms is listed in Table III with two extra assumptions on the gradient, i.e., bounded gradient (BG), and bounded gradient dissimilarity (BGD), which shall be defined in Section IV. Note that BGD can be used to measure the deviation of local gradients after multiple local updates as well as the non-IID extent of data at different workers in FL [86], [89].

The convergence rates of Local SGD, FedAvg and other related algorithms under different assumptions and settings are summarized in Table III. It can be observed that all studies considering strongly convex objectives (or PL condition) use learning rate decay to eliminate the influence of noisy gradient estimation and achieve a similar convergence rate $\mathcal{O}(1/NT)$. For non-convex objectives, they adopt a similar constant learning rate $\mathcal{O}(\sqrt{N/T})$ and achieve a sublinear convergence rate $\mathcal{O}(1/\sqrt{NT})$. Besides, decentralized SGD algorithms were also studied in [90], [91].

All the algorithms listed in Table III aggregate local models to update the global model. In fact, the local information to be aggregated for global model update at the server can be classified into the following three categories.

- **Local Model:** In this case, each worker directly transmits its local model (e.g., \mathbf{x}^t in (3)) to the central server for global model update [76]–[82], [84]–[87], [92].
- **Model Difference:** Model difference refers to the difference of local models before and after local training in one global iteration (e.g., $\mathbf{x}^{t+1} - \mathbf{x}^t$). In this case, the central server receives all workers' model difference and performs a model update step using the average model difference. By applying Lookahead, which is a deep learning optimizer [93], to the update rule in FL, exchanging model difference between the workers and the central server has the following advantages: 1) Model difference exchange is necessary for developing a general local update framework with gradient-based local optimizer [94]; 2) Model difference has decreasing dynamic ranges as iteration proceeds, which facilitates the design of quantization schemes [95], [96] for reducing the communication cost between the workers and server; 3) Exchanging model difference can promote the design

²If an algorithm has a convergence rate of $\mathcal{O}(1/T)$, then it will take $\mathcal{O}(1/\epsilon)$ iterations to achieve accuracy ϵ .

of other local update rules in FL, such as [97]–[100], because it only needs to exchange the difference instead of transmitting specific local information.

- **Local Gradient:** In this case, all workers transmit their local gradients to the central server, which performs a gradient decent step using the average local gradient. As the local gradients are decreasing as the training continues, the gradient information is suitable for alleviating communication burden by applying gradient quantization, sparsification [101], [102] and lazy gradient aggregation [103].

III. SYSTEM MODEL

In this section, we elaborate the whole procedure of the AirFL algorithm considered in this tutorial, including the loss functions, the training steps, the communication schemes, and the aggregation steps.

A. FL over Wireless Networks

We consider a wireless FL system that consists of a single-antenna edge server and N single-antenna edge devices indexed by set $\mathcal{N} = \{1, 2, \dots, N\}$. Each edge device $n \in \mathcal{N}$ has a local dataset $\mathcal{D}_n = \{\mathbf{x}_{ni}, y_{ni}\}_{i=1}^{D_n}$ with D_n data samples. All edge devices collaboratively learn a shared global model by communicating with the edge server without moving their private raw datasets. For each edge device n , $\theta_n \in \mathbb{R}^d$ is the local model trained based on its local dataset \mathcal{D}_n and $F_n : \mathbb{R}^d \rightarrow \mathbb{R}$ is the local loss function, defined as

$$F_n(\theta_n) := \frac{1}{D_n} \sum_{i=1}^{D_n} f_n(\theta_n; \mathbf{x}_{ni}, y_{ni}), \quad (8)$$

where $f_n : \mathbb{R}^d \rightarrow \mathbb{R}$ denotes the sample-wise loss function defined by the learning task. For example, the sample-wise loss function of the linear regression problem is given by $f_n(\theta_n; \mathbf{x}_{ni}, y_{ni}) = \frac{1}{2} |\mathbf{x}_{ni} \theta_n - y_{ni}|^2$, and that of the logistic regression is $f_n(\theta_n; \mathbf{x}_{ni}, y_{ni}) = \log(1 + e^{-y_{ni} \mathbf{x}_{ni}^T \theta})$.

Our goal is to learn a shared global model by minimizing the weighted sum of the edge devices' local loss functions. This can be formulated as the following optimization problem:

$$\mathcal{P} : \underset{\theta \in \mathbb{R}^d}{\text{minimize}} \quad F(\theta) := \sum_{n=1}^N p_n F_n(\theta), \quad (9)$$

where $\theta \in \mathbb{R}^d$ is the global model with dimension d , $F(\cdot)$ is the objective function defined by the learning task, and $p_n > 0$ is the aggregation weight satisfying $\sum_{n=1}^N p_n = 1$. Generally, the aggregation weight p_n can be simply set as D_n/D , where $D = \sum_{n=1}^N D_n$ is the total number of data samples from all edge devices [5]. Besides, the weights can be designed to promote fairness [104], personalization [105], and efficiency of device sampling [106]. The solution to problem (9), i.e., the global minimum θ^* , is defined as

$$\theta^* := \arg \min_{\theta \in \mathbb{R}^d} F(\theta). \quad (10)$$

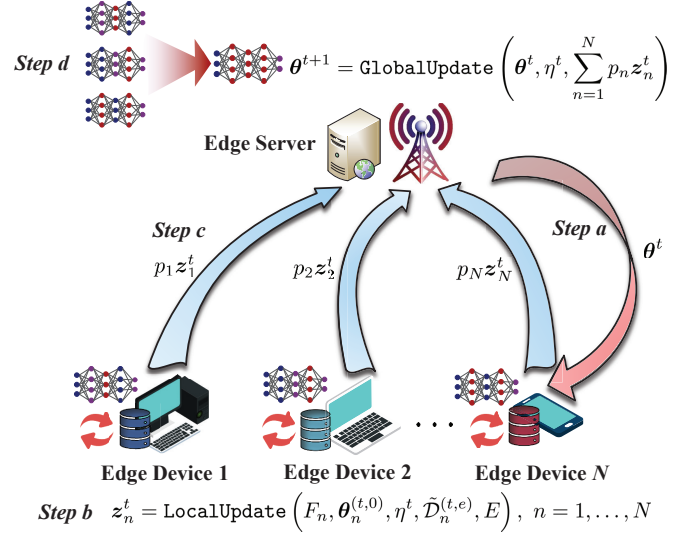


Fig. 2. Illustration of the FL procedure.

As illustrated in Fig 2, during each communication round t , the computation and transmission steps between the edge server and edge devices can be summarized as follows:

- **Step a:** The edge server broadcasts the global model θ^t to all edge devices;
- **Step b:** After receiving the global model θ^t , edge device $n \in \mathcal{N}$ initializes its local model by setting $\theta_n^{(t,0)} = \theta^t$, and performs $E \geq 1$ epoch of local updates with respect to the local mini-batch set $\tilde{\mathcal{D}}_n^{(t,e)}$ with $\tilde{D}_n^{(t,e)}$ samples, $e \in [0, \dots, E-1]$, via

$$z_n^t := \text{LocalUpdate}(F_n, \theta_n^{(t,0)}, \eta^t, \tilde{\mathcal{D}}_n^{(t,e)}, E), \quad (11)$$

where $\text{LocalUpdate}(\cdot) : \mathbb{R}^d \rightarrow \mathbb{R}^d$ denotes the local model update operator, η^t is the learning rate, and $z_n^t \in \mathbb{R}^d$ is the output vector of the operator. If the local batch size equals to the local sample size, i.e., $\tilde{D}_n^{(t,e)} = D_n$, then the mini-batch stochastic gradient becomes a full-batch one.

- **Step c:** All edge devices send the local information (e.g., local model, model difference, and local gradient) $p_n z_n^t$ to the edge server³;
- **Step d:** The edge server receives all the local information and updates the global model θ^{t+1} by performing

$$\theta^{t+1} := \text{GlobalUpdate}\left(\theta^t, \eta^t, \sum_{n=1}^N p_n z_n^t\right), \quad (12)$$

where $\text{GlobalUpdate}(\cdot) : \mathbb{R}^d \rightarrow \mathbb{R}^d$ denotes the global model update operator, i.e., model aggregation.

The iterative training process continues until a desired model accuracy is attained.

In this article, we aim to analyze the convergence of FL via first-order optimization method. Specifically, we consider the state-of-the-art algorithm FEDAVG [5] with local vanilla

³In this paper, we only consider full device participation. The discussion on partial device participation can be found in Section VI-E

SGD optimizer in our analysis. The local SGD optimizer of FEDAVG is performed as follows

$$\theta_n^{(t,e+1)} \triangleq \theta_n^{(t,e)} - \eta^t \mathbf{g}_n^{(t,e)}, \quad e \in [0, \dots, E-1], \quad (13)$$

where $\mathbf{g}_n^{(t,e)}$ is the abbreviation for $\mathbf{g}_n(\theta_n^{(t,e)}) = \frac{1}{|\tilde{\mathcal{D}}_n^{(t,e)}|} \sum_{i \in \tilde{\mathcal{D}}_n^{(t,e)}} \nabla f_n(\theta_n^{(t,e)}; \mathbf{x}_{ni}, y_{ni})$ and denotes the mini-batch stochastic gradient estimate of the local loss function $F_n(\theta)$ with respect to $\theta_n^{(t,e)}$ and the local mini-batch set $\tilde{\mathcal{D}}_n^{(t,e)}$ in the local iteration e of the communication round t .

Remark 1. *It is worth noting that different from the algorithms listed in Table III, notation T in our FL model refers to the total number of communication rounds. This means that the number of local computation for each edge device is $E \times T$ in this paper but T in those literature.*

Remark 2. *The local model update operator (11) has different forms, resulting in different \mathbf{z}_n^t , i.e., model difference, local gradient, and local model. For different forms of \mathbf{z}_n^t , the global update should be adjusted accordingly.*

We first consider the situation that \mathbf{z}_n^t in (11) is the accumulated local gradients (i.e., model difference in other literature) [94], which can be written as

$$\mathbf{z}_n^t = \Delta \theta_n^{t+1} \triangleq \theta_n^{(t,E)} - \theta_n^{(t,0)} = -\eta^t \sum_{e=0}^{E-1} \mathbf{g}_n^{(t,e)}. \quad (14)$$

The edge server then aggregates all the accumulated local gradients and updates the global model θ^{t+1} by performing

$$\theta^{t+1} = \theta^t + \sum_{n=1}^N p_n \mathbf{z}_n^t. \quad (15)$$

B. AirComp-based FEDAVG (AIRFEDAVG)

In this paper, we mainly consider the transmission of local information from edge devices to the edge server over multiple-access fading channels in the uplink. The downlink transmission is assumed to be error-free [61], [62] as the edge server has a greater transmit power than the edge devices. Note that the convergence of FL over a noisy downlink is studied in [50], [59], [107], [108].

With the conventional orthogonal multiple access schemes [109], N edge devices are assigned with N orthogonal frequency/time resource blocks to transmit their local information. The edge server needs to successfully decode the transmitted information of all edge devices for global model update, which may be of low spectrum efficiency. To address this challenge, AirComp [24], as a non-orthogonal multiple access scheme, was proposed to exploit the waveform superposition property by enabling all edge devices to synchronously transmit their local information over the same channel. Moreover, a critical observation made by [28] is that the waveform superposition property of AirComp is a perfect fit for model aggregation at the edge server. Prior works [28] demonstrate that AirComp enables fast and spectrum-efficient model aggregation for wireless FL.

In this paper, all edge devices adopt AirComp to communicate with the edge server with perfect synchronization. We assume a block flat-fading channel and each communication block comprises d time slots for a d -dimensional local model to be transmitted, during which the channel coefficients remain unchanged. By denoting α_n^t as the precoder of edge device n , the received signal at the edge server in communication round t is given by

$$\hat{\mathbf{s}}^t = \sum_{n=1}^N h_n^t \alpha_n^t p_n \mathbf{z}_n^t + \mathbf{w}^t, \quad (16)$$

where $h_n^t \in \mathbb{C}$ is the channel coefficient for edge device n in the t -th communication round, and $\mathbf{w}^t \in \mathbb{R}^d \sim \mathcal{CN}(0, \sigma_w^2 \mathbf{I}_d)$ is the additive white Gaussian noise (AWGN) vector. In each model aggregation, AirFL suffers from the channel fading and the additive noise. To characterize the detrimental impact of the channel distortions, channel fading causes different magnitudes for different edge devices, and the additive noise of each communication round may stack up and further cause the FL model to diverge. These issues inspire us to design power control policies for magnitude alignment and signal processing schemes to reduce the impact of noise, thereby improving the training performance of AirFL.

As in most of the existing literature on AirComp [28], [57], [61], we assume that perfect channel state information (CSI) is available at each edge device and the edge sever. Each edge device is required to perform power control to make the received signal satisfy magnitude alignment for model aggregation. By exploiting the CSI, each edge device can implement channel inversion by multiplying the local information by its inverse channel coefficient to compensate for both amplitude and phase of the fading channel, which is

$$\alpha_n^t := \sqrt{\beta^t} \frac{(h_n^t)^H}{|h_n^t|^2}, \quad (17)$$

where β^t is the denoising factor at the edge server. Then the estimated signal at the edge server is⁴

$$\hat{\mathbf{y}}^t := \frac{\hat{\mathbf{s}}^t}{\sqrt{\beta^t}} = \sum_{n=1}^N p_n \mathbf{z}_n^t + \tilde{\mathbf{w}}^t, \quad (18)$$

where $\tilde{\mathbf{w}}^t \sim \mathcal{N}(0, \frac{\sigma_w^2}{\beta^t} \mathbf{I}_d)$ is the equivalent noise vector. It is clear that the signal estimated by the edge server is distorted by noise, which is different from the error-free case. Such an imperfect estimation causes a model aggregation error (MAE), which refers to the difference between the estimated signal of the edge server and the error-free one, i.e.,

$$\boldsymbol{\varepsilon}^t := \hat{\mathbf{y}}^t - \bar{\mathbf{y}}^t, \quad (19)$$

where $\bar{\mathbf{y}}^t = \sum_{n=1}^N p_n \mathbf{z}_n^t$. The MAE is dominated by the additive noise with estimated signal (18) at the edge server.

⁴In this paper, the transmitted signal of edge device n is the local information multiplied by weight p_n , i.e., the edge server receives the weighted sum of the transmitted local information. When $p_1 = \dots = p_N = 1/N$, the edge devices transmit only the local information without scaling by $1/N$, while the edge server needs to perform global averaging by multiplying $1/N$ for post-processing.

Algorithm 1: AIRFEDAVG-M Algorithm

1 Algorithm of the Edge Server:
2 Initialize the global model and broadcast it to all edge devices. Set $t = 0$;
3 while $t \leq T$ **do**
4 **wait** until receiving the perturbed and aggregated signal via AirComp (16);
5 **post-process** the received signal by dividing the denoising factor (18);
6 **update** global model via (21);
7 **broadcast** the updated global model to all edge devices;
8 **set** $t \leftarrow t + 1$;
9 end

1 Algorithm of the n -th Edge Device:
2 Initialization: local model, $\eta^0, t = 0$;
3 while $t \leq T$ **do**
4 **wait** until receiving global model from edge server;
5 **update** local model via (14);
6 **send** the pre-processed and precoded accumulated local gradients to edge server synchronously with respect to time and frequency;
7 **set** $t \leftarrow t + 1$.
8 end

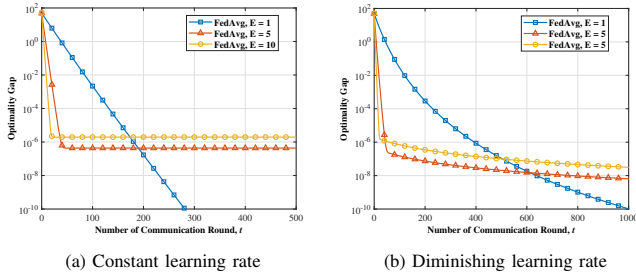


Fig. 3. FEDAVG with $E = 1$, $E = 5$, and $E = 10$ under constant learning rate and learning rate decay for federated linear regression problems.

Remark 3. Besides, the channel inversion method we adopt has some variants. For instance, in [53], [99], [110], the authors considered a threshold for channel gains of edge devices to filter out edge devices in deep fading, leading to partial device participation. The threshold-based channel inversion can be summarized as

$$\alpha_n^t := \begin{cases} 0, & |h_n^t| < \gamma, \\ \sqrt{\beta^t} \frac{(h_n^t)^H}{|h_n^t|^2}, & |h_n^t| \geq \gamma, \end{cases} \quad (20)$$

where γ is the pre-determined threshold. Under threshold-based channel inversion, full device participation reduces to partial device participation.

We first consider the scenario where edge device n performs multiple local updates (i.e., $E > 1$) and the accumulated local gradient (i.e., model difference) in (14) is transmitted. This algorithm is named AIRFEDAVG-MULTIPLE (AIRFEDAVG-M) and is detailed in Algorithm 1, which has the following global

update operator

$$\hat{\theta}^{t+1} = \hat{\theta}^t + \hat{g}^t. \quad (21)$$

where $\hat{\theta}^t$ represents the noisy global model. We will discuss other two forms of z_n^t (i.e., local gradient and local model) in Section V.

However, according to [111], [112], FEDAVG with multiple local updates cannot optimally converge in some convex problems, e.g., federated least square and logistic regression, under the constant learning rate. As depicted in Fig. 3, FEDAVG with single local update converges directly to the optimal point under the constant learning rate, while FEDAVG with multiple local updates converges to a surrogate fixed point instead of the optimal point, resulting in a non-diminishing optimality gap. This is because multiple local updates may possibly be biased (refer to details in Section V), and the decaying learning rate can reduce such a bias in analogous to variance reduction of decaying learning rate on SGD. Using learning rate decay can address this problem [76], [88], which is verified in Fig. 3(b) with convergence speed slowed down. In view of this, together with the conclusions in Section II, the setting of learning rate η^t in AIRFEDAVG-M is chosen as follows:

- For strongly convex objective functions, we use a diminishing learning rate for algorithm analysis to attain diminishing optimality gap.
- For non-convex objective functions, we use a diminishing learning rate for algorithm analysis as well. Besides, we also present convergence results with constant learning rate, in terms of to achieve convergence rate and error bound on the average norm of the global gradient, which is related to the number of edge devices, the number of local updates, and the number of communication rounds,

IV. CONVERGENCE ANALYSIS FOR AIRFEDAVG-M

In this section, we start by establishing the convergence analysis of AIRFEDAVG-M over a noisy uplink channel. Our analysis is based on several basic and widely-used assumptions.

Assumption 3 (L -Smoothness). F_1, \dots, F_N are all L -smooth.

Assumption 4 (μ -Strong Convexity). F_1, \dots, F_N are all μ -strongly convex.

Assumption 5 (Unbiased Gradient and Bounded Variance). Each edge device can query an unbiased stochastic gradient with bounded variance:

$$\begin{aligned} \mathbb{E} [g_n^t] &= \nabla F_n(\theta^t), \\ \mathbb{E} [\|g_n^t - \nabla F_n(\theta^t)\|_2^2] &\leq \sigma_n^2, \end{aligned}$$

where σ_n^2 is inversely proportional to the local mini-batch size \tilde{D}_n^t , for $n = 1, \dots, N$.

Assumption 6 (Bounded Gradient Dissimilarity (BGD)). There exist constants $\beta_1 \geq 1$ and $\beta_2 \geq 0$, such that

$$\sum_{n=1}^N p_n \|\nabla F_n(\mathbf{x})\|_2^2 \leq \beta_2 + \beta_1 \|\nabla F(\mathbf{x})\|_2^2.$$

Note that if the local datasets of all devices are i.i.d., then it holds that $\beta_1 = 1$, and $\beta_2 = 0$.

A. Strongly Convex Case

1) *Main Results and Analysis*: The convergence for AIRFEDAVG-M is stated in **Theorem 1** for strongly convex objectives.

Theorem 1 (Convergence of AIRFEDAVG-M under Strong Convexity with Learning Rate Decay). *With Assumptions 3, 4, 5, and 6, if learning rate $0 < \eta^t \leq \min \left\{ \frac{1}{L\sqrt{2E(E-1)(2\beta_1+1)}}, \frac{1}{2LE} \right\}$, then the upper bound on the cumulative gap after T communication rounds is given by*

$$\begin{aligned} \mathbb{E} \left[F(\hat{\theta}^T) \right] - F^* &\leq \underbrace{\left[F(\hat{\theta}^0) - F^* \right] M^0 + C_1 \sum_{t=0}^{T-1} (\eta^t)^3 M^{t+1}}_{(a)} \\ &+ \underbrace{C_2 \sum_{t=0}^{T-1} (\eta^t)^2 M^{t+1}}_{(b)} + \underbrace{C_3 \sum_{t=0}^{T-1} \text{MSE}^t M^{t+1}}_{(c)}, \end{aligned} \quad (22)$$

where constants $M^t = \prod_{i=t}^{T-1} (1 - \frac{\mu\eta^i E}{2})$, $M^T = 1$, $C_1 = \frac{L^2 E(E-1)(2\beta_1+1)}{4\beta_1} \left[\sum_{n=1}^N p_n \sigma_n^2 + 2E\beta_2 \right]$, $C_2 = LE \sum_{n=1}^N p_n^2 \sigma_n^2$, and $C_3 = \frac{L}{2}$. In addition, the MSE is a function of MAE in each communication round, and can be written as

$$\text{MSE}^t(\epsilon^t) := \mathbb{E} \left[\|\epsilon^t\|_2^2 \right] = \mathbb{E} \left[\|\tilde{w}^t\|_2^2 \right] = \frac{\sigma_w^2}{\beta^t}, \quad (23)$$

where the expectation is taken over the distribution of the random variable ϵ^t .

Proof. Please refer to Appendix A-B. \square

Remark 4. The key observations of **Theorem 1** include: term (a) is caused by bounded variance, non-IID data, and multiple local updates; term (b) is caused by gradient estimation variance; term (c) reflects the impact of the mean square error (MSE) caused by MAE on the convergence bound, which is dominated by the noise power and the denoising factor.

To analyze the convergence of partial sums (a), (b), and (c) in **Theorem 1**, we introduce a key lemma to support our theoretical analysis.

Lemma 1 (Lemma 25 in [113]). *Let sequences $\{s_1(t)\}_{t \geq 0}$ and $\{s_2(t)\}_{t \geq 0}$ be*

$$s_1(t) = \frac{a_1}{(t+1)^{\delta_1}}, \quad s_2(t) = \frac{a_2}{(t+1)^{\delta_2}}, \quad t \geq 0,$$

with $a_1, a_2, \delta_2 \geq 0$ and $0 \leq \delta_1 \leq 1$. If $\delta_1 = \delta_2$, then there exists a constant φ , such that for a large enough positive integer $j < T$,

$$0 \leq \sum_{t=j}^{T-1} \left[s_2(t) \left(\prod_{i=t+1}^{T-1} (1 - s_1(i)) \right) \right] \leq \varphi. \quad (24)$$

Moreover, if $\delta_1 < \delta_2$, then for an arbitrary j , we have

$$\lim_{T \rightarrow \infty} \sum_{t=j}^{T-1} \left[s_2(t) \left(\prod_{i=t+1}^{T-1} (1 - s_1(i)) \right) \right] = 0. \quad (25)$$

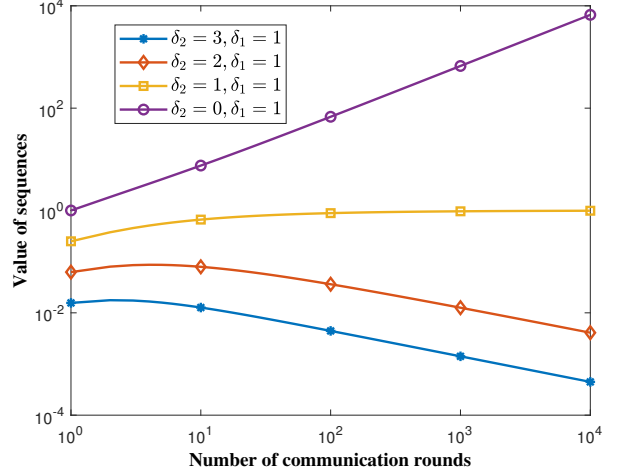


Fig. 4. Values of the sequences versus number of communication rounds with different (δ_1, δ_2) pairs in **Lemma 1**.

Proof. Please refer to [113, Appendix C]. \square

We carry out numerical experiments to illustrate the convergence of partial sums with different (δ_1, δ_2) pairs, as presented in **Lemma 1**. The value of sequences against the number of communication rounds in the log-scale is demonstrated in Fig. 4 with $(\delta_1, \delta_2) \in \{(1, 0), (1, 1), (1, 2), (1, 3)\}$. Specifically, we set the learning rate as

$$\eta^t = \frac{\eta^0}{t+1}, \quad \eta^0 = \min \left\{ \frac{1}{L\sqrt{2E(E-1)(2\beta_1+1)}}, \frac{1}{2LE} \right\},$$

for further analysis, which satisfies condition (4) in Section II.

Term (a) in **Theorem 1** can be reformulated as

$$C_1 \sum_{t=0}^{T-1} \left[\left(\frac{\eta^0}{t+1} \right)^3 \prod_{i=t+1}^{T-1} \left(1 - \frac{\mu E \eta^0 / 2}{i+1} \right) \right],$$

which is equivalent to (25) with $j = 0$, $a_1 = \frac{\mu E \eta^0}{2}$, $\delta_1 = 1$, $a_2 = (\eta^0)^3$ and $\delta_2 = 3$ in **Lemma 1**. This indicates that term (a) of (22) in **Theorem 1** is diminishing as $T \rightarrow \infty$ because $\delta_1 < \delta_2$. The convergent property is illustrated in Fig. 4 with $(\delta_1, \delta_2) = (1, 3)$.

Similarly, the diminishing property of term (b) of (22) in **Theorem 1** can be verified by setting $j = 0$, $a_1 = \frac{\mu E \eta^0}{2}$, $\delta_1 = 1$, $a_2 = (\eta^0)^2$, and $\delta_2 = 2$ in **Lemma 1**. The diminishing property is also illustrated in Fig. 4 with $(\delta_1, \delta_2) = (1, 2)$.

However, to analyze the convergence property of term (c), it hinges on whether MSE satisfies the conditions in **Lemma 1**. Therefore, it is required to provide elaborate classification with respect to the MSE for further discussion.

2) *Case Study*: According to (23), the MSE is determined by the noise power and denoising factor. To discuss the influence of the MSE on term (c), we consider the following cases.

- **The MSE approaches to zero in each communication round.** In this case, term (c) in (22) is eliminated, which means AIRFEDAVG-M approximates to error-free FEDAVG. In addition, for asymptotic analysis, if $\text{MSE}^t \rightarrow 0$, we must have $\sigma_w^2 \rightarrow 0$ or $\beta^t \rightarrow \infty$, which demands an

infinite large SNR. However, neither of the two conditions is practical in real AirComp systems since we cannot control the noise power and the transmit power is limited.

- **The MSE is a positive constant in each communication round.** In this case, we have

$$\text{MSE}^t \sim (\eta^t)^0 = 1,$$

which means that for the strongly convex case, term (c) is non-diminishing as presented in Fig. 4 with $(\delta_1, \delta_2) = (1, 0)$.

- **The MSE is proportional to the diminishing learning rate.** For strongly convex case, term (c) converges if and only if the following condition holds

$$\text{MSE}^t \sim (\eta^t)^\delta = \left(\frac{\eta^0}{t+1} \right)^\delta, \quad \delta > 1, \quad (26)$$

without requiring an infinite large SNR. This condition can be directly derived from **Lemma 1**.

In summary, we are unable to obtain a convergent upper bound for strongly convex case of AIRFEDAVG-M without properly designing the AirComp system to make the MSE caused by model aggregation satisfy condition (26). Hence, the impact of the MAE caused by the wireless channel needs to be carefully studied.

According to (23), to achieve convergence guarantee for AIRFEDAVG-M, one possible approach is to jointly design the transmit scalar and the denoising factor $\sqrt{\beta^t}$. As inspired, a lot of recent efforts applied the precoding and denoising techniques to ensure the decaying property of term (c) and further provided an upper bound for the convergence optimality gap [53]. In this tutorial, we verify the observations by adopting an exemplifying denoising factor design and deriving some insightful conclusions regarding the convergence rate and optimality gap, which are presented as follows.

According to the convergence analysis on the sequences of the upper bound, the convergence of the upper bound can be guaranteed and the impact of the additive noise can be compensated as long as the denoising factor satisfies the following condition:

$$(\beta^t)^{-1} \sim (\eta^t)^\delta, \quad \delta > 1, \quad (27)$$

which can be directly derived by combining (23) and (26). The transmit power constraint in communication round t for edge device n is given by

$$\mathbb{E} \left[\|\alpha_n^t p_n \mathbf{z}_n^t\|_2^2 \right] \leq d \times P_0,$$

where P_0 is the transmit power, and the SNR can be written as

$$\text{SNR} := \frac{P_0}{\sigma_w^2}. \quad (28)$$

Based on the transmit power constraint, we adopt a denoising factor that takes the norm of local information into account to mitigate the detrimental influence caused by the additive noise, i.e.,

$$\beta^t := \min_{n \in \mathcal{N}} \frac{|h_n^t|^2 d P_0}{\|p_n \mathbf{z}_n^t\|_2^2}. \quad (29)$$

Under this setup, the information recovered by the edge server is an unbiased estimation of the transmit information. However, this setting may be suboptimal especially in deep fading scenarios [47]. Since $\mathbf{z}_n^t = -\eta^t \sum_{e=0}^{E-1} \mathbf{g}_n^{(t,e)}$, the denoising factor can be further written as

$$(\beta^t)^{-1} = (\eta^t)^2 \max_{n \in \mathcal{N}} \frac{\left\| p_n \sum_{e=0}^{E-1} \mathbf{g}_n^{(t,e)} \right\|_2^2}{|h_n^t|^2 d P_0} \sim (\eta^t)^2.$$

Condition (27) can be proved to hold according to [53, **Lemma A.2**] with the BG assumption, which is presented as follows.

Assumption 7 (Bounded Gradient (BG)). *The expected squared norm of stochastic gradient of each edge device is bounded by*

$$\mathbb{E}[\|\mathbf{g}_n^{(t,e)}\|_2^2] \leq G^2, \quad \forall n,$$

where $G > 0$ is a constant.

The denoising factor can be further specified as

$$(\beta^t)^{-1} = \frac{\tilde{G}^2 E (\eta^t)^2}{d N^2 P_0}, \quad (30)$$

by **Assumption 7**, where $\tilde{G}^2 = G^2 \max_{n \in \mathcal{N}} \frac{v_n^2}{|h_n^t|^2}$ with $v_n = N p_n$, and $\sum_{n=1}^N v_n = N$. This indicates that **Assumption 7** is not necessary in error-free transmission scenarios, but usually needed in wireless FL scenarios [47], [49], [53], [60], [66]. By substituting (30) into (23), the MSE of model aggregation can be written as

$$\text{MSE}^t = \frac{\sigma_w^2 \tilde{G}^2 E (\eta^t)^2}{d N^2 P_0} = \frac{\tilde{G}^2 E (\eta^t)^2}{d N^2 \text{SNR}},$$

where the MSE is inversely proportional to SNR.

This transmission scheme leverages the decaying property of the accumulated local gradients to eliminate the impact of receiver noise as the training process proceeds. Similarly, the authors in [59] proposed an SNR control policy, which requires that the noise power decays with respect to communication rounds, i.e.,

$$(\sigma_w^t)^2 \sim \mathcal{O} \left(\frac{1}{t^2} \right).$$

This scheme coincides with our statement because decaying the power of noise $\tilde{\mathbf{w}}^t$ with fixed denoising factor is equivalent to setting β^t as in (27).

Subsequently, we have the following corollary for the strongly convex case to derive the diminishing optimality gap and convergence rate for AIRFEDAVG-M.

Corollary 1 (Optimality Gap of AIRFEDAVG-M under Strong Convexity with Learning Rate Decay). *If the learning rate is set as $\eta^t = \frac{6}{E\mu(\tau+t)}$, with $\tau = \frac{3L}{\mu}$, the optimality gap $\mathbb{E} [F(\hat{\theta}^T)] - F^*$ of the strongly convex case of AIRFEDAVG-M converges to zero with rate*

$$\mathbb{E} [F(\hat{\theta}^T)] - F^* \leq \mathcal{O} \left(\frac{A_1}{E^2 \mu^3 T^2} \right) + \mathcal{O} \left(\frac{B_1}{N E \mu^2 T} \right), \quad (31)$$

where $A_1 = L^2(E-1)(2+1/\beta_1)[\bar{\sigma}^2 + E\beta_2]$, $B_1 = L\Sigma + L/dN\text{SNR}$, $\Sigma = N\sigma^2$, $\bar{\sigma}^2 = \sum_{n=1}^N p_n \sigma_n^2$, and $\sigma^2 = \sum_{n=1}^N p_n^2 \sigma_n^2$.

In order to achieve bound (31), the number of local updates is bounded by

$$E \leq \frac{6(2\beta_1 + 1)\bar{\sigma}^2 + 12\beta_1(\sigma^2 + \tilde{G}^2/dN^2\text{SNR})}{\beta_1\mu(F(\hat{\theta}^0) - F^*) - 12\beta_2(2\beta_1 + 1)}. \quad (32)$$

Proof. Please refer to Appendix C. \square

Remark 5. The right hand side of (31) is dominated by $\mathcal{O}((NET)^{-1})$, and the additional error decays faster with rate $\mathcal{O}((ET)^{-2})$. It is obvious that AIRFEDAVG-M in the strongly convex case with proper denoising factor achieves linear speed up in terms of the number of local updates and the number of edge devices.

B. Non-Convex Case

1) *Main Results and Analysis:* We derive **Theorem 2** for the error bound of the non-convex objectives.

Theorem 2 (Convergence of AIRFEDAVG-M under Non-convexity with Learning Rate Decay). *Let Assumptions 3, 5, and 6 hold. If the diminishing learning rate satisfies $0 < \eta^t \leq \min \left\{ \frac{1}{L\sqrt{2E(E-1)(2\beta_1+1)}}, \frac{1}{2LE} \right\}$, then the weighted average norm of global gradients after T communication rounds is upper bounded by*

$$\begin{aligned} & \frac{1}{\Phi} \sum_{t=0}^{T-1} \eta^t \mathbb{E} \left[\left\| \nabla F(\hat{\theta}^t) \right\|_2^2 \right] \\ & \leq \frac{4 \left[F(\hat{\theta}^0) - F^{\text{inf}} \right]}{E\Phi} + \underbrace{\frac{4C_1}{E\Phi} \sum_{t=0}^{T-1} (\eta^t)^3}_{(a)} + \underbrace{\frac{4C_2}{E\Phi} \sum_{t=0}^{T-1} (\eta^t)^2}_{(b)} \\ & \quad + \underbrace{\frac{4C_3}{E\Phi} \sum_{t=0}^{T-1} \text{MSE}^t}_{(c)}, \end{aligned} \quad (33)$$

where $\Phi = \sum_{j=0}^{T-1} \eta^j$.

Proof. Please refer to Appendix A-B. \square

Similarly, to analyze the convergence of each sequence in **Theorem 2**, we introduce a key lemma to support our theoretical analysis for the non-convex case.

Lemma 2 (Stolz–Cesàro Theorem). *Let $\{a_n\}_{n \geq 1}$ and $\{b_n\}_{n \geq 1}$ be two sequences of real numbers. Assume that $\{b_n\}_{n \geq 1}$ is a strictly monotone and divergent sequence, and the following limit exists:*

$$\lim_{n \rightarrow \infty} \frac{a_{n+1} - a_n}{b_{n+1} - b_n} = \ell.$$

Then we have the following limit

$$\lim_{n \rightarrow \infty} \frac{a_n}{b_n} = \ell.$$

Using the same diminishing learning rate as the strongly convex case, the partial sum $\Phi = \sum_{j=0}^{T-1} \eta^j$ diverges due to the property of harmonic series. For term (a) in **Theorem 2**,

its convergent property can be easily verified by **Lemma 2**, which is a common criterion for proving the convergence of a sequence, as the numerator $a_T = \sum_{t=0}^{T-1} (\eta^t)^3$ is of higher order than the denominator $b_T = \Phi = \sum_{t=0}^{T-1} \eta^t$. Similarly, the diminishing property of term (b) in **Theorem 2** can be verified as well.

As in the strongly convex case, to analyze the convergence property of term (c) in **Theorem 2**, it is also required to provide elaborate classification with respect to the MSE. According to **Lemmas 1** and **2**, the properties of terms (a), (b), and (c) in the above two theorems are equivalent. In view of this, the convergence condition of the MSE for non-convex cases with learning rate decay is identical to that in strongly convex cases.

To conclude, the denoising factor adopted in the previous section can also be applied in the non-convex case, which guarantees the convergence property of term (c) in **Theorem 2**.

2) *Case Study:* For case study in the non-convex case with denoising factor (30), we have the following two corollaries for the diminishing error bound and convergence rate.

Corollary 2 (Error Bound of AIRFEDAVG-M under Non-Convexity with Learning Rate Decay). *Given learning rate $\eta^t = \frac{\eta^0}{t+1}$, and $\eta^0 = \min \left\{ \frac{1}{L\sqrt{2E(E-1)(2\beta_1+1)}}, \frac{1}{2LE} \right\}$, the error bound of AIRFEDAVG-M under non-convexity is diminishing, i.e.,*

$$\frac{1}{\Phi} \sum_{t=0}^{T-1} \eta^t \mathbb{E} \left[\left\| \nabla F(\hat{\theta}^t) \right\|_2^2 \right] \xrightarrow{T \rightarrow \infty} 0. \quad (34)$$

Proof. By combining (6), (33) and (30), we obtain (34). \square

Corollary 3 (Error Bound of AIRFEDAVG-M under Non-convexity with Constant Learning Rate). *When the learning rate is a constant satisfying*

$$\eta = \frac{1}{L} \sqrt{\frac{N}{ET}} \leq \min \left\{ \frac{1}{L\sqrt{2E(E-1)(2\beta_1+1)}}, \frac{1}{2LE} \right\},$$

the minimal gradient norm of the global objective function of AIRFEDAVG-M is bounded as follows

$$\begin{aligned} & \min_{t \in [T]} \mathbb{E} \left[\left\| \nabla F(\hat{\theta}^t) \right\|_2^2 \right] \leq \frac{1}{T} \sum_{t=0}^{T-1} \mathbb{E} \left[\left\| \nabla F(\hat{\theta}^t) \right\|_2^2 \right] \\ & \leq \mathcal{O} \left(\frac{1 + \Sigma}{\sqrt{NET}} \right) + \mathcal{O} \left(\frac{\tilde{C}N(\bar{\sigma}^2 + E\beta_2)}{ET} \right) \\ & \quad + \mathcal{O} \left(\frac{1}{d\text{SNR}\sqrt{N^3ET}} \right), \end{aligned} \quad (35)$$

where $\Sigma = N\sigma^2$ and $\tilde{C} = \frac{(E-1)(2\beta_1+1)}{\beta_1}$. The right hand side of the inequality is dominated by $\mathcal{O} \left(\frac{1+\Sigma}{\sqrt{NET}} \right)$.

It is worth noting that **Corollary 3** recovers the results of the error-free case by setting $\sigma_w^2 = 0$, i.e., $\text{SNR} \rightarrow \infty$ in [94].

Remark 6. The impact of receiver noise on the convergence of AIRFEDAVG-M is mathematically similar to the gradient estimation noise caused by vanilla SGD. In addition, we

observe from **Corollaries 1 and 3** that a lower SNR amplifies the optimality gap for strongly convex cases and the error bound for non-convex objectives.

Remark 7. It is clear that for both strongly convex and non-convex objectives, a greater number of local updates leads to a faster convergence rate at the cost of worsening the impact of non-IID data by enlarging the optimality gap in **Corollary 1** and the error bound in **Corollary 3**. Moreover, by setting $E = 1$ for AIRFEDAVG-M, the impact caused by non-IID data is eliminated. This means that by setting $E = 1$ and $\sigma_w^2 = 0$ in **Corollary 1** and **3**, the result is consistent with the standard convergence rate for vanilla SGD [75] for both strongly convex and non-convex cases without data heterogeneity.

To conclude, AIRFEDAVG-M ($E \geq 1$) is a typical example of AIRFEDAVG in terms of algorithm analysis. Other important results will be discussed in the following section.

V. VARIANTS OF AIRFEDAVG

As mentioned previously, local model, model difference and local gradient are three different forms of local information that can be exchanged between the edge server and edge devices for global model aggregation. In error-free FEDAVG, these different forms are equivalent and transferable from each other in the training process. However, with AirComp (18), the variants of AIRFEDAVG are no longer identical due to the additive noise in each communication round. In this section, different variants of AIRFEDAVG will be presented, and the insights and results of these variations will be analyzed and discussed.

A. AIRFEDAVG with Local Gradients

Although AIRFEDAVG-M is an effective algorithm for AirFL [49], [53], [55], [59], [60], [66]–[68], [71], it faces several issues as follows.

- In (14), if local gradients are not multiplied by the learning rate, then

$$\mathbf{z}_n^t = \Delta \theta_n^{t+1} / \eta^t \triangleq - \sum_{e=0}^{E-1} \mathbf{g}_n^{(t,e)}.$$

In this case, the global update is given by

$$\hat{\theta}^{t+1} \stackrel{(19)}{=} \hat{\theta}^t + \eta^t \left(\sum_{n=1}^N p_n \mathbf{z}_n^t + \varepsilon^t \right). \quad (36)$$

If the learning rate changes every local update in one communication round, i.e., $\eta^t \rightarrow \eta^{(t,e)}$, then this scheme cannot be well generalized because it is difficult to select $\eta^{(t,e)}$ for obtaining \mathbf{z}_n^t and model aggregation.

- From **Remark 7**, we know that a larger number of local updates enlarges the aggregation bias due to non-IID data [86]. To be more specific, for $E = 1$ and $\theta_n^{(t,1)} = \theta_n^{(t,0)} - \eta^t \mathbf{g}_n^{(t,0)}$, $\theta_n^{(t,1)} - \theta_n^{(t,0)}$ is an unbiased estimator of $-\eta^t \nabla F(\theta^t)$. However, for $E = 2$, we have

$$\theta_n^{(t,2)} = \theta_n^{(t,0)} - \eta^t \mathbf{g}_n^{(t,0)} - \eta^t \mathbf{g}_n^{(t,1)},$$

and $\theta_n^{(t,2)} - \theta_n^{(t,0)}$ is neither the unbiased estimator of $-\eta^t \nabla F(\theta^t)$ nor that of $-\eta^t \nabla F(\theta^t - \eta^t \nabla F(\theta^t))$ [95]. This reflects the advantage of single local update.

- From the results of AIRFEDAVG-M, we know that the requirements for the MSE in AIRFEDAVG-M is quite stringent, i.e., the upper bound of AIRFEDAVG-M cannot converge with an arbitrary MSE. Simply setting $E = 1$ in AIRFEDAVG-M still requires strict restrictions on the model aggregation MSE.

To tackle these challenges, we propose to exploit an important variant of AIRFEDAVG. Specially, when $E = 1$, the local computation can directly be local gradient estimation without performing a decent step, i.e.,

$$\mathbf{z}_n^t = \mathbf{g}_n^{(t,0)}. \quad (37)$$

We name this algorithm as AIRFEDAVG with single local gradient, AIRFEDAVG-S. The global update of AIRFEDAVG-S is

$$\hat{\theta}^{t+1} = \hat{\theta}^t - \eta^t \hat{\mathbf{y}}^t \stackrel{(19)}{=} \hat{\theta}^t - \eta^t (\bar{\mathbf{y}}^t + \varepsilon^t), \quad (38)$$

where $\hat{\mathbf{y}}^t$ is defined in (18) and $\bar{\mathbf{y}}^t = \sum_{n=1}^N p_n \mathbf{z}_n^t$.

As to the convergence analysis for AIRFEDAVG-S, the model aggregation of this algorithm is special. Compared with the global model update in AIRFEDAVG-M ($E = 1$) (21), it is observed that the MAE of AIRFEDAVG-S is naturally multiplied by the learning rate for model aggregation while AIRFEDAVG-M does not have this property, which implies that the convergence of these two algorithms may not be identical and simply setting $E = 1$ in the convergence results of AIRFEDAVG-M is improper. Assume that this property is prone to relax the requirements on the model aggregation MSE as discussed in the previous section. We will prove this conjecture.

The setting of learning rate η^t in AIRFEDAVG-S can be chosen as follows:

- For strongly convex objective functions, we unify to use a diminishing learning rate to attain diminishing optimality gap. The results for constant learning rate are presented as corollaries for non-diminishing optimality gap.
- For non-convex objective functions, we use a diminishing learning rate for convergence analysis as well. In addition, we will present convergence results with constant learning rate in terms of the convergence rate and the error bound.

1) *Main Results and Case Study:* To analyze the impact of receive noise in AIRFEDAVG-S, we summarize the convergence results with respect to the MSE in **Theorem 3** for strongly convex objectives.

Theorem 3 (Convergence of AIRFEDAVG-S under Strong Convexity with Learning Rate Decay). *Let Assumption 3, 4 and 5 hold, where L, μ, σ_n are defined. If the decaying learning rate satisfies $0 < \eta^t \leq \frac{1}{L}$, then the upper bound*

on the optimality gap after T communication rounds is given by

$$\begin{aligned} & \mathbb{E} \left[F(\hat{\theta}^T) \right] - F^* \\ & \leq \left[F(\hat{\theta}^0) - F^* \right] P^0 + \frac{L}{2} \sum_{t=0}^{T-1} (\eta^t)^2 (\sigma^2 + \text{MSE}^t) P^{t+1}, \end{aligned} \quad (39)$$

where $P^t = \prod_{i=t}^{T-1} (1 - \mu\eta^i)$, $P^T = 1$, and MSE^t is defined in (23).

Proof. Please refer to Appendix B-B. \square

Using **Lemma 1**, we can easily prove that for strongly convex objective functions, the last term of (39) is a convergent sequence for all three conditions of the MSE listed in Section IV-A2. The following two corollaries for the strongly convex cases can be obtained based on **Theorem 3**.

Corollary 4 (Optimality Gap of AIRFEDAVG-S under Convexity with Constant Learning Rate). *If the learning rate is a constant satisfying $\eta^t = \eta = \frac{1}{L}$, the optimality gap $\mathbb{E} \left[F(\hat{\theta}^T) \right] - F^*$ of the convex case of AIRFEDAVG-S can be bounded by*

$$\begin{aligned} \mathbb{E} \left[F(\hat{\theta}^T) \right] - F^* & \leq \left(1 - \frac{\mu}{L} \right)^T \left[F(\hat{\theta}^0) - F^* \right] \\ & \quad + \left(1 - \frac{\mu}{L} \right)^{T-t-1} \frac{1}{2L} \sum_{t=0}^{T-1} (\sigma^2 + \text{MSE}^t). \end{aligned} \quad (40)$$

The second term of the right hand side is a non-diminishing term. Note that this is the most frequently-used conclusion in wireless FL literature with respect to AIRFEDAVG-S. Subsequently, to provide case study with respect to the denoising factor (29), we have the following corollary for the strongly convex case.

Corollary 5 (Optimality Gap of AIRFEDAVG-S under Convexity with Learning Rate Decay). *If the precoding factor is a constant, and the learning rate is set as $\eta^t = \frac{2}{\mu(\tau+t)}$, with $\tau = \frac{2L}{\mu}$, then the optimality gap $\mathbb{E} \left[F(\hat{\theta}^T) \right] - F^*$ of the convex case of AIRFEDAVG-S converges to zero with rate*

$$\mathbb{E} \left[F(\hat{\theta}^T) \right] - F^* \leq \mathcal{O} \left(\frac{\tilde{B}}{\mu^2 NT} \right), \quad (41)$$

where $\tilde{B} = \max \left\{ 2L(\Sigma + \frac{\tilde{G}^2}{dN\text{SNR}}), \mu^2 N\tau(F(\hat{\theta}^0) - F^*) \right\}$.

Proof. Please refer to Appendix D. \square

Note that this result is equivalent to the statements in [52], [76] with respect to the convergence rate. According to **Corollary 4** and **Corollary 5**, we can conclude that in the strongly convex case, the expected objective values converge linearly to a neighborhood of the optimal value for AIRFEDAVG-S with a constant learning rate. However the impact of MAE, i.e., the model aggregation MSE, hinders further convergence to the optimal solution. On the other hand, it can converge to the optimal point at the expense of achieving a slower sublinear convergence speed, which is in the order of $\mathcal{O}(1/NT)$.

Besides, the convergence results for non-convex objectives with diminishing learning rate can be found in **Theorem 4**.

Theorem 4 (Convergence of AIRFEDAVG-S under Non-convexity with Learning Rate Decay). *Let Assumptions 3 and 5 hold, and the learning rate satisfy $0 < \eta^t \leq \frac{1}{L}$. The weighted average norm of global gradients after T communication rounds is upper bounded by*

$$\begin{aligned} & \frac{1}{\Phi} \sum_{t=0}^{T-1} \eta^t \mathbb{E} \left[\left\| \nabla F(\hat{\theta}^t) \right\|_2^2 \right] \\ & \leq \frac{2}{\Phi} \left[F(\hat{\theta}^0) - F^{\text{inf}} \right] + \frac{L}{\Phi} \sum_{t=0}^{T-1} (\eta^t)^2 (\sigma^2 + \text{MSE}^t). \end{aligned} \quad (42)$$

Proof. Please refer to Appendix B-B. \square

Similar to the non-convex objective functions, the last term of **Theorem 4** is a convergent sequence for all three conditions of the MSE listed in Section IV-A2 by **Lemma 2**. In addition, the following corollary for non-convex case and denoising factor (29) can be obtained based on **Theorem 4**.

Corollary 6 (Error Bound of AIRFEDAVG-S under Non-convexity with Constant Learning Rate). *When the constant learning rate is given by*

$$\eta = \frac{1}{L} \sqrt{\frac{N}{T}} \leq \frac{1}{L},$$

the minimal gradient norm of the global objective function of the unbiased AIRFEDAVG-S will be bounded by

$$\begin{aligned} & \min_{t \in [T]} \mathbb{E} \left[\left\| \nabla F(\hat{\theta}^t) \right\|_2^2 \right] \leq \frac{1}{T} \sum_{t=0}^{T-1} \mathbb{E} \left[\left\| \nabla F(\hat{\theta}^t) \right\|_2^2 \right] \\ & \leq \mathcal{O} \left(\frac{1 + \Sigma}{\sqrt{NT}} \right) + \mathcal{O} \left(\frac{1}{d\text{SNR}\sqrt{N^3T}} \right), \end{aligned} \quad (43)$$

where the right hand side is dominated by $\mathcal{O} \left(\frac{1 + \Sigma}{\sqrt{NT}} \right)$.

2) *Comparison with AIRFEDAVG-M:* Compared with AIRFEDAVG-M ($E = 1$), we have the following corollary.

Corollary 7 (Equivalence of AIRFEDAVG-M ($E = 1$) and AIRFEDAVG-S). *When the denoising factor design satisfies (29), AIRFEDAVG-M ($E = 1$) and AIRFEDAVG-S are identical regardless of the strongly convex or non-convex objectives.*

Proof. For AIRFEDAVG-M ($E = 1$), we have

$$\text{MSE}_M^t = \frac{\sigma_w^2}{\beta^t} = (\eta^t)^2 \max_{n \in \mathcal{N}} \frac{\left\| p_n \mathbf{g}_n^{(t,0)} \right\|_2^2}{|h_n^t|^2 d\text{SNR}}.$$

For AIRFEDAVG-S, we have

$$\text{MSE}_S^t = \frac{\sigma_w^2}{\beta^t} = \max_{n \in \mathcal{N}} \frac{\left\| p_n \mathbf{g}_n^{(t,0)} \right\|_2^2}{|h_n^t|^2 d\text{SNR}}.$$

Obviously, we have

$$\text{MSE}_M^t = (\eta^t)^2 \text{MSE}_S^t.$$

It is worth noting that **Corollary 7** can be derived by comparing **Corollary 1** with **Corollary 5** for strongly convex case, and **Corollary 3** with **Corollary 6** for non-convex case. \square

To conclude, for both strongly convex and non-convex cases, AIRFEDAVG-S can be generalized by AIRFEDAVG-M with denoising factor in (29). With a constant MSE, AIRFEDAVG-S is more robust to receiver noise than AIRFEDAVG-M. This is due to the fact that MSE is multiplied by the learning rate, which is either decaying or a small real number, compared with AIRFEDAVG-M ($E = 1$).

Furthermore, the comparisons between AIRFEDAVG-M and AIRFEDAVG-S are discussed in the following.

Remark 8. In AIRFEDAVG-S, the detrimental impact of the additive noise on the optimality gap for strongly convex cases and the error bound for non-convex cases is relatively small compared with AIRFEDAVG-M, as the last terms of (39) and (42) converge with arbitrary model aggregation MSE.

Remark 9. Note that **Theorems 3 and 4**, together with AIRFEDAVG-M ($E = 1$) in **Theorems 1 and 2**, do not depend on **Assumption 6**, which indicates that performing only one local update has the potential to avoid the impact of heterogeneous data to some extent in comparison to the periodic averaging algorithms such as AIRFEDAVG-M. This confirms the discussion in **Remark 7**. This phenomenon is also illustrated in Fig. 5.

Remark 10. To compare the performance of AIRFEDAVG-M and AIRFEDAVG-S, we take the case study of non-convex case for example, where the denoising factor satisfies (27). Comparing **Corollary 2** with **Corollary 6**, it is clear that the number of communication rounds in AIRFEDAVG-M can be reduced by the number of local updates E , whose maximum is in the order of $\min \left\{ \mathcal{O} \left(\frac{T+(2\beta_1+1)N}{(2\beta_1+1)N} \right), \mathcal{O} \left(\frac{T}{N} \right) \right\}$. In summary, compared with AIRFEDAVG-S, AIRFEDAVG-M reduces the heavy communication cost, while guaranteeing faster convergence. However, AIRFEDAVG-M has more stringent requirements for the model aggregation MSE, while those requirements are quite loose in AIRFEDAVG-S. In addition, AIRFEDAVG-M may suffer from aggregation bias caused by non-IID data, while AIRFEDAVG-S is more robust to data heterogeneity at the cost of slower convergence speed.

In a nutshell, we have the following conclusions for algorithm selection.

- For the relatively simple learning task with strongly convex objectives, to support lightweight algorithm design, AIRFEDAVG-S is preferred with either constant or decaying learning rate to avoid non-diminishing optimality gap caused by multiple local updates, as in most recent works [36], [37], [44]–[48], [52], [57], [58], [61]–[64].
- For training non-convex DNNs and CNNs, the communication overhead is a critical issue due to the high dimensional model parameters. Since reducing the number of communication rounds between the edge devices and edge server alleviates the communication overhead, AIRFEDAVG-M algorithm is strongly recommended [49], [53], [55], [59], [60], [66]–[68], [71] based on the analysis above. AIRFEDAVG-S is also a practical algorithm to train non-convex DNNs in some extreme scenarios, for example, highly non-IID data distribution across edge

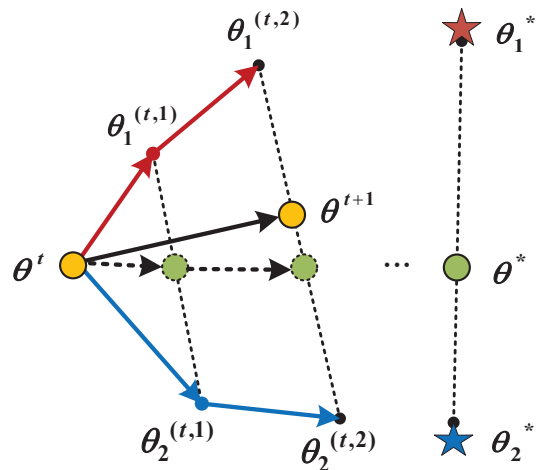


Fig. 5. Model aggregation bias caused by data heterogeneity of AIRFEDAVG-M for 2 edge devices with 2 local updates, i.e., $N = 2$, and $E = 2$. The stars represent the local optima of two edge devices while the circle in green is the global optima. The circles in yellow represent the global model for AIRFEDAVG-M. The dotted circles in green illustrate the global model for fully synchronized AIRFEDAVG-S.

devices.

B. AIRFEDAVG with Local Model

As an equivalent variant of FEDAVG, if the output of the local update operator is the local model parameter, i.e.,

$$z_n^t = \theta_n^{(t,E)}, \quad (44)$$

the global model update becomes

$$\hat{\theta}^{t+1} = \hat{y}^t, \quad (45)$$

for AIRFEDAVG with local model (AIRFEDMODEL). Besides, the impact mechanism of the additive noise for AIRFEDMODEL and AIRFEDAVG-M is the same, i.e., adding the noise directly to the model aggregation step without multiplying the learning rate.

In this section, we will present the convergence results in **Corollary 8** for AIRFEDMODEL by generalizing the analysis from Section IV.

Theorem 5 (Succession from AIRFEDAVG-M to AIRFEDMODEL). In **Theorems 1 and 2**, we present the convergence results of AIRFEDAVG-M with strongly convex and non-convex objective functions, respectively. Due to the fact that the impact mechanism of the additive noise is identical for AIRFEDAVG-M and AIRFEDMODEL, the convergence results of AIRFEDMODEL is mathematically the same as that of AIRFEDAVG-M with the output of the local update operator being set as $z_n^t = \theta_n^{(t,E)}$, which reflects the flexibility and extensibility of our convergence analysis framework.

Here we take the strongly convex case with $E = 1$ and a diminishing learning rate for case study.

Corollary 8 (Convergence of AIRFEDMODEL ($E = 1$) under Strong Convexity). With **Assumptions 3, 4, 5, and 6**, if the decaying learning satisfies $0 < \eta^t \leq \frac{1}{L}$, then the upper bound

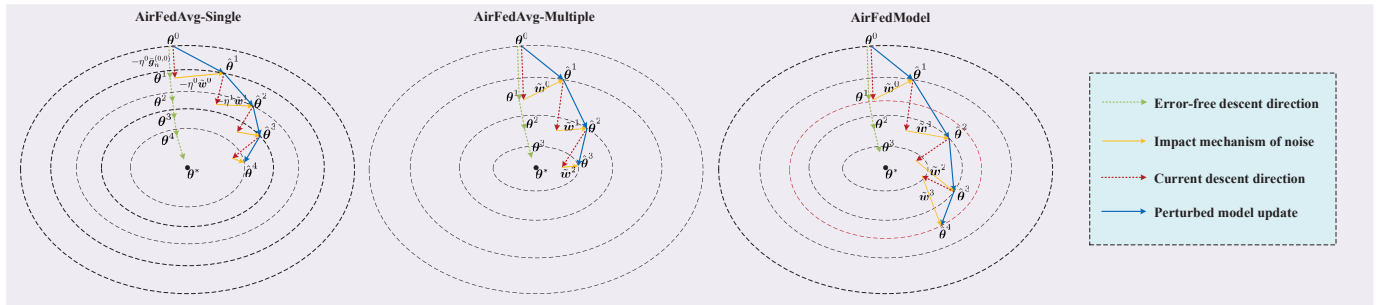


Fig. 6. The impact of the additive noise on the convergence for AIRFEDAVG-S, AIRFEDAVG-M and AIRFEDMODEL. The tighter the ellipse set is, the slower the convergence rate it represents. The dotted lines in green represent the error-free iterates of FEDAVG and the dotted lines in red represent the current descent direction from the perturbed global model $\hat{\theta}$. The yellow arrows are the impact mechanisms of the additive noise, \tilde{w}^t for AIRFEDAVG-M and AIRFEDMODEL and $-\eta^t \tilde{w}^t$ for AIRFEDAVG-S. The noise vector leads to an offset on the descent direction of the initialization point and that of every global model hereafter. For AIRFEDAVG-M and AIRFEDAVG-S, existing approaches can eliminate the impact of noise as the training procedure proceeds, but not for AIRFEDMODEL.

of the optimality gap after T communication rounds is given by

$$\mathbb{E} \left[F(\hat{\theta}^T) \right] - F^* \leq \left[F(\hat{\theta}^0) - F^* \right] Q^0 + C_{21} \sum_{t=0}^{T-1} (\eta^t)^2 Q^{t+1} + C_3 \sum_{t=0}^{T-1} \text{MSE}^t Q^{t+1}, \quad (46)$$

where $Q^t = \prod_{i=t}^{T-1} (1 - \frac{\mu\eta^i}{2})$, $Q^T = 1$, $C_{21} = L\sigma^2$, and $C_3 = \frac{L}{2}$.

However, the optimality gap for strongly convex case and error bound for non-convex case are non-diminishing unless the MSE approaches to zero in each communication round when the model parameter is transmitted in AIRFEDMODEL according to the analysis and results in Section IV-A2. In order to support this conclusion, suppose that each local model parameter is bounded by a constant, i.e.,

$$\mathbb{E}[\|\theta_n^{(t,E)}\|_2^2] \leq \Theta^2,$$

where $\Theta > 0$ is a constant, then by (29), the model aggregation MSE can be written as

$$\text{MSE}^t = \frac{\sigma_w^2 \tilde{\Theta}^2}{dN^2 P_0} = \frac{\tilde{\Theta}^2}{dN^2 \text{SNR}},$$

where $\tilde{\Theta}^2 = \Theta^2 \max_{n \in \mathcal{N}} \frac{v_n^2}{|h_n^t|^2}$. This indicates that the local model has neither decaying property like the accumulated local gradients (proportional to η^2) nor has the property as AIRFEDAVG-S, where the receiver noise is multiplied by the learning rate, as depicted in Fig. 6.

In this case, if the model parameters to be aggregated are perturbed, and the aggregation bias caused by stacked perturbations cannot be eliminated over time. This results in the model parameter being off the track, and the entire training procedure will be ruined. Then our FL model is very likely to fail to converge, unless $\text{MSE}^t \rightarrow 0$, which approximates to the error-free case or under an infinite large SNR.

For strongly convex cases, the non-convergence property of AIRFEDMODEL is reflected in the non-diminishing optimality gap. However, for non-convex DNNs and CNNs, highly precise model parameter is required in the training process, which means the training loss of AIRFEDMODEL may diverge after only a few communication rounds.

In fact, there are few works considering transmitting local model parameter via AirComp [22], [50], [56], [59]. We believe that AIRFEDMODEL is not an appropriate choice for the aforementioned reasons. We will verify our findings in Section VII.

VI. DISCUSSIONS

In this section, we further extend the analysis of AIRFEDAVG-M and AIRFEDAVG-S with unbiased MAE to the biased MAE cases for practical implementations. Other extensions are also discussed.

A. Signal Processing Schemes

In Section III, we adopt channel inversion (17) with denoising factor (29) for signal pre-processing and post-processing. However, there are also efforts that consider other signal pre-processing and post-processing methods and precoding (denoising) factors to improve the communication efficiency.

1) *Normalization Methods*: To facilitate power control, the transmitted symbols can be normalized to have zero mean and unit variance. The normalization and de-normalization procedure is summarized in [22]. This signal pre-processing scheme facilitates the MSE minimization problem considered in [28], [37], [55].

2) *Multi-antenna Scenarios*: In order to make full use of the spatial multiplexing, effectively resist the influence of multipath fading, and improve communication quality, multi-antenna technology has been widely applied. Although our work mainly focuses on the single-input-single-output (SISO) scenario, it can also be extended to the single-input-multiple-output (SIMO), multiple-input-single-output (MISO), and multiple-input-multiple-output (MIMO) scenarios for AirFL [114]. For each time slot, the estimated signal can be generalized as

$$y := \frac{1}{\sqrt{\beta}} \sum_{n=1}^N b_n p_n z_n + \frac{1}{\sqrt{\beta}} w. \quad (47)$$

With N_t antennas at edge devices and N_r antennas at the edge server for SIMO, MISO and MIMO systems, the settings of P_n and w are shown in Table IV, where $\mathbf{m} \in \mathbb{C}^{N_r}$ denotes the receive beamforming vector. Then, a uniform-forcing based precoder can be designed based on Table IV [115].

TABLE IV
PARAMETER SETTINGS FOR TRANSCIEVERS WITH DIFFERENT NUMBER
OF ANTENNAS

Scenario \ Value	SISO	MISO	SIMO	MIMO
b_n	$h_n \alpha_n$	$\mathbf{h}_n^T \alpha_n$	$\mathbf{m}^H \mathbf{h}_n \alpha_n$	$\mathbf{m}^H \mathbf{H}_n \alpha_n$
w	w	w	$\mathbf{m}^H \mathbf{w}$	$\mathbf{m}^H \mathbf{w}$

For instance, for the SIMO scenario, the precoding factor can be set as

$$\alpha_n = \sqrt{\beta} \frac{(\mathbf{m}^H \mathbf{h}_n)^H}{\|\mathbf{m}^H \mathbf{h}_n\|_2^2}, \quad (48)$$

where the denoising factor is set based on the case study in the previous sections

$$\beta := \min_{n \in \mathcal{N}} \frac{P_0 \|\mathbf{m}^H \mathbf{h}_n\|_2^2}{|p_n z_n|^2}. \quad (49)$$

The MSE is thus given by

$$\text{MSE} := \frac{\|\mathbf{m}\|_2^2 \sigma_w^2}{\beta} = \frac{\|\mathbf{m}\|_2^2}{\text{SNR}} \max_{n \in \mathcal{N}} \frac{|p_n z_n|^2}{\|\mathbf{m}^H \mathbf{h}_n\|_2^2}. \quad (50)$$

This illustrates that our convergence analysis framework can be directly applied in multi-antenna scenarios, where the receive beamforming vector design [28] and learning rate optimization [55] by MSE minimization were considered.

3) *Compressive Sensing Scheme*: The communication overhead is enormous as the model dimensions of the DNNs and CNNs are typically high-dimensional. To reduce the dimension of the gradient information to be transmitted by the edge devices, compressive sensing was considered in [61], [66], [116]. In the following, we take AIRFEDAVG-M with compressive sensing for a case study. In particular, the sparsification procedure is given by

$$\Delta \theta_{n,t+1}^{sp} = \text{Top}_k(\Delta \theta_n^{t+1}), \quad (51)$$

where operator $\text{Top}_k(\cdot)$ sets all elements of $\Delta \theta_n^{t+1}$ to zero but the first k largest ones. Subsequently, a consensus mapping matrix \mathbf{A} is used for compression of the sparsified vector $\Delta \theta_{n,t+1}^{sp}$, i.e.,

$$\Delta \theta_{n,t+1}^{cp} = \mathbf{A} \Delta \theta_{n,t+1}^{sp}, \quad (52)$$

and the local information to be transmitted is $\mathbf{z}_n^t = \Delta \theta_{n,t+1}^{cp}$. In this case, together with the AirComp model in Section III, the estimated signal at the edge server is given by

$$\begin{aligned} \hat{\mathbf{y}}_{cp}^t &= \sum_{n=1}^N p_n \mathbf{z}_n^t + \tilde{\mathbf{w}}^t \\ &= \mathbf{A} \sum_{n=1}^N p_n \Delta \theta_{n,t+1}^{sp} + \tilde{\mathbf{w}}^t = \mathbf{A} \mathbf{x}_{sp} + \tilde{\mathbf{w}}^t. \end{aligned} \quad (53)$$

The edge server can recover the signal for model aggregation by applying the approximate message passing (AMP) algorithm [117]. In view of this, the model aggregation MSE can still be used for analyzing the impact of signal estimation error on the convergence of AirFL. Besides, quantization was also considered in [58] to further reduce communication overhead. When the channel inversion precoder of the edge devices

is imperfect due to the hardware limitation and inaccurate channel estimation along with the imperfect synchronization, the misaligned transmit scheme proposed in [71] can be adopted.

B. Unbiased and Biased MAE

As various communication schemes can be applied in AirFL, different schemes cause different forms of MAE. According to the statistical characteristics of MAE, we can divide the communication model of AirFL into the following two categories:

- **Unbiased AirFL**: The MAE is unbiased from the statistical point view, where the error satisfies

$$\text{Bias}^t := \mathbb{E}[\boldsymbol{\varepsilon}^t] = 0, \quad \text{MSE}^t := \mathbb{E}[\|\boldsymbol{\varepsilon}^t\|_2^2] \neq 0,$$

This indicates that the edge server receives an unbiased estimation of the transmitted signal;

- **Biased AirFL**: The MAE is biased with the error satisfying

$$\text{Bias}^t \neq 0, \quad \text{MSE}^t \neq 0.$$

Opposite to the unbiased case, the edge server receives a biased estimation of the transmitted signal.

We next provide evidence for the classification. With the channel inversion model in (17) and (18), it is guaranteed that the signal estimated by the edge server is only perturbed by the Gaussian noise. In other words, the MAE is given by

$$\boldsymbol{\varepsilon}^t = \tilde{\mathbf{w}}^t \sim \mathcal{N}(0, \frac{\sigma_w^2}{\beta^t} \mathbf{I}_d). \quad (54)$$

As such, by applying channel inversion to compensate for channel fading, the signal after post-processing at the edge server is an unbiased estimation of the transmitted one, which is a special case of unbiased AirFL.

Recently, only compensating for the phase of the fading channel first and then optimizing the power control scheme in AirFL was put forward and applied in [33], [47]–[49], [57], [118]. The basic idea is that the amplitude alignment among the transmitted signals of edge devices is no longer required, e.g., the precoding factor can be set as

$$\alpha_n^t := \sqrt{\beta_n^t} \frac{(h_n^t)^H}{|h_n^t|}, \quad (55)$$

where $\sqrt{\beta_n^t}$ is the power control factor. The estimated signal at the edge server is given by

$$\begin{aligned} \hat{\mathbf{y}}^t &:= \frac{\hat{\mathbf{s}}^t}{\sqrt{\beta^t}} \stackrel{(16)}{=} \frac{1}{\sqrt{\beta^t}} \sum_{n=1}^N h_n^t \alpha_n^t p_n \mathbf{z}_n^t + \tilde{\mathbf{w}}^t \\ &= \frac{1}{\sqrt{\beta^t}} \sum_{n=1}^N |h_n^t| \sqrt{\beta_n^t} p_n \mathbf{z}_n^t + \tilde{\mathbf{w}}^t. \end{aligned} \quad (56)$$

Compared with the channel inversion approach that compensates for both the amplitude and phase of the channel coefficient, this scenario only regards the magnitude of the channel coefficient as aggregation weights.

For the case without magnitude alignment, as presented in (55) and (56), the MAE is given by

$$\varepsilon^t = \sum_{n=1}^N \left(\frac{|h_n^t| \sqrt{\beta_n^t}}{\sqrt{\beta^t}} - 1 \right) p_n \mathbf{z}_n^t + \tilde{\mathbf{w}}^t. \quad (57)$$

In this case, the MAE is not guaranteed to have the zero-mean, which implies the MAE is biased. For instance, the authors in [47] designed transmit power control policies in the fading scenario to minimize the optimality gap caused by the biased MAE.

To summarize, the biasedness of the MAE depends on the transceiver design for AirFL. As the convergence analysis of unbiased MAE has been conducted in previous sections, we shall present the influence caused by the biased MAE on the model convergence in the following. In this paper, we do not compare the learning performance under biased MAE with that of unbiased MAE, but point out the dominant terms of the convergence results under biased MAE for extension.

The results for AIRFEDAVG-M under biased MAE with error ε^t are summarized in **Theorem 6** for strongly convex cases and **Theorem 7** for non-convex cases with a diminishing learning rate, respectively.

Theorem 6 (Convergence of AIRFEDAVG-M with Biased MAE under Strong Convexity). *Let Assumptions 3, 4, 5, and 6 hold. By setting the decaying learning rate as $0 < \eta^t \leq \min \left\{ \frac{1}{L\sqrt{2E(E-1)(4\beta_1+1)}}, \frac{1}{4LE} \right\}$, the upper bound on the optimality gap after T communication rounds is given by*

$$\begin{aligned} & \mathbb{E} \left[F(\hat{\theta}^T) \right] - F^* \\ & \leq \left[F(\hat{\theta}^0) - F^* \right] J^0 + C'_1 \sum_{t=0}^{T-1} (\eta^t)^3 J^{t+1} \\ & + C'_2 \sum_{t=0}^{T-1} (\eta^t)^2 J^{t+1} + \underbrace{\sum_{t=0}^{T-1} \eta^t \left(C'_3 + 2L^2 EMSE^t \right) J^{t+1}}_{(d)} \\ & + \underbrace{C'_4 \sum_{t=0}^{T-1} MSE^t J^{t+1}}_{(e)} + \underbrace{C'_5 \sum_{t=0}^{T-1} \frac{\|\text{Bias}^t\|_2^2}{\eta^t} J^{t+1}}_{(f)}, \end{aligned} \quad (58)$$

where $J^t = \prod_{i=t}^{T-1} (1 - \frac{\mu\eta^i E}{4})$, $J^T = 1$, $C'_1 = \frac{L^2 E(E-1)(4\beta_1+1)}{8\beta_1} [\bar{\sigma}^2 + 2E\beta_2]$, $C'_2 = LE\sigma^2$, $C'_3 = \frac{1}{4}\sigma^2$, $C'_4 = \frac{L}{2}$ and $C'_5 = \frac{1}{E}$.

Proof. Please refer to Appendix A-C for details. \square

Theorem 7 (Convergence of AIRFEDAVG-M with Biased MAE under Non-convexity). *With Assumptions 3, 5, and 6, if the decaying learning rate satisfies $0 < \eta^t \leq \min \left\{ \frac{1}{L\sqrt{2E(E-1)(4\beta_1+1)}}, \frac{1}{4LE} \right\}$, then the weighted average*

norm of global gradients after T communication rounds is upper bounded by

$$\begin{aligned} & \frac{1}{\Phi} \sum_{t=0}^{T-1} \eta^t \mathbb{E} \left[\left\| \nabla F(\hat{\theta}^t) \right\|_2^2 \right] \\ & \leq \frac{8 \left[F(\hat{\theta}^0) - F^{\text{inf}} \right]}{E\Phi} + \frac{8C'_1}{E\Phi} \sum_{t=0}^{T-1} (\eta^t)^3 + \frac{8C'_2}{E\Phi} \sum_{t=0}^{T-1} (\eta^t)^2 \\ & + \underbrace{\frac{8}{E\Phi} \sum_{t=0}^{T-1} \eta^t \left(C'_3 + 2L^2 EMSE^t \right)}_{(d)} + \underbrace{\frac{8C'_4}{E\Phi} \sum_{t=0}^{T-1} MSE^t}_{(e)} \\ & + \underbrace{\frac{8C'_5}{E\Phi} \sum_{t=0}^{T-1} \frac{\|\text{Bias}^t\|_2^2}{\eta^t}}_{(f)}. \end{aligned} \quad (59)$$

Proof. Please refer to Appendix A-C. \square

Remark 11. *Theorems 6 and 7 focus on the convergence results of the strongly convex and non-convex loss functions, respectively. We have the following key observations: term (d) is caused by gradient estimation variance and the model aggregation MSE; term (e) is caused by the model aggregation MSE; term (f) results from the biased MAE. The upper bound is a function of both the model aggregation bias and MSE.*

According to **Lemmas 1** and **2**, for any communication model with biased MAE, both the squared norm of bias, i.e., $\|\text{Bias}^t\|_2^2$, and MSE^t need to be designed or minimized to improve the model training performance of AIRFEDAVG-M for strongly convex and non-convex loss functions. One possible solution is to jointly minimize $\|\text{Bias}^t\|_2^2$ and MSE^t . Without loss of generality, the optimization problem can be established as

$$\begin{aligned} \mathcal{P}_1 : \quad & \text{minimize} \quad \lambda MSE^t + (1 - \lambda) \|\text{Bias}^t\|_2^2 \\ & \text{subject to} \quad 0 \leq \beta_n^t \leq P_n^{\text{max}}, \forall n \in \mathcal{N}, t \in [T], \end{aligned} \quad (60)$$

where P_n^{max} is the maximum transmit power for edge device n . This key observation is in line with the work in [49]. Another possible solution is to ensure these two variables satisfy the following condition with learning rate decay:

$$MSE^t \sim (\eta^t)^{\rho_1}, \quad \text{Bias}^t \sim (\eta^t)^{\rho_2}, \quad \rho_1, \rho_2 > 1. \quad (61)$$

However, this method may be difficult to be applied in practical systems.

To conclude, we mainly discuss the convergence results and intuitions for AIRFEDAVG-M with biased MAE, which are corresponding to the analysis in Section IV. In comparison, when the MAE is unbiased, the upper bound is a function of the model aggregation MSE. Otherwise it is related to both the squared norm of bias and the MSE.

Besides, the convergence results for AIRFEDAVG-S with biased MAE are summarized in **Theorem 8** for strongly convex cases and **Theorem 9** for non-convex cases, respectively.

Theorem 8 (Convergence of AIRFEDAVG-S with Biased MAE under Strong Convexity). *With Assumptions 3, 4 and*

5, if the decaying learning rate with $0 < \eta^t \leq \frac{1}{4L}$, then the upper bound on the cumulative gap after T communication rounds is given by

$$\begin{aligned} & \mathbb{E} \left[F(\hat{\theta}^T) \right] - F^* \\ & \leq \left[F(\hat{\theta}^0) - F^* \right] Q^0 + \frac{1}{2} \sum_{t=0}^{T-1} \eta^t \|\text{Bias}^t\|_2^2 Q^{t+1} \\ & \quad + \frac{L}{2} \sum_{t=0}^{T-1} (\eta^t)^2 \left[\text{MSE}^t + \|\text{Bias}^t\|_2^2 + \sigma^2 \right] Q^{t+1}. \end{aligned} \quad (62)$$

Proof. Please refer to Appendix A-C. \square

Theorem 9 (Convergence of AIRFEDAVG-S with Biased MAE under Non-convexity). *With Assumptions 3, 5, and 6, if the decaying learning rate satisfies $0 < \eta^t \leq \frac{1}{4L}$, then the weighted average norm of global gradients after T communication rounds is upper bounded by*

$$\begin{aligned} & \frac{1}{\Phi} \sum_{t=0}^{T-1} \eta^t \mathbb{E} \left[\left\| \nabla F(\hat{\theta}^t) \right\|_2^2 \right] \\ & \leq \frac{4}{\Phi} \left[F(\hat{\theta}^0) - F^{\text{inf}} \right] + \frac{2}{\Phi} \sum_{t=0}^{T-1} \eta^t \|\text{Bias}^t\|_2^2 \\ & \quad + \frac{2L}{\Phi} \sum_{t=0}^{T-1} (\eta^t)^2 \left[\text{MSE}^t + \|\text{Bias}^t\|_2^2 + \sigma^2 \right]. \end{aligned} \quad (63)$$

Proof. Please refer to Appendix A-C. \square

Combining the above two theorems, we notice that the upper bound is dominated by the square norm of bias, i.e., $\|\text{Bias}^t\|_2^2$, which converges to an error floor if $\|\text{Bias}^t\|_2^2$ is a constant. Compared to AIRFEDAVG-S with unbiased MAE, the main challenge is to minimize $\|\text{Bias}^t\|_2^2$ for achieving better training performance of AIRFEDAVG-S with biased MAE for both strongly convex and non-convex objectives. Our observation is in line with the work in [47], which focuses on AIRFEDAVG-S with biased MAE. In addition, another possible solution with learning rate decay is that

$$\text{Bias}^t \sim (\eta^t)^\rho, \quad \rho > 0. \quad (64)$$

It is clear that with biased MAE, AIRFEDAVG-S is different from AIRFEDAVG-M in the dominant term of the optimality gap for strongly convex objectives and the error bound for non-convex ones.

In a nutshell, we discuss the practical signal processing approaches and their impact on MAE in this section. Then we provide convergence results for AIRFEDAVG-M and AIRFEDAVG-S with biased MAE.

C. Extension to Other Optimization Methods

1) *Different Local Optimizers:* This paper mainly considers first-order optimization methods for local model updating, i.e., vanilla SGD. In fact, the local optimizer can be extended to other gradient-based methods, e.g., SGD with proximal gradients, momentum [94], [118]. Moreover, ideas and insights obtained in this paper can also be applied in AirFL with zeroth-order optimization [99] and second-order optimization [119], [120].

2) *Different Optimization Methods:* The aforementioned optimization methods are all primal. AirFL with Peaceman-Rachford splitting was first considered in [110], which can be classified as a primal-dual method, to address the non-optimality of AIRFEDAVG-M with a constant learning rate. By applying the similar convergence analysis approach, the illustration of bounding the MAE is given in [110, Theorem 2]. Without gradient information, it is worth investigating that whether transmitting local model parameter via AirComp leads to convergence after multiple communication rounds.

D. Extension to Other Network Architectures

1) *Decentralized Networks:* This paper considers a star-topology network consisting of a central edge server, and N distributed edge devices, where the device-to-server (D2S) communication links are dominated. To alleviate the communication overhead caused by D2S links, decentralized networks exploiting device-to-device (D2D) links with an arbitrary topology has recently attracted a lot of attention [121], e.g., decentralized (gossip) SGD [90], [91] and hybrid SGD [92]. Besides, AirFL in wireless D2D networks was studied in [29].

2) *Multi-cell Networks:* Due to the mobility of the edge devices and the rapid development in connected intelligence, the co-existence of different FL tasks in multi-cell networks will become a new paradigm in the future. [33] extends AirFL to multi-cell networks with different learning tasks for inter-cell interference management. In addition, End-Edge-Cloud hierarchical FL architecture has been proposed to exploit more data while reducing the costly communication with the cloud [122], [123]. Convergence analysis for hierarchical AirFL has been studied in [34].

3) *Other Networks:* To overcome the detrimental effect of channel fading in wireless networks, RIS has been proposed to reconfigure the propagation channels and thus support reliable model aggregation of AirFL [36]–[38], [124]. In particular, the convergence of RIS-assisted AirFL can still be covered in this tutorial, which only leads to different expressions for MSE or bias. Moreover, unlike static networks considered in this tutorial, UAV or satellite aided FL systems [125]–[129], which consider mobile edge server or edge devices, lead to new challenges in terms of communication schemes and algorithm design. There are also open problems and interesting directions for future study.

E. Extension to Partial Device Participation

This paper mainly considers the convergence of AIRFEDAVG with full device participation. However, due to the limited communication resources and the heterogeneous channel conditions, only a part of edge devices may participate in the model training. For instance, in [53], [99], [110], the authors adopted a threshold-based method as described in (20) to filter out edge devices with poor channel conditions, leading to partial device participation. The convergence of AIRFEDAVG with partial device participation is worth further study.

Partial device participation can be divided into the following three cases.

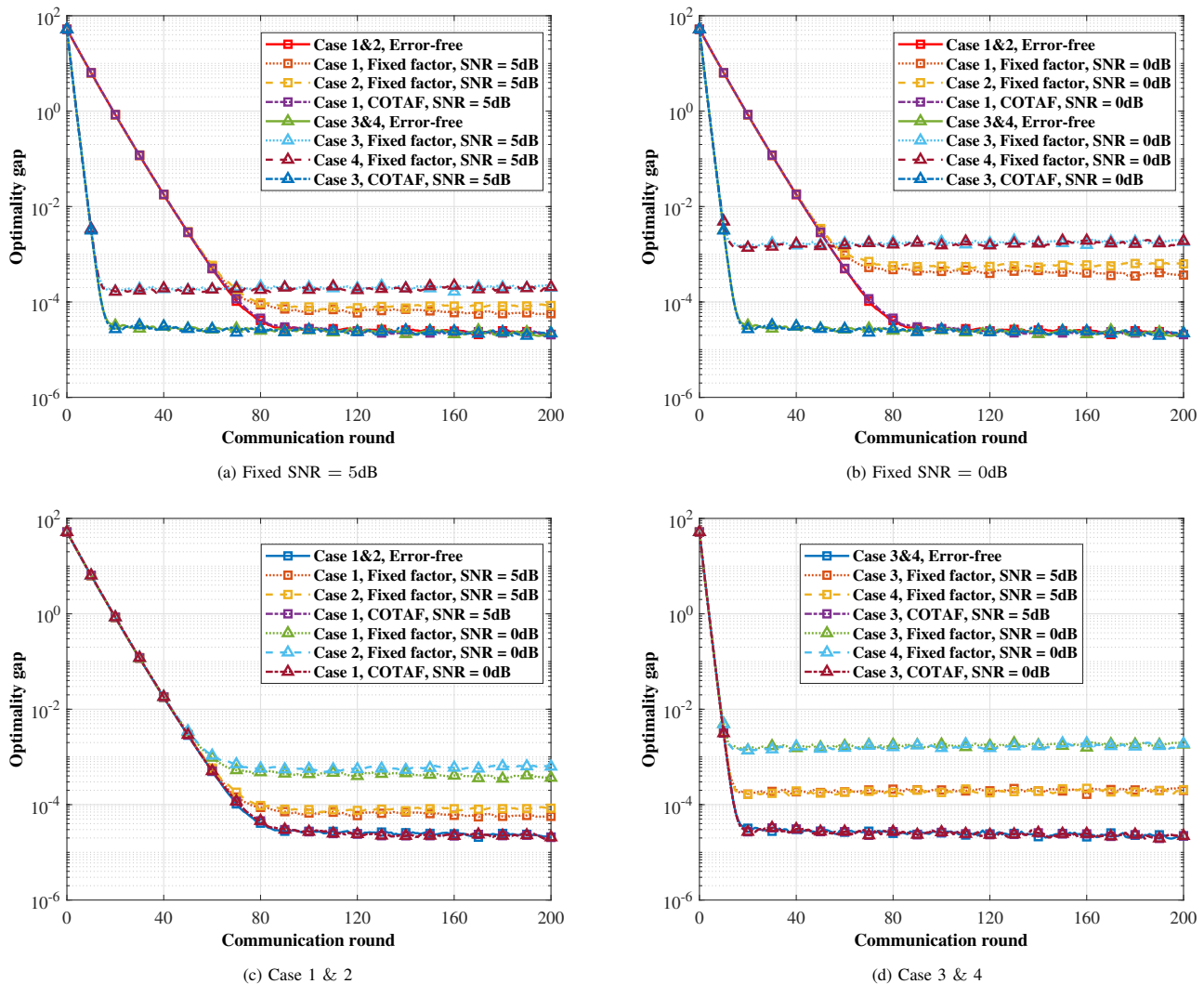


Fig. 7. Simulation results for linear regression on the synthetic dataset.

- Non-uniform sampling of edge devices. The edge server actively schedules a part of edge devices before the global model dissemination non-uniformly. Different scheduling policies based on edge devices' computation capability, channel condition, norm of local model, beamforming, or contribution can be applied to select a subset of edge devices [10]–[12], [28], [50], [130]–[132].
- Uniform sampling of edge devices. In this category, the probability of each edge device participating in the training process in each communication round is uniform [70].
- Arbitrary participation of edge devices. Edge devices participate in the model training in an arbitrary way, i.e., arriving and leaving the system without grant of edge server, which makes the convergence of FL algorithm more complicated [133]–[135].

F. Other Potential Extensions

Firstly, although AirFedModel is not convergent in low SNR scenarios from our analysis, a potential research direction is to provide convergence guarantees for this algorithm.

Secondly, while this paper considers that all edge devices perform an equal number of local updates, the heterogeneity in computation capabilities leads to variations in the number of local epochs across edge devices in each communication round. Furthermore, each edge device's number of local epochs can also vary across different communication rounds. This brings new challenges to the convergence analysis and system design of AirFL [94], [136], [137], which is an attractive extension.

Finally, data heterogeneity may severely degrade the overall learning performance [138]. To handle non-IID data, personalization is a leading approach for each edge device to train a personalized local model, which mainly consists of multi-task FL [139] and meta-learning [140]. This technique has been applied in AirFL [141]. The performance of other solutions such as [142], which introduces a proximal term to the local objectives to minimize the model divergence, also worth investigating in the presence of wireless fading channels.

VII. NUMERICAL EVALUATIONS

In this section, we evaluate the performance of AIRFEDAVG-M, AIRFEDAVG-S, and AIRFEDMODEL

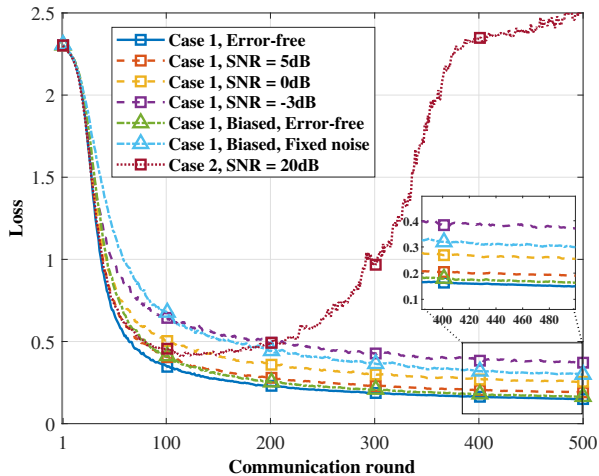
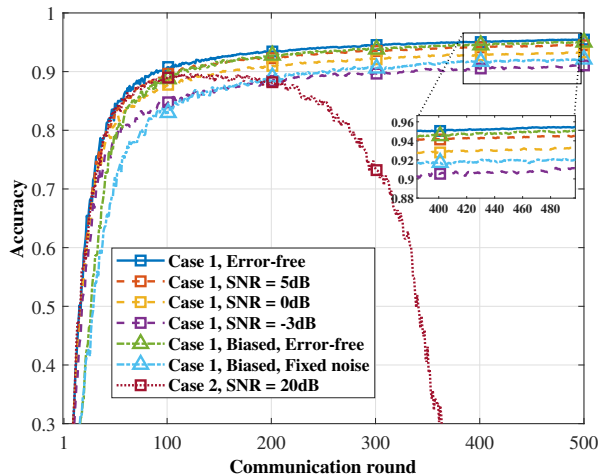
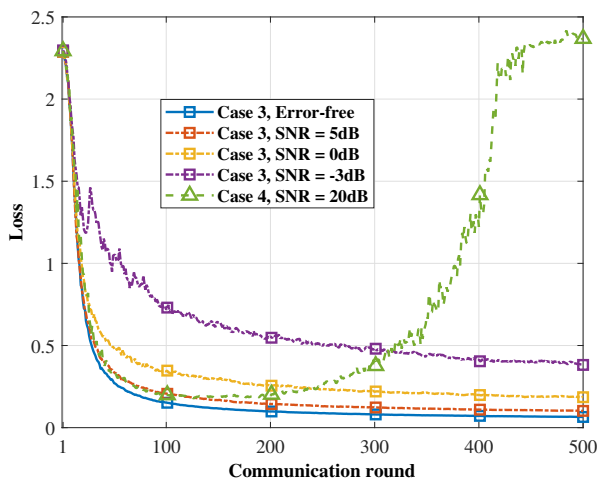
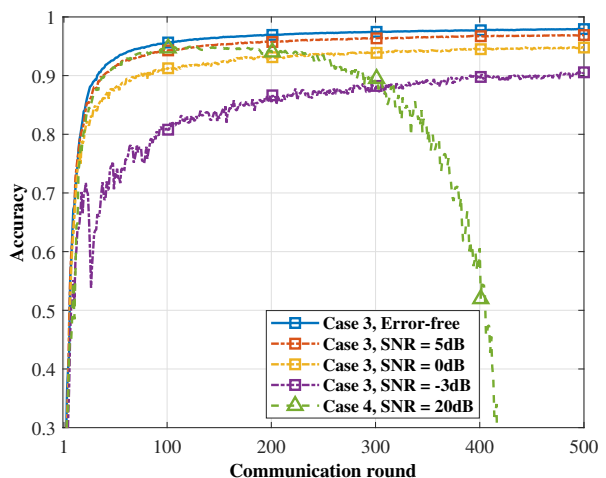
(a) Loss of AIRFEDAVG-S and AIRFEDMODEL ($E = 1$)(b) Test accuracy of AIRFEDAVG-S and AIRFEDMODEL ($E = 1$)(c) Loss of AIRFEDAVG-M and AIRFEDMODEL ($E = 5$)(d) Test accuracy of AIRFEDAVG-M and AIRFEDMODEL ($E = 5$)

Fig. 8. Simulation results for the CNN model on the MNIST dataset over AWGN channel.

with both strongly convex and non-convex loss functions. All experiments are averaged over 5 independent runs. For simplicity, we use Case 1–4 to represent AIRFEDAVG-S, AIRFEDMODEL ($E = 1$), AIRFEDAVG-M and AIRFEDMODEL ($E > 1$), respectively.

A. Strongly Convex Case: Linear Regression on Synthetic Dataset

We consider a linear regression problem for the strongly convex case on the synthetic dataset. In particular, the dataset of each edge device \mathcal{D}_n is randomly generated by

$$\mathbf{b}_n = \mathbf{A}_n \mathbf{x}_0 + v_n, \quad \forall n \in \mathcal{N}, \quad (65)$$

where $\mathbf{x}_0 \in \mathbb{R}^d$ is a random parameter with standard Gaussian distribution $\mathcal{N}(0, \mathbf{I}_d)$ and the sample-wise noise vectors are independently generated as $v_n \stackrel{i.i.d.}{\sim} \mathcal{N}(0, \sigma^2 \mathbf{I}_{D_n})$. Random matrices $\mathbf{A}_n \in \mathbb{R}^{D_n \times d}$ is generated by $(\mathbf{A}_n)_{uv} \stackrel{i.i.d.}{\sim} \mathcal{N}(0, 1)$, for all $n \in \mathcal{N}$, $u \in [D_n]$ and $v \in [d]$.

The local loss function for each edge device n is given by

$$F_n(\theta) = \frac{1}{2D_n} \|\mathbf{A}_n \theta - \mathbf{b}_n\|_2^2, \quad (66)$$

which is strongly convex.

We numerically evaluate the optimality gap $\mathbb{E}[F(\hat{\theta})] - F(\theta^*)$ with respect to $T = 200$ communication rounds in the following benchmarks in AWGN channel for comparison:

- **Error-free AIRFEDAVG-M and AIRFEDAVG-S:** Conventional FL without channel fading and noise, where the number of local updates is $E = 5$ for AIRFEDAVG-M.
- **AirFedAvg with Fixed Precoding Factor:** The precoding factor is fixed since the starting round by

$$\alpha_n^t = \frac{\sqrt{dP_0}}{\max_{n \in \mathcal{N}} \|p_n \mathbf{z}_n^0\|_2}, \quad t \in [T]. \quad (67)$$

- **AIRFEDAVG-M and AIRFEDAVG-S with Designed Precoding Factor:** The precoding factor is designed as

$$\alpha_n^t = \frac{\sqrt{dP_0}}{\max_{n \in \mathcal{N}} \|p_n \mathbf{z}_n^t\|_2}, \quad t \in [T], \quad (68)$$

which is named COTAF for abbreviation [53].

Consider there are $N = 25$ edge devices and the model with dimension $d = 100$. The size of local dataset satisfies $D_n \in [D_{\min}, D_{\max}]$ with mean $\bar{D} = 500$, where $D_{\min} = 300$ and $D_{\max} = 1200$. The local batch size is 128 and we

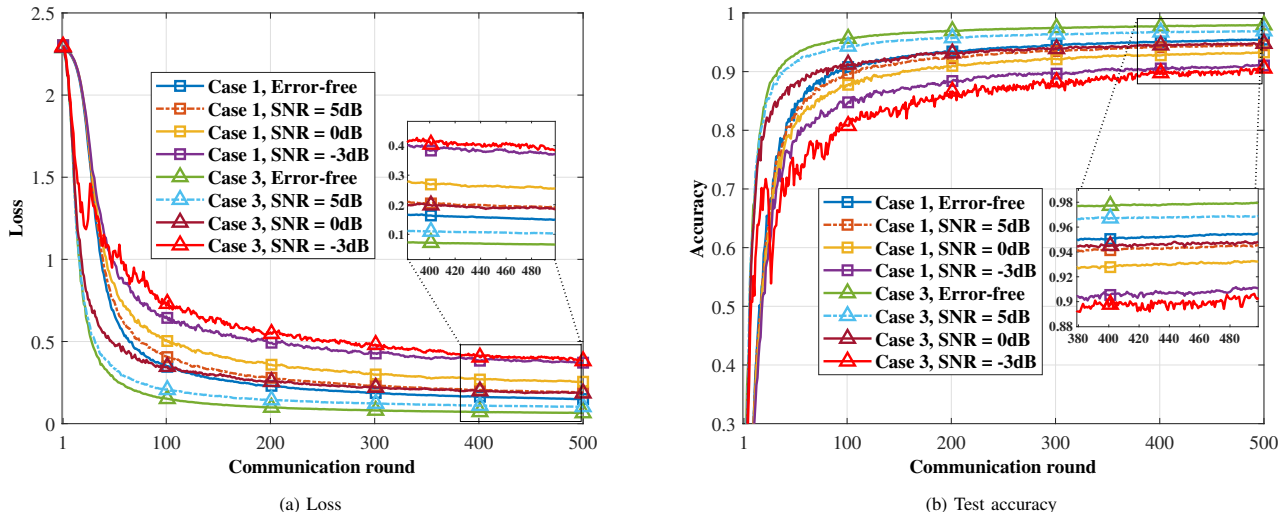


Fig. 9. Comparison of AIRFEDAVG-M and AIRFEDAVG-S for the CNN model on the MNIST dataset over AWGN channel.

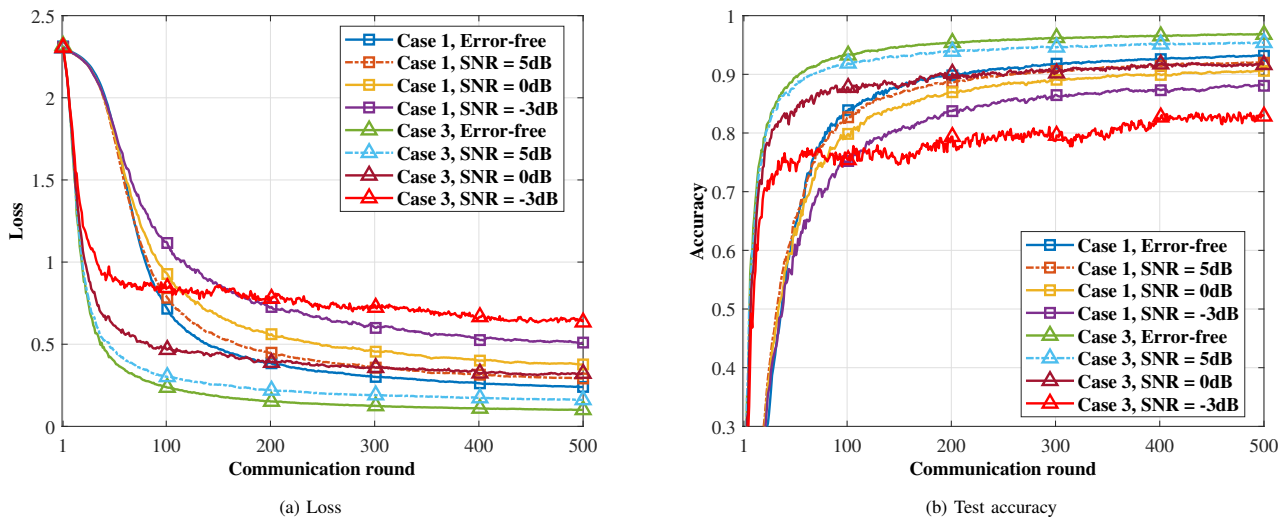


Fig. 10. Comparison of AIRFEDAVG-M and AIRFEDAVG-S for the CNN model on the MNIST dataset over Rayleigh fading channel.

evaluate the convergence performance under different SNR, where $\text{SNR} = P_0/\sigma_w^2$.

Here we set the parameters as

$$\begin{aligned} \sigma^2 &= 0.20, \quad \text{SNR} \in \{5\text{dB}, 0\text{dB}\}, \\ \eta^0 &= 0.1, \quad \eta^t = \frac{\eta^0}{1+0.002 \times t}. \end{aligned}$$

Experimental results are illustrated in Fig. 7. The observations made from Fig. 7 can be concluded as follows:

- From Figs. 7(a) and 7(b), it is clear that under fixed SNR, AIRFEDAVG-S and AIRFEDAVG-M with COTAF precoder have the same performance as the error-free setting.
- For fixed SNR and fixed precoding factor, the performance is worse compared with designed COTAF precoder for all cases. Meanwhile, AIRFEDAVG-S has a smaller optimality gap than AIRFEDMODEL and AIRFEDAVG-M, which is in line with our analysis in **Remark 8** that the AIRFEDAVG-S is less sensitive to the model aggregation MSE, i.e., the denoising factor design and AIRFEDAVG-M is on the contrary.

- From Figs. 7(c) and 7(d), it is obvious that the lower the SNR is, the bigger the optimality gap for all cases but COTAF, which means this precoding scheme is more robust to noisy channel and is capable of eliminating the impact of receiver noise through the training process.
- Subsequently, AIRFEDAVG-M converges faster with $E = 5$ local updates than AIRFEDAVG-S to achieve linear speedup for fewer communication rounds as analyzed in **Remark 10**.

B. Non-Convex Case I: CNN on MNIST Dataset

Next we validate our theorems and remarks by considering handwritten digits classification on the MNIST dataset [143], which consists of 60,000 training images and 10,000 images for testing with 28×28 pixels of 10 digits. The training dataset is uniformly distributed over $N = 50$ edge devices. We assume non-IID data distribution, where the original training dataset is first sorted by labels, and then randomly assigned to all edge devices. Each edge device can access only two sorts of labels.

For the learning model, we consider the non-convex CNN model, which has two 5×5 convolution layers, a full connected

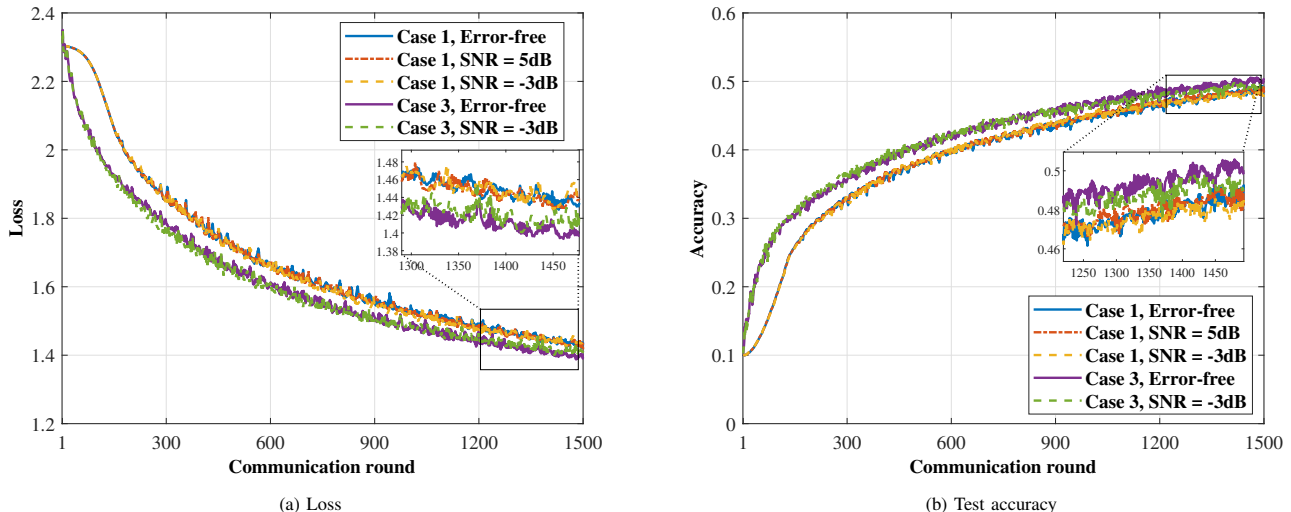


Fig. 11. Comparison of AIRFEDAVG-M and AIRFEDAVG-S for the CNN model on the CIFAR-10 dataset over Rayleigh fading channel.

layers with 320 units and ReLU activation, and a final output layer with softmax. The first convolution layer has 10 channels and the second one has 20 channels, which are both followed by ReLU activation and 2×2 max pooling. The total number of model parameters is $d = 21840$ and the number of local updates for AIRFEDAVG is set as $E = 5$ unless specified otherwise. The local batch size is 10 and the learning rate is initially set as $\eta^0 = 0.1$ for AWGN channel and $\eta^0 = 0.05$ for Rayleigh fading channel and decays with $\eta^t = \frac{\eta^0}{1+0.005 \times t}$ in each communication round and the SNR is selected from the set $\{-3\text{dB}, 0\text{dB}, 5\text{dB}\}$. We run the experiments on PyTorch version 1.10.2 with python version 3.6.

We consider the loss and test accuracy over $T = 500$ communication rounds of the following benchmarks for comparison:

- **Error-free AIRFEDAVG-M and AIRFEDAVG-S:** Conventional FL without channel fading and noise.
- **AIRFEDAVG-M and AIRFEDAVG-S with Designed Precoding Factor:** The precoding factor is described in (68) in AWGN channel and (29) for Rayleigh fading channel.
- **AIRFEDMODEL over High SNR with Designed Precoding Factor:** For AWGN channel, the SNR is set to be up to 20dB to verify the divergence of Case 2 and 4.
- **Biased MAE for AIRFEDAVG-S:** The power control policy proposed in [47] for gradient transmission with noise power $\sigma_w^2 = 0.01$ for fixed noise case and $\sigma_w^2 = 0$ for error-free case.

TABLE V
HIGHEST ACHIEVABLE TEST ACCURACY FOR AWGN CHANNEL

MAE	Scheme	Case 1	Case 3 ($E=5$)	Case 3 ($E=10$)
Unbiased	Error-free	95.5%	98.0%	98.5%
	SNR = 5dB	94.5%	96.9%	97.6%
	SNR = 0dB	93.3%	94.9%	96.2%
	SNR = -3dB	91.1%	94.4%	94.7%
Biased	Error-free	95.1%	—	—
	Fixed Noise	92.1%	—	—

Experimental results are illustrated in Figs. 8 and 9. From

Figs. 8(a) and 8(c), it is clear that although under a high SNR, AIRFEDMODEL still cannot converge in the presence of complicated neural networks, let alone a lower SNR. A further increase in the SNR, up to 30dB, will not make it converge. This is because in neural networks, the model parameter should be highly precise, which is of very low tolerance in perturbation. However, even in very low SNR regime, the convergence of AIRFEDAVG-M and AIRFEDAVG-S is guaranteed, which confirms our earlier reasoning that transmitting local model parameter via AirComp is not a good choice. Similar to the convex case, the higher the SNR is, the better the performance of AIRFEDAVG will be for all cases. In addition, AIRFEDAVG-M converges faster with $E = 5$ local updates than AIRFEDAVG-S to achieve linear speedup, as analyzed in **Remark 7**. But with a low SNR, using the same learning rate as AIRFEDAVG-M will degrade the learning performance. As analyzed in **Theorem 2**, the initial learning rate should be smaller. After the tuning on the learning rate, the highest achievable accuracy on non-IID MNIST dataset of different cases is summarized in Table V. From Table V, more local updates lead to better learning performance under the same precoding factor design, which may be caused by a better stationary point for the non-convex objective function, but requiring smaller learning rate. The experiments concerning AIRFEDAVG-S with biased MAE are only demonstrated for validating the convergence property. As depicted in Fig. 10, the training performance is degraded in fading channel compared with that of AWGN channel. Although channel inversion is exploited to compensate for the fading channel, it still has huge influence reflected by the precoding factor. Last but not least, with a high SNR, AIRFEDAVG-M has better performance and faster convergence speed than AIRFEDAVG-S. However, it is clear that AIRFEDAVG-S is more robust to the fading channel even in a very low SNR due to the impact mechanism of the noise discussed in **Remark 10**.

C. Non-Convex Case II: CNN on CIFAR-10 Dataset

Finally we validate our theorems and remarks by considering image classification on the CIFAR-10 dataset [144], which

consists of 50,000 training images and 10,000 images for testing with $32 \times 32 \times 3 = 3072$ features. The training dataset is uniformly distributed over $N = 50$ edge devices. We consider non-IID data distribution, where the original training dataset is first sorted by labels, and then randomly assigned to all edge devices. Specially, the situation of extreme non-IID data is considered in this experiments, where each edge device can access only one shard of label.

For the learning model, we consider the non-convex CNN model and the architecture of this model is listed in the following table. The total number of model parameters is $d = 62006$ and the number of local updates for AIRFEDAVG is set as $E = 5$ unless specified otherwise. The local batch size is 50 and the learning rate is initially set as $\eta^0 = 0.05$ and decays with $\eta^t = \frac{\eta^0}{1+0.001 \times t}$ in each communication round and the SNR is selected from the set $\{-3\text{dB}, 5\text{dB}\}$.

TABLE VI
CNN ARCHITECTURE FOR CIFAR-10

Layer Type	Size
Convolution + ReLU	$5 \times 5 \times 6$
Max Pooling	2×2
Convolution + ReLU	$5 \times 5 \times 16$
Max Pooling	2×2
Fully Connected + ReLU	400×120
Fully Connected + ReLU	120×84
Fully Connected	84×10

We consider the loss and test accuracy over $T = 1500$ communication rounds. Experimental results are illustrated in Fig. 11. For extreme non-IID case of CIFAR-10 dataset, where each edge device can only access one category of data, the model aggregation MSE is not dominant any more, but the non-IID data degrading the learning performance. In this case, as analyzed in **Remark 9**, AIRFEDAVG-M suffers from highly non-IID data, and the linear speedup advantage over AIRFEDAVG-S is no longer obvious. In addition, greater receiver noise for model aggregation may have the potential to help the vanilla SGD method escape from saddle points [145], [146].

VIII. CONCLUDING REMARKS

In this tutorial, we investigated the first-order optimization algorithm AIRFEDAVG, where MAE is introduced in each communication round due to the receiver noise. We first adopted channel inversion scheme, and provided convergence analysis for AIRFEDAVG-M algorithm and obtained the results for strongly convex objectives and non-convex ones with diminishing learning rate. Based on these results, we provided mathematical convergence guarantees for the optimality gap of the strongly convex case and the error bound of the non-convex case, and derived the convergence rate for both cases. We further extended the algorithm to AIRFEDAVG-S and AIRFEDMODEL. Last but not least, we discussed the communication schemes in AirFL for practical implementations and extended our analysis to biased MAE. Our simulations were consistent with the theoretical analysis for the impact of noise and non-IID data, and convergence rate.

Several insightful conclusions can be obtained as follows.

- Firstly, the convergence of the optimality gap of AIRFEDAVG-M in the strongly convex case and error bound in the non-convex case hinge on the model aggregation MSE, which is dominated by the noise power and denoising factor. In addition, the MSE should satisfy a certain condition to guarantee the convergence. For strongly convex objective function, the convergence rate of AIRFEDAVG-M is $\mathcal{O}\left(\frac{1}{NET}\right)$ with diminishing learning rate while that of non-convex case is $\mathcal{O}\left(\frac{1}{\sqrt{NET}}\right)$ with designed constant learning rate, which achieves linear speedup in terms of the number of local updates and the number of edge devices.
- Secondly, it may not be a good choice to transmit local model in AIRFEDMODEL, which may cause divergence of the algorithm unless the MSE approaches to zero.
- Thirdly, the convergence of the optimality gap of AIRFEDAVG-S in strongly convex case and error bound in non-convex hinge on the model aggregation MSE as well, but the requirements on the MSE is not stringent. Under the same precoding and denoising factor design as AIRFEDAVG-M, AIRFEDAVG-S witnesses convergence rate $\mathcal{O}\left(\frac{1}{NT}\right)$ in strongly convex case and $\mathcal{O}\left(\frac{1}{\sqrt{NT}}\right)$ in non-convex case, respectively.
- In terms of the comparison between AIRFEDAVG-M and AIRFEDAVG-S, AIRFEDAVG-M converges faster and is more communication-efficient, but is more sensitive to the receiver noise and non-IID data. At the cost of convergence speed, AIRFEDAVG-S is observed to be more robust to receiver noise. There is an interesting trade-off between convergence rate and algorithm robustness. Besides, the consensus for AIRFEDAVG-M and AIRFEDAVG-S is that the lower SNR it is, the worse the learning performance will be.
- In the end, when the MAE is biased, the convergence bound is dominated by both MSE and the squared norm of bias for AIRFEDAVG-M, and the squared norm of bias for AIRFEDAVG-S.

There are many open directions to extend this tutorial. For instance, different federated optimization algorithms and network architectures can be applied in AirFL for further analysis. More practical scenarios such as multi-antennas system, RIS and UAV assisted AirFL, and FL over satellite networks are promising directions to be investigated.

APPENDIX A

CONVERGENCE ANALYSIS FOR MAE IN AIRFEDAVG-M

This section summarizes the method of convergence analysis for MAE in AIRFEDAVG-M. In terms of perturbation in GD and SGD algorithms, [147] is served as a guidance to this paper

A. Preliminaries

We denote $\mathbf{d}_n^t = \frac{1}{E} \sum_{e=0}^{E-1} \mathbf{g}_n^{(t,e)}$ and $\mathbf{h}_n^t = \frac{1}{E} \sum_{e=0}^{E-1} \nabla F_n(\boldsymbol{\theta}_n^{(t,e)})$. It is clear that $\mathbb{E}[\mathbf{d}_n^t - \mathbf{h}_n^t] = 0, \forall n$ and $\mathbb{E}[\langle \mathbf{d}_i^t - \mathbf{h}_i^t, \mathbf{d}_j^t - \mathbf{h}_j^t \rangle] = 0, \forall i \neq j$.

Lemma 3. Suppose $\{A_k\}_{k=1}^T$ is a sequence of random matrices and $\mathbb{E}[A_k | A_{k-1}, A_{k-2}, \dots, A_1] = \mathbf{0}, \forall k$. Then we have

$$\mathbb{E} \left[\left\| \sum_{k=1}^T A_k \right\|_F^2 \right] = \sum_{k=1}^T \mathbb{E} \left[\|A_k\|_F^2 \right]. \quad (69)$$

Lemma 4. Let **Assumption 5** hold and we have

$$\mathbb{E} \left[\left\| \sum_{n=1}^N p_n \mathbf{d}_n^t \right\|_2^2 \right] \leq \frac{2}{E} \sum_{n=1}^N p_n^2 \sigma_n^2 + 2\mathbb{E} \left[\left\| \sum_{n=1}^N p_n \mathbf{h}_n^t \right\|_2^2 \right]. \quad (70)$$

Proof. By applying the fact that $\|\mathbf{a} + \mathbf{b}\|_2^2 \leq 2\|\mathbf{a}\|_2^2 + 2\|\mathbf{b}\|_2^2$, we have

$$\begin{aligned} & \mathbb{E} \left[\left\| \sum_{n=1}^N p_n \mathbf{d}_n^t \right\|_2^2 \right] \\ & \leq 2\mathbb{E} \left[\left\| \sum_{n=1}^N p_n (\mathbf{d}_n^t - \mathbf{h}_n^t) \right\|_2^2 \right] + 2\mathbb{E} \left[\left\| \sum_{n=1}^N p_n \mathbf{h}_n^t \right\|_2^2 \right] \\ & = 2 \sum_{n=1}^N p_n^2 \mathbb{E} \left[\|\mathbf{d}_n^t - \mathbf{h}_n^t\|_2^2 \right] + 2\mathbb{E} \left[\left\| \sum_{n=1}^N p_n \mathbf{h}_n^t \right\|_2^2 \right] \\ & = \frac{2}{E^2} \sum_{n=1}^N p_n^2 \sum_{e=0}^{E-1} \mathbb{E} \left[\left\| \mathbf{g}_n^{(t,e)} - \nabla F_n(\boldsymbol{\theta}_n^{(t,e)}) \right\|_2^2 \right] \\ & \quad + 2\mathbb{E} \left[\left\| \sum_{n=1}^N p_n \mathbf{h}_n^t \right\|_2^2 \right] \\ & \leq \frac{2}{E} \sum_{n=1}^N p_n^2 \sigma_n^2 + 2\mathbb{E} \left[\left\| \sum_{n=1}^N p_n \mathbf{h}_n^t \right\|_2^2 \right]. \quad (71) \end{aligned}$$

where the second equality follows from **Lemma 3**, and the last inequality holds by **Assumption 5**. \square

By applying **Assumption 3** for global loss function, we obtain

$$\begin{aligned} F(\hat{\boldsymbol{\theta}}^{t+1}) - F(\hat{\boldsymbol{\theta}}^t) & \leq \left\langle \boldsymbol{\varepsilon}^t - \eta^t E \sum_{n=1}^N p_n \mathbf{d}_n^t, \nabla F(\hat{\boldsymbol{\theta}}^t) \right\rangle \\ & \quad + \frac{L}{2} \left\| \boldsymbol{\varepsilon}^t - \eta^t E \sum_{n=1}^N p_n \mathbf{d}_n^t \right\|_2^2. \quad (72) \end{aligned}$$

Taking an expectation on the mini-batch stochastic gradient for both sides of (72), we obtain

$$\begin{aligned} & \mathbb{E} \left[F(\hat{\boldsymbol{\theta}}^{t+1}) - F(\hat{\boldsymbol{\theta}}^t) \right] \\ & \leq \mathbb{E} \left[\left\langle \boldsymbol{\varepsilon}^t - \eta^t E \sum_{n=1}^N p_n \mathbf{d}_n^t, \nabla F(\hat{\boldsymbol{\theta}}^t) \right\rangle \right] \\ & \quad + \frac{L}{2} \mathbb{E} \left[\left\| \boldsymbol{\varepsilon}^t - \eta^t E \sum_{n=1}^N p_n \mathbf{d}_n^t \right\|_2^2 \right] \\ & = \left[\nabla F(\hat{\boldsymbol{\theta}}^t) \right]^\top \mathbb{E} [\boldsymbol{\varepsilon}^t] - E\eta^t \left[\nabla F(\hat{\boldsymbol{\theta}}^t) \right]^\top \mathbb{E} \left[\sum_{n=1}^N p_n \mathbf{d}_n^t \right] \end{aligned}$$

$$\begin{aligned} & + \frac{L}{2} \mathbb{E} \left[\|\boldsymbol{\varepsilon}^t\|_2^2 \right] + \frac{L(\eta^t)^2 E^2}{2} \mathbb{E} \left[\left\| \sum_{n=1}^N p_n \mathbf{d}_n^t \right\|_2^2 \right] \\ & - L\eta^t E \mathbb{E} \left[(\boldsymbol{\varepsilon}^t)^\top \sum_{n=1}^N p_n \mathbf{d}_n^t \right]. \quad (73) \end{aligned}$$

B. Unbiased MAE

Obviously we have $\mathbb{E}[\boldsymbol{\varepsilon}^t] = 0$. We suppose $\mathbb{E}[\|\boldsymbol{\varepsilon}^t\|_2^2] = \frac{\sigma_w^2}{\beta^t} \neq 0$, then (73) can be reformulated as

$$\begin{aligned} & \mathbb{E} \left[F(\hat{\boldsymbol{\theta}}^{t+1}) - F(\hat{\boldsymbol{\theta}}^t) \right] \\ & = -\frac{\eta^t E}{2} \|\nabla F(\hat{\boldsymbol{\theta}}^t)\|_2^2 - \frac{\eta^t E}{2} \mathbb{E} \left[\left\| \sum_{n=1}^N p_n \mathbf{h}_n^t \right\|_2^2 \right] \\ & \quad + \frac{\eta^t E}{2} \mathbb{E} \left[\left\| \sum_{n=1}^N p_n \mathbf{h}_n^t - \nabla F(\hat{\boldsymbol{\theta}}^t) \right\|_2^2 \right] \\ & \quad + \frac{L(\eta^t)^2 E^2}{2} \mathbb{E} \left[\left\| \sum_{n=1}^N p_n \mathbf{d}_n^t \right\|_2^2 \right] + \frac{L}{2} \frac{\sigma_w^2}{\beta^t}, \quad (74) \end{aligned}$$

where the equality holds for the fact that $\mathbb{E}[\mathbf{d}_n^t - \mathbf{h}_n^t] = 0, \forall n$, and that $2\langle \mathbf{a}, \mathbf{b} \rangle = \|\mathbf{a}\|_2^2 + \|\mathbf{b}\|_2^2 - \|\mathbf{a} - \mathbf{b}\|_2^2$.

Using **Lemma 4**, we have

$$\begin{aligned} & \mathbb{E} \left[F(\hat{\boldsymbol{\theta}}^{t+1}) - F(\hat{\boldsymbol{\theta}}^t) \right] \\ & \leq -\frac{\eta^t E}{2} \|\nabla F(\hat{\boldsymbol{\theta}}^t)\|_2^2 \\ & \quad + \frac{\eta^t E}{2} (2\eta^t E L - 1) \mathbb{E} \left[\left\| \sum_{n=1}^N p_n \mathbf{h}_n^t \right\|_2^2 \right] + \frac{L}{2} \frac{\sigma_w^2}{\beta^t} \\ & \quad + \frac{\eta^t E}{2} \mathbb{E} \left[\left\| \sum_{n=1}^N p_n \mathbf{h}_n^t - \nabla F(\hat{\boldsymbol{\theta}}^t) \right\|_2^2 \right] + (\eta^t)^2 L E \sum_{n=1}^N p_n^2 \sigma_n^2 \\ & \leq -\frac{\eta^t E}{2} \|\nabla F(\hat{\boldsymbol{\theta}}^t)\|_2^2 + (\eta^t)^2 L E \sum_{n=1}^N p_n^2 \sigma_n^2 + \frac{L}{2} \frac{\sigma_w^2}{\beta^t} \\ & \quad + \frac{\eta^t E}{2} \underbrace{\mathbb{E} \left[\left\| \sum_{n=1}^N p_n \mathbf{h}_n^t - \nabla F(\hat{\boldsymbol{\theta}}^t) \right\|_2^2 \right]}_{T_1}, \quad (75) \end{aligned}$$

where the second inequality holds by $\eta^t \leq \frac{1}{2LE}$.

To give an upper bound of T_1 , since $\hat{\boldsymbol{\theta}}_n^{(t,0)} = \hat{\boldsymbol{\theta}}^t$, we have

$$\begin{aligned} T_1 & = \mathbb{E} \left[\left\| \sum_{n=1}^N p_n \left[\mathbf{h}_n^t - \nabla F_n(\hat{\boldsymbol{\theta}}_n^{(t,0)}) \right] \right\|_2^2 \right] \\ & \leq \sum_{n=1}^N p_n \mathbb{E} \left[\left\| \mathbf{h}_n^t - \nabla F_n(\hat{\boldsymbol{\theta}}_n^{(t,0)}) \right\|_2^2 \right] \\ & = \sum_{n=1}^N p_n \mathbb{E} \left[\left\| \nabla F_n(\hat{\boldsymbol{\theta}}_n^{(t,0)}) - \frac{1}{E} \sum_{e=0}^{E-1} \nabla F_n(\hat{\boldsymbol{\theta}}_n^{(t,e)}) \right\|_2^2 \right] \\ & = \sum_{n=1}^N p_n \mathbb{E} \left[\left\| \frac{1}{E} \sum_{e=0}^{E-1} \left[\nabla F_n(\hat{\boldsymbol{\theta}}_n^{(t,0)}) - \nabla F_n(\hat{\boldsymbol{\theta}}_n^{(t,e)}) \right] \right\|_2^2 \right] \end{aligned}$$

$$\begin{aligned}
&\leq \frac{1}{E} \sum_{n=1}^N p_n \sum_{e=0}^{E-1} \mathbb{E} \left[\left\| \nabla F_n(\hat{\theta}_n^{(t,0)}) - \nabla F_n(\hat{\theta}_n^{(t,e)}) \right\|_2^2 \right] \\
&\leq \sum_{n=1}^N p_n \underbrace{\left\{ \frac{L^2}{E} \sum_{e=0}^{E-1} \mathbb{E} \left[\left\| \hat{\theta}_n^{(t,0)} - \hat{\theta}_n^{(t,e)} \right\|_2^2 \right] \right\}}_{T_2}, \quad (76)
\end{aligned}$$

where the first and the second inequality holds by Jensen's Inequality, which is $\left\| \sum_{n=1}^N p_n \mathbf{x}_n \right\|_2^2 \leq \sum_{n=1}^N p_n \|\mathbf{x}_n\|_2^2$, while the last inequality follows **Assumption 3**.

Next, we give an upper bound of the term T_2 . From (13) and the fact that $\|\mathbf{a} + \mathbf{b}\|_2^2 \leq 2\|\mathbf{a}\|_2^2 + 2\|\mathbf{b}\|_2^2$, we have

$$\begin{aligned}
T_2 &= (\eta^t)^2 \mathbb{E} \left[\left\| \sum_{k=0}^{e-1} \mathbf{g}_n^{(t,k)} \right\|_2^2 \right] \\
&\leq 2(\eta^t)^2 \mathbb{E} \left[\left\| \sum_{k=0}^{e-1} \left[\mathbf{g}_n^{(t,k)} - \nabla F_n(\hat{\theta}_n^{(t,k)}) \right] \right\|_2^2 \right] \\
&\quad + 2(\eta^t)^2 \mathbb{E} \left[\left\| \sum_{k=0}^{e-1} \nabla F_n(\hat{\theta}_n^{(t,k)}) \right\|_2^2 \right] \\
&= 2(\eta^t)^2 \sum_{k=0}^{e-1} \mathbb{E} \left[\left\| \mathbf{g}_n^{(t,k)} - \nabla F_n(\hat{\theta}_n^{(t,k)}) \right\|_2^2 \right] \\
&\quad + 2(\eta^t)^2 \mathbb{E} \left[\left\| \sum_{k=0}^{e-1} \nabla F_n(\hat{\theta}_n^{(t,k)}) \right\|_2^2 \right] \\
&\leq 2e\sigma_n^2(\eta^t)^2 + 2(\eta^t)^2 e \sum_{k=0}^{e-1} \mathbb{E} \left[\left\| \nabla F_n(\hat{\theta}_n^{(t,k)}) \right\|_2^2 \right] \\
&\leq 2e\sigma_n^2(\eta^t)^2 \\
&\quad + 2(\eta^t)^2 e \sum_{k=0}^{E-1} \left\{ 2\mathbb{E} \left[\left\| \nabla F_n(\hat{\theta}_n^{(t,k)}) - \nabla F_n(\hat{\theta}_n^{(t,0)}) \right\|_2^2 \right] \right. \\
&\quad \left. + 2\mathbb{E} \left[\left\| \nabla F_n(\hat{\theta}_n^{(t,0)}) \right\|_2^2 \right] \right\} \\
&\leq 2e\sigma_n^2(\eta^t)^2 + 4(\eta^t)^2 e \sum_{k=0}^{E-1} \left\{ L^2 \mathbb{E} \left[\left\| \hat{\theta}_n^{(t,k)} - \hat{\theta}_n^{(t,0)} \right\|_2^2 \right] \right. \\
&\quad \left. + \mathbb{E} \left[\left\| \nabla F_n(\hat{\theta}_n^{(t,0)}) \right\|_2^2 \right] \right\}, \quad (77)
\end{aligned}$$

where the second inequality follows Jensen's Inequality and **Assumption 5**, and the last inequality holds by **Assumption 3**. In this case, we have

$$\begin{aligned}
\frac{L^2}{E} \sum_{e=0}^{E-1} T_2 &\leq \frac{L^2}{E} \sum_{e=0}^{E-1} 2e\sigma_n^2(\eta^t)^2 \\
&\quad + \frac{L^2}{E} \sum_{e=0}^{E-1} 4(\eta^t)^2 e \sum_{k=0}^{E-1} \left\{ L^2 \mathbb{E} \left[\left\| \hat{\theta}_n^{(t,k)} - \hat{\theta}_n^{(t,0)} \right\|_2^2 \right] \right. \\
&\quad \left. + \mathbb{E} \left[\left\| \nabla F_n(\hat{\theta}_n^{(t,0)}) \right\|_2^2 \right] \right\} \\
&\leq L^2 \sigma_n^2 (\eta^t)^2 (E-1) + H^t \frac{L^2}{E} \sum_{e=0}^{E-1} T_2
\end{aligned}$$

$$+ H^t \mathbb{E} \left[\left\| \nabla F_n(\hat{\theta}_n^{(t,0)}) \right\|_2^2 \right], \quad (78)$$

where $H^t = 2L^2(\eta^t)^2 E(E-1) < \frac{E-1}{2E} < 1$. After rearranging, we obtain

$$\frac{L^2}{E} \sum_{e=0}^{E-1} T_2 \leq \frac{L^2 \sigma_n^2 (\eta^t)^2 (E-1)}{1-H^t} + \frac{H^t \mathbb{E} \left[\left\| \nabla F_n(\hat{\theta}_n^{(t,0)}) \right\|_2^2 \right]}{1-H^t}. \quad (79)$$

By substituting (79) into (76), we have

$$\begin{aligned}
T_1 &\leq \sum_{n=1}^N p_n \frac{L^2 \sigma_n^2 (\eta^t)^2 (E-1)}{1-H^t} \\
&\quad + \frac{H^t}{1-H^t} \sum_{n=1}^N p_n \mathbb{E} \left[\left\| \nabla F_n(\hat{\theta}_n^{(t,0)}) \right\|_2^2 \right] \\
&\leq \frac{L^2 (\eta^t)^2 (E-1)}{1-H^t} \sum_{n=1}^N p_n \sigma_n^2 \\
&\quad + \frac{H^t}{1-H^t} \left[\beta_1 \left\| \nabla F(\hat{\theta}^t) \right\|_2^2 + \beta_2 \right]. \quad (80)
\end{aligned}$$

By substituting (80) into (75), we have

$$\begin{aligned}
&\mathbb{E} \left[F(\hat{\theta}^{t+1}) - F(\hat{\theta}^t) \right] \\
&\leq -\frac{\eta^t E}{2} \left(1 - \frac{H^t \beta_1}{1-H^t} \right) \left\| \nabla F(\hat{\theta}^t) \right\|_2^2 \\
&\quad + \frac{(\eta^t)^3 L^2 E (E-1)}{2(1-H^t)} \sum_{n=1}^N p_n \sigma_n^2 + (\eta^t)^2 L E \sum_{n=1}^N p_n^2 \sigma_n^2 \\
&\quad + \frac{\eta^t H^t E \beta_2}{2(1-H^t)} + \frac{L \sigma_w^2}{2 \beta^t}. \quad (81)
\end{aligned}$$

If $H^t \leq \frac{1}{2\beta_1+1}$, then it follows that $1 - \frac{H^t \beta_1}{1-H^t} \geq \frac{1}{2}$, which requires $\eta^t \leq \frac{1}{L\sqrt{2E(E-1)(2\beta_1+1)}}$. Then (81) can be simplified as

$$\begin{aligned}
&\mathbb{E} \left[F(\hat{\theta}^{t+1}) - F(\hat{\theta}^t) \right] \\
&\leq -\frac{\eta^t E}{4} \mathbb{E} \left[\left\| \nabla F(\hat{\theta}^t) \right\|_2^2 \right] + (\eta^t)^3 C_1 + (\eta^t)^2 C_2 + \frac{C_3}{\beta^t}, \quad (82)
\end{aligned}$$

where $C_1 = \frac{L^2 E (E-1) (2\beta_1+1)}{4\beta_1} \left[\sum_{n=1}^N p_n \sigma_n^2 + 2E\beta_2 \right]$, $C_2 = L E \sum_{n=1}^N p_n^2 \sigma_n^2$, and $C_3 = \frac{L}{2} \sigma_w^2$.

1) *Strongly Convex Case:* When **Assumption 4** holds, i.e., the strongly convex case, we have the following results:

$$\begin{aligned}
&\mathbb{E} \left[F(\hat{\theta}^{t+1}) - F(\hat{\theta}^t) \right] \\
&\leq -\frac{\mu \eta^t E}{2} \mathbb{E} \left[F(\hat{\theta}^t) - F^* \right] + (\eta^t)^3 C_1 + (\eta^t)^2 C_2 + \frac{C_3}{\beta^t}. \quad (83)
\end{aligned}$$

By rearranging (83), we obtain

$$\begin{aligned}
\mathbb{E} \left[F(\hat{\theta}^{t+1}) - F^* \right] &\leq \left(1 - \frac{\mu \eta^t E}{2} \right) \mathbb{E} \left[F(\hat{\theta}^t) - F^* \right] \\
&\quad + (\eta^t)^3 C_1 + (\eta^t)^2 C_2 + \frac{C_3}{\beta^t}. \quad (84)
\end{aligned}$$

Applying (84) recursively for t from 0 to $T - 1$, we can obtain the cumulative upper bound after T communication rounds shown as follows

$$\begin{aligned} & \mathbb{E} \left[F(\hat{\boldsymbol{\theta}}^T) \right] - F^* \\ & \leq \prod_{t=0}^{T-1} \rho^t [F(\boldsymbol{\theta}^0) - F^*] \\ & + \sum_{t=0}^{T-1} \left\{ \left[(\eta^t)^3 C_1 + (\eta^t)^2 C_2 + \frac{C_3}{\beta^t} \right] \prod_{i=t+1}^{T-1} \rho^i \right\}, \end{aligned} \quad (85)$$

where $\rho^t = 1 - \frac{\mu\eta^t E}{2} \geq 0$. At last, the constraint on the learning rate satisfies

$$\begin{aligned} 0 < \eta^t & \leq \min \left\{ \frac{1}{L\sqrt{2E(E-1)}(2\beta_1+1)}, \frac{1}{2LE}, \frac{2}{\mu E} \right\} \\ & = \min \left\{ \frac{1}{L\sqrt{2E(E-1)}(2\beta_1+1)}, \frac{1}{2LE} \right\}. \end{aligned} \quad (86)$$

2) *Non-Convex Case*: When **Assumption 4** does not hold, i.e., the non-convex case, we have the corresponding results.

By rearranging (82), we obtain

$$\begin{aligned} \eta^t \mathbb{E} \left[\left\| \nabla F(\hat{\boldsymbol{\theta}}^t) \right\|_2^2 \right] & \leq \frac{4\mathbb{E} \left[F(\hat{\boldsymbol{\theta}}^t) - F(\hat{\boldsymbol{\theta}}^{t+1}) \right]}{E} \\ & + \frac{4C_1}{E} (\eta^t)^3 + \frac{4C_2}{E} (\eta^t)^2 + \frac{4C_3}{E\beta^t}. \end{aligned} \quad (87)$$

Then, summing both sides of (87) for t from 0 to $T - 1$, we have

$$\begin{aligned} & \sum_{t=0}^{T-1} \eta^t \mathbb{E} \left[\left\| \nabla F(\hat{\boldsymbol{\theta}}^t) \right\|_2^2 \right] \\ & \leq \frac{4 \left[F(\boldsymbol{\theta}^{(0,0)}) - F^{\text{inf}} \right]}{E} + \frac{4C_1}{E} \sum_{t=0}^{T-1} (\eta^t)^3 + \frac{4C_2}{E} \sum_{t=0}^{T-1} (\eta^t)^2 \\ & + \frac{4C_3}{E} \sum_{t=0}^{T-1} \frac{1}{\beta^t}. \end{aligned} \quad (88)$$

Dividing (88) by $\sum_{t=0}^{T-1} \eta^t$, we complete the proof.

C. Biased MAE

Obviously we have $\mathbb{E}[\boldsymbol{\varepsilon}^t] \neq 0$, $\mathbb{E}[\|\boldsymbol{\varepsilon}^t\|_2^2] \neq 0$. By applying the relationship between arithmetic and geometric mean to (73), i.e., $|\mathbf{x}^\top \mathbf{y}| \leq \frac{p\|\mathbf{x}\|_2^2}{2} + \frac{\|\mathbf{y}\|_2^2}{2p}$, it yields

$$\begin{aligned} & \mathbb{E} \left[F(\hat{\boldsymbol{\theta}}^{t+1}) - F(\hat{\boldsymbol{\theta}}^t) \right] \\ & \leq \frac{E\eta^t \left\| \nabla F(\hat{\boldsymbol{\theta}}^t) \right\|_2^2}{4} + \frac{\|\mathbb{E}[\boldsymbol{\varepsilon}^t]\|_2^2}{E\eta^t} \\ & - E\eta^t \left[\nabla F(\hat{\boldsymbol{\theta}}^t) \right]^\top \mathbb{E} \left[\sum_{n=1}^N p_n \mathbf{h}_n^t \right] + \frac{L}{2} \mathbb{E} \left[\|\boldsymbol{\varepsilon}^t\|_2^2 \right] \\ & + \frac{L(\eta^t)^2 E^2}{2} \mathbb{E} \left[\sum_{n=1}^N p_n \mathbf{d}_n^t \right] \end{aligned}$$

$$+ L\eta^t E \left\{ 2L\mathbb{E} \left[\|\boldsymbol{\varepsilon}^t\|_2^2 \right] + \frac{\mathbb{E} \left[\left\| \sum_{n=1}^N p_n \mathbf{d}_n^t \right\|_2^2 \right]}{8L} \right\}. \quad (89)$$

Combining (89) with **Lemma 4** and (80), we obtain

$$\begin{aligned} & \mathbb{E} \left[F(\hat{\boldsymbol{\theta}}^{t+1}) - F(\hat{\boldsymbol{\theta}}^t) \right] \\ & \leq -\frac{\eta^t E}{4} \left(1 - \frac{2H^t \beta_1}{1-H^t} \right) \left\| \nabla F(\hat{\boldsymbol{\theta}}^t) \right\|_2^2 \\ & + (\eta^t)^3 \frac{L^2 E(E-1)}{2(1-H^t)} \sum_{n=1}^N p_n \sigma_n^2 + (\eta^t)^2 LE \sum_{n=1}^N p_n^2 \sigma_n^2 \\ & + \eta^t \left[\frac{H^t E \beta_2}{2(1-H^t)} + \frac{1}{4} \sum_{n=1}^N p_n^2 \sigma_n^2 + 2L^2 E \mathbb{E} \left[\|\boldsymbol{\varepsilon}^t\|_2^2 \right] \right] \\ & + \frac{L}{2} \mathbb{E} \left[\|\boldsymbol{\varepsilon}^t\|_2^2 \right] + (\eta^t)^{-1} \frac{\|\mathbb{E}[\boldsymbol{\varepsilon}^t]\|_2^2}{E}. \end{aligned} \quad (90)$$

If $H^t \leq \frac{1}{4\beta_1+1}$, then it follows that $1 - \frac{2H^t \beta_1}{1-H^t} \geq \frac{1}{2}$, which requires $\eta^t \leq \frac{1}{L\sqrt{2E(E-1)}(4\beta_1+1)}$. Then (90) can be simplified as

$$\begin{aligned} & \mathbb{E} \left[F(\hat{\boldsymbol{\theta}}^{t+1}) - F(\hat{\boldsymbol{\theta}}^t) \right] \\ & \leq -\frac{\eta^t E}{8} \left\| \nabla F(\hat{\boldsymbol{\theta}}^t) \right\|_2^2 \\ & + (\eta^t)^3 \frac{L^2 E(E-1)(4\beta_1+1)}{8\beta_1} \left[\sum_{n=1}^N p_n \sigma_n^2 + 2E\beta_2 \right] \\ & + (\eta^t)^2 LE \sum_{n=1}^N p_n^2 \sigma_n^2 + \eta^t \left[\frac{1}{4} \sum_{n=1}^N p_n^2 \sigma_n^2 + 2L^2 E \mathbb{E} \left[\|\boldsymbol{\varepsilon}^t\|_2^2 \right] \right] \\ & + \frac{L}{2} \mathbb{E} \left[\|\boldsymbol{\varepsilon}^t\|_2^2 \right] + (\eta^t)^{-1} \frac{\|\mathbb{E}[\boldsymbol{\varepsilon}^t]\|_2^2}{E}. \end{aligned} \quad (91)$$

Finally we can obtain **Theorems 6** and **7** respectively with the same method in **Appendix A-B**.

APPENDIX B

CONVERGENCE ANALYSIS FOR MAE IN AIRFEDAVG-S

This section summarizes the method of convergence analysis for MAE in AIRFEDAVG-S.

A. Preliminaries

First we have

$$\hat{\boldsymbol{\theta}}^{t+1} = \hat{\boldsymbol{\theta}}^t - \eta^t \hat{\mathbf{y}}^t. \quad (92)$$

By applying **Assumption 3** for global loss function, we obtain

$$F(\hat{\boldsymbol{\theta}}^{t+1}) - F(\hat{\boldsymbol{\theta}}^t) \leq -\eta^t \left\langle \hat{\mathbf{y}}^t, \nabla F(\hat{\boldsymbol{\theta}}^t) \right\rangle + \frac{L(\eta^t)^2}{2} \left\| \hat{\mathbf{y}}^t \right\|_2^2. \quad (93)$$

Taking an expectation on the mini-batch stochastic gradient for both sides of (93), and denoting $\bar{\mathbf{y}}^t = \sum_{n=1}^N p_n \mathbf{g}_n^{(t,0)}$, we obtain

$$\begin{aligned} & \mathbb{E} \left[F(\hat{\boldsymbol{\theta}}^{t+1}) - F(\hat{\boldsymbol{\theta}}^t) \right] \\ & \leq -\eta^t \mathbb{E} \left[\left\langle \hat{\mathbf{y}}^t, \nabla F(\hat{\boldsymbol{\theta}}^t) \right\rangle \right] + \frac{L(\eta^t)^2}{2} \mathbb{E} \left[\left\| \hat{\mathbf{y}}^t \right\|_2^2 \right] \end{aligned}$$

$$\begin{aligned}
&= -\eta^t \left\| \nabla F(\hat{\theta}^t) \right\|_2^2 - \eta^t \left[\nabla F(\hat{\theta}^t) \right]^\top \mathbb{E} [\varepsilon^t] \\
&+ \frac{L(\eta^t)^2}{2} \mathbb{E} \left[\left\| \bar{\mathbf{y}}^t \right\|_2^2 \right] + L(\eta^t)^2 \left[\nabla F(\hat{\theta}^t) \right]^\top \mathbb{E} [\varepsilon^t] \\
&+ \frac{L(\eta^t)^2}{2} \mathbb{E} \left[\left\| \varepsilon^t \right\|_2^2 \right], \tag{94}
\end{aligned}$$

where the equality holds by **Assumption 5** and the fact that $\nabla F(\hat{\theta}^t) = \sum_{n=1}^N p_n \nabla F_n(\hat{\theta}^t)$.

B. Unbiased MAE

Obviously we have $\mathbb{E}[\varepsilon^t] = 0$. We suppose $\mathbb{E}[\|\varepsilon^t\|_2^2] = \sigma_w^2/\beta^t \neq 0$, then (94) can be reformulated as

$$\begin{aligned}
&\mathbb{E} \left[F(\hat{\theta}^{t+1}) - F(\hat{\theta}^t) \right] \\
&\leq -\eta^t \left\| \nabla F(\hat{\theta}^t) \right\|_2^2 + \frac{L(\eta^t)^2}{2} \mathbb{E} \left[\left\| \bar{\mathbf{y}}^t \right\|_2^2 \right] + \frac{L(\eta^t)^2}{2} \frac{\sigma_w^2}{\beta^t}, \tag{95}
\end{aligned}$$

Next, to further give a bound on $\mathbb{E}[\|\bar{\mathbf{y}}^t\|_2^2]$, we only need to give a bound on $\mathbb{E}[\|\bar{\mathbf{g}}^t\|_2^2]$

$$\begin{aligned}
\mathbb{E} \left[\left\| \bar{\mathbf{y}}^t \right\|_2^2 \right] &= \mathbb{E} \left[\left\| \sum_{n=1}^N p_n \mathbf{g}_n^t - \nabla F(\hat{\theta}^t) + \nabla F(\hat{\theta}^t) \right\|_2^2 \right] \\
&= \mathbb{E} \left[\left\| \sum_{n=1}^N p_n \mathbf{g}_n^t - \nabla F(\hat{\theta}^t) \right\|_2^2 \right] + \left\| \nabla F(\hat{\theta}^t) \right\|_2^2 \\
&= \mathbb{E} \left[\left\| \sum_{n=1}^N p_n \left[\mathbf{g}_n^t - \nabla F_n(\hat{\theta}^t) \right] \right\|_2^2 \right] + \left\| \nabla F(\hat{\theta}^t) \right\|_2^2 \\
&= \sum_{n=1}^N p_n^2 \mathbb{E} \left[\left\| \mathbf{g}_n^t - \nabla F_n(\hat{\theta}^t) \right\|_2^2 \right] + \left\| \nabla F(\hat{\theta}^t) \right\|_2^2 \\
&\leq \sum_{n=1}^N p_n^2 \sigma_n^2 + \left\| \nabla F(\hat{\theta}^t) \right\|_2^2, \tag{96}
\end{aligned}$$

where the second equality and the last inequality hold by **Assumption 5**.

By substituting (96) into (95), we can obtain

$$\begin{aligned}
\mathbb{E} \left[F(\hat{\theta}^{t+1}) - F(\hat{\theta}^t) \right] &\leq -\eta^t \left(1 - \frac{L\eta^t}{2} \right) \left\| \nabla F(\hat{\theta}^t) \right\|_2^2 \\
&+ \frac{L(\eta^t)^2}{2} \left(\sum_{n=1}^N p_n^2 \sigma_n^2 + \frac{\sigma_w^2}{\beta^t} \right). \tag{97}
\end{aligned}$$

1) *Strongly Convex Case:* When **Assumption 4** holds, i.e., the strongly convex case, we have the following results.

$$\begin{aligned}
\mathbb{E} \left[F(\hat{\theta}^{t+1}) - F(\hat{\theta}^t) \right] &\leq -2\mu\eta^t \left(1 - \frac{L\eta^t}{2} \right) \left[F(\hat{\theta}^t) - F^* \right] \\
&+ \frac{L(\eta^t)^2}{2} \left(\sum_{n=1}^N p_n^2 \sigma_n^2 + \frac{\sigma_w^2}{\beta^t} \right), \tag{98}
\end{aligned}$$

where the inequality holds by **Assumption 4**. By rearranging (98), we have

$$\mathbb{E} \left[F(\hat{\theta}^{t+1}) - F^* \right]$$

$$\begin{aligned}
&\leq \left[1 - 2\mu\eta^t \left(1 - \frac{L\eta^t}{2} \right) \right] \mathbb{E} \left[F(\hat{\theta}^t) - F^* \right] \\
&+ \frac{L(\eta^t)^2}{2} \left(\sum_{n=1}^N p_n^2 \sigma_n^2 + \frac{\sigma_w^2}{\beta^t} \right) \\
&\leq (1 - \mu\eta^t) \mathbb{E} \left[F(\hat{\theta}^t) - F^* \right] + \frac{L(\eta^t)^2}{2} \left(\sum_{n=1}^N p_n^2 \sigma_n^2 + \frac{\sigma_w^2}{\beta^t} \right), \tag{99}
\end{aligned}$$

where the last inequality holds by $\eta^t \leq \frac{1}{L}$.

Applying this recursively for t from 0 to $T-1$, and we can finish the proof.

2) *Non-Convex Case:* When **Assumption 4** does not hold, i.e., the non-convex case, we have the corresponding results.

By rearranging (97), we have

$$\eta^t \mathbb{E} \left[\left\| \nabla F(\hat{\theta}^t) \right\|_2^2 \right] \leq 2\mathbb{E} \left[F(\hat{\theta}^t) - F(\hat{\theta}^{t+1}) \right] + 2C(\eta^t)^2. \tag{100}$$

Then, by summing both sides of (100) for t from 0 to $T-1$ and dividing (101) by $\sum_{t=0}^{T-1} \eta^t$, we finally arrive at the weighted sum of the global gradient

$$\begin{aligned}
\frac{\sum_{t=0}^{T-1} \eta^t \mathbb{E} \left[\left\| \nabla F(\hat{\theta}^t) \right\|_2^2 \right]}{\sum_{t=0}^{T-1} \eta^t} &\leq \frac{2 \left[F(\hat{\theta}^0) - F^{\text{inf}} \right]}{\sum_{t=0}^{T-1} \eta^t} \\
&+ \frac{2C \sum_{t=0}^{T-1} (\eta^t)^2}{\sum_{t=0}^{T-1} \eta^t}. \tag{101}
\end{aligned}$$

C. Biased MAE

In this case, we have $\mathbb{E}[\varepsilon^t] \neq 0$, $\mathbb{E}[\|\varepsilon^t\|_2^2] \neq 0$. By applying the relationship between arithmetic and geometric mean to (94), i.e., $|(\sqrt{\eta}\mathbf{x})^\top(\sqrt{\eta}\mathbf{y})| \leq \frac{\eta\|\mathbf{x}\|_2^2}{2} + \frac{\eta\|\mathbf{y}\|_2^2}{2}$ and combining with (96), it can be reformulated as

$$\begin{aligned}
&\mathbb{E} \left[F(\hat{\theta}^{t+1}) - F(\hat{\theta}^t) \right] \\
&\leq -\eta^t \left\| \nabla F(\hat{\theta}^t) \right\|_2^2 + \frac{\eta^t}{2} \left\| \nabla F(\hat{\theta}^t) \right\|_2^2 + \frac{\eta^t}{2} \mathbb{E} [\varepsilon^t]_2^2 \\
&+ \frac{L(\eta^t)^2}{2} \left[\left\| \nabla F(\hat{\theta}^t) \right\|_2^2 + \mathbb{E} [\varepsilon^t]_2^2 \right] + \frac{L(\eta^t)^2}{2} \mathbb{E} \left[\left\| \varepsilon^t \right\|_2^2 \right] \\
&+ \frac{L(\eta^t)^2}{2} \left[\sum_{n=1}^N p_n^2 \sigma_n^2 + \left\| \nabla F(\hat{\theta}^t) \right\|_2^2 \right] \\
&= -\frac{\eta^t}{2} (1 - 2L\eta^t) \left\| \nabla F(\hat{\theta}^t) \right\|_2^2 + \frac{\eta^t}{2} \mathbb{E} [\varepsilon^t]_2^2 \\
&+ (\eta^t)^2 \frac{L}{2} \left\{ \mathbb{E} \left[\left\| \varepsilon^t \right\|_2^2 \right] + \mathbb{E} [\varepsilon^t]_2^2 + \sum_{n=1}^N p_n^2 \sigma_n^2 \right\} \\
&\leq -\frac{\eta^t}{4} \left\| \nabla F(\hat{\theta}^t) \right\|_2^2 + \frac{\eta^t}{2} \mathbb{E} [\varepsilon^t]_2^2 \\
&+ (\eta^t)^2 \frac{L}{2} \left\{ \mathbb{E} \left[\left\| \varepsilon^t \right\|_2^2 \right] + \mathbb{E} [\varepsilon^t]_2^2 + \sum_{n=1}^N p_n^2 \sigma_n^2 \right\}, \tag{102}
\end{aligned}$$

where the second inequality holds by the constraint on the learning rate $\eta^t \leq \frac{1}{4L}$.

Finally we can obtain **Theorem 8** and **9** respectively with the same method in **Appendix B-B**.

APPENDIX C
PROOF OF COROLLARY 1

For communication round $t \rightarrow t+1$, we have

$$\begin{aligned} & \mathbb{E} \left[F(\hat{\theta}^{t+1}) - F^* \right] \\ & \leq \left(1 - \frac{\mu\eta^t E}{2} \right) \mathbb{E} \left[F(\hat{\theta}^t) - F^* \right] + (\eta^t)^3 A + (\eta^t)^2 B. \end{aligned} \quad (103)$$

where $A = \frac{L^2 E(E-1)(2\beta_1+1)}{4\beta_1} \left[\sum_{n=1}^N p_n \sigma_n^2 + 2E\beta_2 \right]$ and $B = LE \sum_{n=1}^N p_n^2 \sigma_n^2 + L\tilde{G}^2 E/dN^2 \text{SNR}$. We want to prove by induction that there exist τ and η^t , such that

$$\Delta^t \leq (\eta^t)^2 \gamma A + \eta^t \gamma B.$$

where $\Delta^t = \mathbb{E} \left[F(\hat{\theta}^t) \right] - F^*$. Suppose that this holds for $t > 0$. For round $t+1$, we have

$$\begin{aligned} \Delta^{t+1} & \leq \left(1 - \frac{\mu\eta^t E}{2} \right) \Delta^t + (\eta^t)^3 A + (\eta^t)^2 B \\ & \leq \left(1 - \frac{\mu\eta^t E}{2} \right) [(\eta^t)^2 \gamma A + \eta^t \gamma B] + (\eta^t)^3 A + (\eta^t)^2 B \\ & = \left[\gamma \left(1 - \frac{\mu\eta^t E}{2} \right) + \eta^t \right] [(\eta^t)^2 A + \eta^t B]. \end{aligned} \quad (104)$$

We want to prove that

$$\left[\gamma \left(1 - \frac{\mu\eta^t E}{2} \right) + \eta^t \right] \eta^t \leq \tau \eta^{t+1}, \quad (105)$$

$$\left[\gamma \left(1 - \frac{\mu\eta^t E}{2} \right) + \eta^t \right] (\eta^t)^2 \leq \tau (\eta^{t+1})^2. \quad (106)$$

By setting

$$\begin{cases} \eta^t = \frac{6}{E\mu(t+\tau)}, \\ \gamma = \frac{6}{E\mu}, \end{cases} \quad (107)$$

we can show that it is equivalent to proving

$$\begin{cases} (t+\tau-2)(t+\tau-1) \leq (t+\tau)^2, \\ (t+\tau+1)^2(t+\tau-2) \leq (t+\tau)^3, \end{cases} \quad (108)$$

which are obvious for $\tau = \frac{3L}{\mu}$.

In this case, we have

$$\begin{aligned} \Delta^t & \leq \left[\frac{6}{E\mu(t+\tau)} \right]^2 \frac{6}{E\mu} A + \frac{6}{E\mu(t+\tau)} \frac{6}{E\mu} B \\ & = \frac{216A}{E^3 \mu^3 (t+\tau)^2} + \frac{36B}{E^2 \mu^2 (t+\tau)}. \end{aligned} \quad (109)$$

For $t=0$, it follows that

$$\Delta^0 \leq \frac{216A}{E^3 \mu^3 \tau^2} + \frac{36B}{E^2 \mu^2 \tau}. \quad (110)$$

Then the constraint on E can be obtained by

$$E \leq \frac{6(2\beta_1+1)\bar{\sigma}^2 + 12\beta_1(\sigma^2 + \tilde{G}^2/dN^2 \text{SNR})}{\beta_1 \mu (F(\hat{\theta}^0) - F^*) - 12\beta_2(2\beta_1+1)}, \quad (111)$$

where $\bar{\sigma}^2 = \sum_{n=1}^N p_n \sigma_n^2$ and $\sigma^2 = \sum_{n=1}^N p_n^2 \sigma_n^2$.

The upper bound after T communication rounds is then given by

$$\begin{aligned} \Delta^T & \leq \frac{216A}{E^3 \mu^3 (T+\tau)^2} + \frac{36B}{E^2 \mu^2 (T+\tau)} \\ & = \mathcal{O} \left(\frac{A_1}{E^2 \mu^3 T^2} \right) + \mathcal{O} \left(\frac{B_1}{E \mu^2 T} \right) \end{aligned} \quad (112)$$

where $A_1 = L^2(E-1)(2+1/\beta_1)[\bar{\sigma}^2 + E\beta_2]$, $B_1 = L\sigma^2 + L/dN^2 \text{SNR}$.

APPENDIX D
PROOF OF COROLLARY 5

Similarly, we prove this by induction. Let $\delta^t = \mathbb{E} \left[F(\hat{\theta}^t) \right] - F^*$, $C = \frac{L}{2} (\Sigma/N + G^2/dN^2 \text{SNR})$, and define $u = \max \left\{ \frac{\beta^2 C}{\beta\mu-1}, \delta^0 \tau \right\}$, $\tau > 0$. If the learning rate is set to be $\eta^t = \frac{\beta}{\tau+t}$ such that $\eta^0 \leq \min \left\{ \frac{1}{\mu}, \frac{1}{L} \right\} = \frac{1}{L}$. Then by applying induction method, first it is clearly that $\delta^0 \leq \frac{u}{\tau}$. Second, assume that when $n=t$, we have

$$\delta^t \leq \frac{u}{\tau+t}. \quad (113)$$

At last, when $n=t+1$,

$$\begin{aligned} \delta^{t+1} & \leq \left(1 - \frac{\beta\mu}{\tau+t} \right) \frac{u^t}{\tau+t} + \frac{\beta^2 C}{(\tau+t)^2} \\ & = \frac{\tau+t-1}{(\tau+t)^2} u - \frac{\beta\mu-1}{(\tau+t)^2} \left(u - \frac{\beta^2 C}{\beta\mu-1} \right) \\ & \leq \frac{\tau+t-1}{(\tau+t)^2} u \\ & \leq \frac{\tau+t-1}{(\tau+t)^2-1} u = \frac{u}{\tau+t+1}, \end{aligned} \quad (114)$$

where the second inequality holds by $\beta > \frac{1}{\mu}$ and $u = \max \left\{ \frac{\beta^2 C}{\beta\mu-1}, \delta^0 \tau \right\}$.

Specifically, if we choose $\beta = \frac{2}{\mu}$ and $\tau = \frac{2L}{\mu}$, then $\eta^t = \frac{2}{\mu(\tau+t)}$ and

$$\mathbb{E}[F(\hat{\theta}^t)] - F^* \leq \frac{\max\{4C, \mu^2 \tau \delta^0\}}{\mu^2 (\tau+t)}. \quad (115)$$

After T total communication rounds, we have

$$\begin{aligned} \mathbb{E}[F(\hat{\theta}^T)] - F^* & \leq \frac{\max\{4C, \mu^2 \tau \delta^0\}}{\mu^2 (\tau+T)} \\ & = \mathcal{O} \left(\frac{\max\{4C, \mu^2 \tau \delta^0\}}{\mu^2 T} \right). \end{aligned} \quad (116)$$

REFERENCES

- [1] K. B. Letaief, W. Chen, Y. Shi, J. Zhang, and Y.-J. A. Zhang, "The roadmap to 6G: AI empowered wireless networks," *IEEE Commun. Mag.*, vol. 57, no. 8, pp. 84–90, 2019.
- [2] Y. Shi, K. Yang, T. Jiang, J. Zhang, and K. B. Letaief, "Communication-efficient edge AI: Algorithms and systems," *IEEE Commun. Surveys Tuts.*, vol. 22, no. 4, pp. 2167–2191, 2020.
- [3] K. B. Letaief, Y. Shi, J. Lu, and J. Lu, "Edge artificial intelligence for 6G: Vision, enabling technologies, and applications," *IEEE J. Sel. Areas Commun.*, vol. 40, no. 1, pp. 5–36, 2022.
- [4] Y. Shi, K. Yang, Z. Yang, and Y. Zhou, "Mobile edge artificial intelligence: Opportunities and challenges," Amsterdam, The Netherlands: Elsevier, Aug. 2021.

- [5] B. McMahan, E. Moore, D. Ramage, S. Hampson, and B. A. y Arcas, "Communication-efficient learning of deep networks from decentralized data," in *Proc. Int. Conf. Artificial Intell. Stat. (AISTATS)*, 2017, pp. 1273–1282.
- [6] K. Bonawitz, H. Eichner, W. Grieskamp, D. Huba, A. Ingerman, V. Ivanov, C. Kiddon, J. Konečný, S. Mazzocchi, H. B. McMahan et al., "Towards federated learning at scale: System design," *arXiv preprint arXiv:1902.01046*, 2019.
- [7] J. Park, S. Samarakoon, M. Bennis, and M. Debbah, "Wireless network intelligence at the edge," *Proc. IEEE*, vol. 107, no. 11, pp. 2204–2239, 2019.
- [8] T. Li, A. K. Sahu, A. Talwalkar, and V. Smith, "Federated learning: Challenges, methods, and future directions," *IEEE Signal Process. Mag.*, vol. 37, no. 3, pp. 50–60, 2020.
- [9] S. Wang, T. Tuor, T. Salonidis, K. K. Leung, C. Makaya, T. He, and K. Chan, "Adaptive federated learning in resource constrained edge computing systems," *IEEE J. Sel. Areas Commun.*, vol. 37, no. 6, pp. 1205–1221, 2019.
- [10] W. Shi, S. Zhou, Z. Niu, M. Jiang, and L. Geng, "Joint device scheduling and resource allocation for latency constrained wireless federated learning," *IEEE Trans. Wireless Commun.*, vol. 20, no. 1, pp. 453–467, 2021.
- [11] M. Chen, Z. Yang, W. Saad, C. Yin, H. V. Poor, and S. Cui, "A joint learning and communications framework for federated learning over wireless networks," *IEEE Trans. Wireless Commun.*, vol. 20, no. 1, pp. 269–283, 2021.
- [12] M. Chen, H. Vincent Poor, W. Saad, and S. Cui, "Convergence time optimization for federated learning over wireless networks," *IEEE Trans. Wireless Commun.*, vol. 20, no. 4, pp. 2457–2471, 2021.
- [13] J. Ren, G. Yu, and G. Ding, "Accelerating DNN training in wireless federated edge learning systems," *IEEE J. Sel. Areas Commun.*, vol. 39, no. 1, pp. 219–232, 2021.
- [14] M. Zhang, G. Zhu, S. Wang, J. Jiang, Q. Liao, C. Zhong, and S. Cui, "Communication-efficient federated edge learning via optimal probabilistic device scheduling," *IEEE Trans. Wireless Commun.*, vol. 21, no. 10, pp. 8536–8551, 2022.
- [15] Z. Yang, M. Chen, W. Saad, C. S. Hong, and M. Shikh-Bahaei, "Energy efficient federated learning over wireless communication networks," *IEEE Trans. Wireless Commun.*, vol. 20, no. 3, pp. 1935–1949, 2021.
- [16] B. Luo, X. Li, S. Wang, J. Huang, and L. Tassiulas, "Cost-effective federated learning in mobile edge networks," *IEEE J. Sel. Areas Commun.*, vol. 39, no. 12, pp. 3606–3621, 2021.
- [17] M. M. Amiria, D. Gündüz, S. R. Kulkarni, and H. Vincent Poor, "Convergence of update aware device scheduling for federated learning at the wireless edge," *IEEE Trans. Wireless Commun.*, vol. 20, no. 6, pp. 3643–3658, 2021.
- [18] W. Y. B. Lim, J. S. Ng, Z. Xiong, D. Niyato, C. Miao, and D. I. Kim, "Dynamic edge association and resource allocation in self-organizing hierarchical federated learning networks," *IEEE J. Sel. Areas Commun.*, vol. 39, no. 12, pp. 3640–3653, 2021.
- [19] S. Liu, G. Yu, X. Chen, and M. Bennis, "Joint user association and resource allocation for wireless hierarchical federated learning with iid and non-iid data," *IEEE Trans. Wireless Commun.*, vol. 21, no. 10, pp. 7852–7866, 2022.
- [20] W. Wen, Z. Chen, H. H. Yang, W. Xia, and T. Q. S. Quek, "Joint scheduling and resource allocation for hierarchical federated edge learning," *IEEE Trans. Wireless Commun.*, vol. 21, no. 8, pp. 5857–5872, 2022.
- [21] L. Liu, J. Zhang, S. Song, and K. B. Letaief, "Hierarchical federated learning with quantization: Convergence analysis and system design," *IEEE Trans. Wireless Commun.*, vol. 22, no. 1, pp. 2–18, 2023.
- [22] G. Zhu, Y. Wang, and K. Huang, "Broadband analog aggregation for low-latency federated edge learning," *IEEE Trans. Wireless Commun.*, vol. 19, no. 1, pp. 491–506, 2020.
- [23] Y. Shi, Y. Zhou, D. Wen, Y. Wu, C. Jiang, and K. B. Letaief, "Task-oriented communications for 6G: Vision, principles, and technologies," *IEEE Wireless Commun.*, vol. 30, no. 3, pp. 78–85, 2023.
- [24] B. Nazer and M. Gastpar, "Computation over multiple-access channels," *IEEE Trans. Inf. Theory*, vol. 53, no. 10, pp. 3498–3516, 2007.
- [25] G. Zhu, J. Xu, K. Huang, and S. Cui, "Over-the-air computing for wireless data aggregation in massive IoT," *IEEE Wireless Commun.*, vol. 28, no. 4, pp. 57–65, 2021.
- [26] Z. Wang, Y. Zhao, Y. Zhou, Y. Shi, C. Jiang, and K. B. Letaief, "Over-the-air computation: Foundations, technologies, and applications," *arXiv preprint arXiv:2210.10524*, 2022.
- [27] O. Abari, H. Rahul, and D. Katabi, "Over-the-air function computation in sensor networks," *arXiv preprint arXiv:1612.02307*, 2016.
- [28] K. Yang, T. Jiang, Y. Shi, and Z. Ding, "Federated learning via over-the-air computation," *IEEE Trans. Wireless Commun.*, vol. 19, no. 3, pp. 2022–2035, 2020.
- [29] H. Xing, O. Simeone, and S. Bi, "Federated learning over wireless device-to-device networks: Algorithms and convergence analysis," *IEEE J. Sel. Areas Commun.*, vol. 39, no. 12, pp. 3723–3741, 2021.
- [30] Y. Shi, Y. Zhou, and Y. Shi, "Over-the-air decentralized federated learning," in *Proc. IEEE Int. Symp. Inf. Theory (ISIT)*, 2021, pp. 455–460.
- [31] Z. Lin, Y. Gong, and K. Huang, "Distributed over-the-air computing for fast distributed optimization: Beamforming design and convergence analysis," *IEEE J. Sel. Areas Commun.*, vol. 41, no. 1, pp. 274–287, 2022.
- [32] N. Michelusi, "Decentralized federated learning via non-coherent over-the-air consensus," *arXiv preprint arXiv:2210.15806*, 2022.
- [33] Z. Wang, Y. Zhou, Y. Shi, and W. Zhuang, "Interference management for over-the-air federated learning in multi-cell wireless networks," *IEEE J. Sel. Areas Commun.*, vol. 40, no. 8, pp. 2361–2377, 2022.
- [34] O. Aygün, M. Kazemi, D. Gündüz, and T. M. Duman, "Over-the-air federated edge learning with hierarchical clustering," *arXiv preprint arXiv:2207.09232*, 2022.
- [35] Y. Shao, D. Gündüz, and S. C. Liew, "Bayesian over-the-air computation," *IEEE J. Sel. Areas Commun.*, vol. 41, no. 3, pp. 589–606, 2023.
- [36] H. Liu, X. Yuan, and Y.-J. A. Zhang, "Reconfigurable intelligent surface enabled federated learning: A unified communication-learning design approach," *IEEE Trans. Wireless Commun.*, vol. 20, no. 11, pp. 7595–7609, 2021.
- [37] Z. Wang, J. Qiu, Y. Zhou, Y. Shi, L. Fu, W. Chen, and K. B. Letaief, "Federated learning via intelligent reflecting surface," *IEEE Trans. Wireless Commun.*, vol. 21, no. 2, pp. 808–822, 2022.
- [38] Y. Yang, Y. Zhou, Y. Wu, and Y. Shi, "Differentially private federated learning via reconfigurable intelligent surface," *IEEE Internet Things J.*, vol. 9, no. 20, pp. 19728–19743, 2022.
- [39] W. Ni, Y. Liu, Z. Yang, H. Tian, and X. Shen, "Federated learning in multi-RIS-aided systems," *IEEE Internet Things J.*, vol. 9, no. 12, pp. 9608–9624, 2022.
- [40] L. Hu, Z. Wang, H. Zhu, and Y. Zhou, "RIS-assisted over-the-air federated learning in millimeter wave mimo networks," *J. Commun. Inf. Netw.*, vol. 7, no. 2, pp. 145–156, 2022.
- [41] X. Zhong, X. Yuan, H. Yang, and C. Zhong, "Uav-assisted hierarchical aggregation for over-the-air federated learning," in *Proc. IEEE Global Commun. Conf. (GLOBECOM)*, 2022, pp. 807–812.
- [42] Y. Wang, C. Zou, D. Wen, and Y. Shi, "Federated learning over LEO satellite," in *Proc. IEEE GLOBECOM Workshops (GC Wkshps)*, 2022, pp. 1652–1657.
- [43] M. Kim, A. Lee Swindlehurst, and D. Park, "Beamforming vector design and device selection in over-the-air federated learning," *IEEE Trans. Wireless Commun.*, Mar., 2023, doi: 10.1109/TWC.2023.3251339.
- [44] N. Zhang and M. Tao, "Gradient statistics aware power control for over-the-air federated learning," *IEEE Trans. Wireless Commun.*, vol. 20, no. 8, pp. 5115–5128, 2021.
- [45] Y. Sun, S. Zhou, and D. Gündüz, "Energy-aware analog aggregation for federated learning with redundant data," in *Proc. IEEE Int. Conf. Commun. (ICC)*, 2020, pp. 1–7.
- [46] D. Liu and O. Simeone, "Privacy for free: Wireless federated learning via uncoded transmission with adaptive power control," *IEEE J. Sel. Areas Commun.*, vol. 39, no. 1, pp. 170–185, 2020.
- [47] X. Cao, G. Zhu, J. Xu, Z. Wang, and S. Cui, "Optimized power control design for over-the-air federated edge learning," *IEEE J. Sel. Areas Commun.*, vol. 40, no. 1, pp. 342–358, 2022.
- [48] W. Guo, C. Huang, X. Qin, L. Yang, and W. Zhang, "Dynamic clustering and power control for two-tier wireless federated learning," *IEEE Trans. Wireless Commun.*, Jun. 2023, doi: 10.1109/TWC.2023.3288606.
- [49] X. Cao, G. Zhu, J. Xu, and S. Cui, "Transmission power control for over-the-air federated averaging at network edge," *IEEE J. Sel. Areas Commun.*, vol. 40, no. 5, pp. 1571–1586, 2022.
- [50] W. Guo, R. Li, C. Huang, X. Qin, K. Shen, and W. Zhang, "Joint device selection and power control for wireless federated learning," *IEEE J. Sel. Areas Commun.*, vol. 40, no. 8, pp. 2395–2410, 2022.
- [51] Y. Zou, Z. Wang, X. Chen, H. Zhou, and Y. Zhou, "Knowledge-guided learning for transceiver design in over-the-air federated learning," *IEEE Trans. Wireless Commun.*, vol. 22, no. 1, pp. 270–285, 2023.
- [52] H. Guo, A. Liu, and V. K. N. Lau, "Analog gradient aggregation for federated learning over wireless networks: Customized design and

- convergence analysis,” *IEEE Internet Things J.*, vol. 8, no. 1, pp. 197–210, 2021.
- [53] T. Sery, N. Shlezinger, K. Cohen, and Y. C. Eldar, “Over-the-air federated learning from heterogeneous data,” *IEEE Trans. Signal Process.*, vol. 69, pp. 3796–3811, 2021.
- [54] T. Gafni, K. Cohen, and Y. C. Eldar, “Federated learning from heterogeneous data via controlled bayesian air aggregation,” *arXiv preprint arXiv:2303.17413*, 2023.
- [55] C. Xu, S. Liu, Z. Yang, Y. Huang, and K.-K. Wong, “Learning rate optimization for federated learning exploiting over-the-air computation,” *IEEE J. Sel. Areas Commun.*, vol. 39, no. 12, pp. 3742–3756, 2021.
- [56] S. Wang, Y. Hong, R. Wang, Q. Hao, Y.-C. Wu, and D. W. K. Ng, “Edge federated learning via unit-modulus over-the-air computation,” *IEEE Trans. Commun.*, vol. 70, no. 5, pp. 3141–3156, 2022.
- [57] T. Sery and K. Cohen, “On analog gradient descent learning over multiple access fading channels,” *IEEE Trans. Signal Process.*, vol. 68, pp. 2897–2911, 2020.
- [58] G. Zhu, Y. Du, D. Gündüz, and K. Huang, “One-bit over-the-air aggregation for communication-efficient federated edge learning: Design and convergence analysis,” *IEEE Trans. Wireless Commun.*, 2020.
- [59] X. Wei and C. Shen, “Federated learning over noisy channels: Convergence analysis and design examples,” *IEEE Trans. Cogn. Commun. Netw.*, vol. 8, no. 2, pp. 1253–1268, 2022.
- [60] S. Jing and C. Xiao, “Federated learning via over-the-air computation with statistical channel state information,” *IEEE Trans. Wireless Commun.*, vol. 21, no. 11, pp. 9351–9365, 2022.
- [61] M. M. Amiri and D. Gündüz, “Machine learning at the wireless edge: Distributed stochastic gradient descent over-the-air,” *IEEE Trans. Signal Process.*, vol. 68, pp. 2155–2169, 2020.
- [62] M. M. Amiri and D. Gündüz, “Federated learning over wireless fading channels,” *IEEE Trans. Wireless Commun.*, vol. 19, no. 5, pp. 3546–3557, 2020.
- [63] Y. Sun, S. Zhou, Z. Niu, and D. Gündüz, “Dynamic scheduling for over-the-air federated edge learning with energy constraints,” *IEEE J. Sel. Areas Commun.*, vol. 40, no. 1, pp. 227–242, 2022.
- [64] L. Su and V. K. N. Lau, “Data and channel-adaptive sensor scheduling for federated edge learning via over-the-air gradient aggregation,” *IEEE Internet Things J.*, vol. 9, no. 3, pp. 1640–1654, 2022.
- [65] J. Du, B. Jiang, C. Jiang, Y. Shi, and Z. Han, “Gradient and channel aware dynamic scheduling for over-the-air computation in federated edge learning systems,” *IEEE J. Sel. Areas Commun.*, vol. 41, no. 4, pp. 1035–1050, 2023.
- [66] D. Fan, X. Yuan, and Y.-J. A. Zhang, “Temporal-structure-assisted gradient aggregation for over-the-air federated edge learning,” *IEEE J. Sel. Areas Commun.*, vol. 39, no. 12, pp. 3757–3771, 2021.
- [67] H. Sifaou and G. Y. Li, “Robust federated learning via over-the-air computation,” in *Proc. IEEE Int. Wkshp. Mach. Learn. Signal Process. (MLSP)*, 2022, pp. 1–6.
- [68] Z. Lin, H. Liu, and Y.-J. A. Zhang, “Relay-assisted cooperative federated learning,” *IEEE Trans. Wireless Commun.*, vol. 21, no. 9, pp. 7148–7164, 2022.
- [69] A. Elgabli, J. Park, C. B. Issaid, and M. Bennis, “Harnessing wireless channels for scalable and privacy-preserving federated learning,” *IEEE Trans. Commun.*, vol. 69, no. 8, pp. 5194–5208, 2021.
- [70] M. S. E. Mohamed, W.-T. Chang, and R. Tandon, “Privacy amplification for federated learning via user sampling and wireless aggregation,” *IEEE J. Sel. Areas Commun.*, vol. 39, no. 12, pp. 3821–3835, 2021.
- [71] Y. Shao, D. Gündüz, and S. C. Liew, “Federated edge learning with misaligned over-the-air computation,” *IEEE Trans. Wireless Commun.*, vol. 21, no. 6, pp. 3951–3964, 2022.
- [72] L. Li, C. Huang, D. Shi, H. Wang, X. Zhou, M. Shu, and M. Pan, “Energy and spectrum efficient federated learning via high-precision over-the-air computation,” *arXiv preprint arXiv:2208.07237*, 2022.
- [73] L. You, X. Zhao, R. Cao, Y. Shao, and L. Fu, “Broadband digital over-the-air computation for wireless federated edge learning,” *arXiv preprint arXiv:2212.06596*, 2022.
- [74] S. Ghadimi and G. Lan, “Stochastic first- and zeroth-order methods for nonconvex stochastic programming,” *SIAM J. Optim.*, vol. 23, no. 4, pp. 2341–2368, 2013.
- [75] L. Bottou, F. E. Curtis, and J. Nocedal, “Optimization methods for large-scale machine learning,” *Siam Rev.*, vol. 60, no. 2, pp. 223–311, 2018.
- [76] X. Li, K. Huang, W. Yang, S. Wang, and Z. Zhang, “On the convergence of FedAvg on non-IID data,” in *Proc. Int. Conf. Learn. Representations (ICLR)*, 2020.
- [77] S. U. Stich, “Local SGD converges fast and communicates little,” in *Proc. Int. Conf. Learn. Representations (ICLR)*, 2019.
- [78] F. Haddadpour and M. Mahdavi, “On the convergence of local descent methods in federated learning,” *arXiv preprint arXiv:1910.14425*, 2019.
- [79] H. Yu, S. Yang, and S. Zhu, “Parallel restarted SGD with faster convergence and less communication: Demystifying why model averaging works for deep learning,” in *Proc. AAAI Conf. Artificial Intell.*, vol. 33, no. 01, 2019, pp. 5693–5700.
- [80] J. Wang and G. Joshi, “Cooperative SGD: A unified framework for the design and analysis of local-update SGD algorithms,” *J. Mach. Learn. Res.*, vol. 22, no. 213, pp. 1–50, 2021.
- [81] H. Yu, R. Jin, and S. Yang, “On the linear speedup analysis of communication efficient momentum SGD for distributed non-convex optimization,” in *Proc. Int. Conf. Mach. Learn. (ICML)*, vol. 97, Jun. 2019, pp. 7184–7193.
- [82] X. Liang, S. Shen, J. Liu, Z. Pan, E. Chen, and Y. Cheng, “Variance reduced local SGD with lower communication complexity,” *arXiv preprint arXiv:1912.12844*, 2019.
- [83] F. Zhou and G. Cong, “On the convergence properties of a K-step averaging stochastic gradient descent algorithm for nonconvex optimization,” in *Proc. 27th Int. Joint Conf. Artif. Intell. (IJCAI)*, 2018, pp. 3219–3227.
- [84] F. Haddadpour, M. M. Kamani, M. Mahdavi, and V. Cadambe, “Trading redundancy for communication: Speeding up distributed SGD for non-convex optimization,” in *Proc. Int. Conf. Mach. Learn. (ICML)*, vol. 97, Jun. 2019, pp. 2545–2554.
- [85] A. Khaled, K. Mishchenko, and P. Richtarik, “Tighter theory for local SGD on identical and heterogeneous data,” in *Proc. Int. Conf. Artificial Intell. Stat. (AISTATS)*, vol. 108, Aug. 2020, pp. 4519–4529.
- [86] S. P. Karimireddy, S. Kale, M. Mohri, S. Reddi, S. Stich, and A. T. Suresh, “SCAFFOLD: Stochastic controlled averaging for federated learning,” in *Proc. Int. Conf. Mach. Learn. (ICML)*, vol. 119, Jul. 2020, pp. 5132–5143.
- [87] E. Gorbunov, F. Hanzely, and P. Richtarik, “Local SGD: Unified theory and new efficient methods,” in *Proc. Int. Conf. Artificial Intell. Stat. (AISTATS)*, vol. 130, Apr. 2021, pp. 3556–3564.
- [88] Z. Charles and J. Konečný, “On the outsized importance of learning rates in local update methods,” *arXiv preprint arXiv:2007.00878*, 2020.
- [89] X. Zhang, M. Hong, S. Dhople, W. Yin, and Y. Liu, “FedPD: A federated learning framework with adaptivity to non-IID data,” *IEEE Trans. Signal Process.*, vol. 69, pp. 6055–6070, 2021.
- [90] Y. Chen, K. Yuan, Y. Zhang, P. Pan, Y. Xu, and W. Yin, “Accelerating gossip SGD with periodic global averaging,” in *Proc. Int. Conf. Mach. Learn. (ICML)*, vol. 139, Jul. 2021, pp. 1791–1802.
- [91] A. Koloskova, N. Loizou, S. Boreiri, M. Jaggi, and S. Stich, “A unified theory of decentralized SGD with changing topology and local updates,” in *Proc. Int. Conf. Mach. Learn. (ICML)*, vol. 119, Jul. 2020, pp. 5381–5393.
- [92] Y. Guo, Y. Sun, R. Hu, and Y. Gong, “Hybrid local SGD for federated learning with heterogeneous communications,” in *Proc. Int. Conf. Learn. Representations (ICLR)*, 2022.
- [93] M. Zhang, J. Lucas, J. Ba, and G. E. Hinton, “Lookahead optimizer: k steps forward, 1 step back,” in *Proc. Adv. Neural Inf. Process. Syst. (NeurIPS)*, vol. 32, 2019.
- [94] J. Wang, Q. Liu, H. Liang, G. Joshi, and H. V. Poor, “Tackling the objective inconsistency problem in heterogeneous federated optimization,” in *Proc. Adv. Neural Inf. Process. Syst. (NeurIPS)*, 2020.
- [95] A. Reiszadeh, A. Mokhtari, H. Hassani, A. Jadbabaie, and R. Pedarsani, “FedPAQ: A communication-efficient federated learning method with periodic averaging and quantization,” in *Proc. Int. Conf. Artificial Intell. Stat. (AISTATS)*, vol. 108, Aug. 2020, pp. 2021–2031.
- [96] R. Das, A. Acharya, A. Hashemi, S. Sanghavi, I. S. Dhillon, and U. Topcu, “Faster non-convex federated learning via global and local momentum,” *arXiv preprint arXiv:2012.04061*, 2020.
- [97] S. J. Reddi, Z. Charles, M. Zaheer, Z. Garrett, K. Rush, J. Konečný, S. Kumar, and H. B. McMahan, “Adaptive federated optimization,” in *Proc. Int. Conf. Learn. Representations (ICLR)*, 2021.
- [98] Q. Tran Dinh, N. H. Pham, D. Phan, and L. Nguyen, “FedDR—randomized douglas-rachford splitting algorithms for nonconvex federated composite optimization,” in *Proc. Adv. Neural Inf. Process. Syst. (NeurIPS)*, vol. 34, 2021, pp. 30 326–30 338.
- [99] W. Fang, Z. Yu, Y. Jiang, Y. Shi, C. N. Jones, and Y. Zhou, “Communication-efficient stochastic zeroth-order optimization for federated learning,” *IEEE Trans. Signal Process.*, vol. 70, pp. 5058–5073, 2022.
- [100] S. Horváth, M. Sanjabi, L. Xiao, P. Richtarik, and M. Rabbat, “Fed-shuffle: Recipes for better use of local work in federated learning,” *Trans. Mach. Learn. Res.*, 2022.

- [101] D. Rothchild, A. Panda, E. Ullah, N. Ivkin, I. Stoica, V. Braverman, J. Gonzalez, and R. Arora, "FetchSGD: Communication-efficient federated learning with sketching," in *Proc. Int. Conf. Mach. Learn. (ICML)*, vol. 119, Jul. 2020, pp. 8253–8265.
- [102] Y. Wang, Y. Xu, Q. Shi, and T.-H. Chang, "Quantized federated learning under transmission delay and outage constraints," *IEEE J. Sel. Areas Commun.*, vol. 40, no. 1, pp. 323–341, 2022.
- [103] T. Chen, G. Giannakis, T. Sun, and W. Yin, "Lag: Lazily aggregated gradient for communication-efficient distributed learning," in *Proc. Adv. Neural Inf. Process. Syst. (NeurIPS)*, vol. 31, 2018.
- [104] T. Li, M. Sanjabi, A. Beirami, and V. Smith, "Fair resource allocation in federated learning," in *Proc. Int. Conf. Learn. Representations (ICLR)*, 2020.
- [105] M. Zhang, K. Sapra, S. Fidler, S. Yeung, and J. M. Alvarez, "Personalized federated learning with first order model optimization," in *Proc. Int. Conf. Learn. Representations (ICLR)*, 2021.
- [106] L. Wang, Y. Guo, T. Lin, and X. Tang, "Client selection in nonconvex federated learning: Improved convergence analysis for optimal unbiased sampling strategy," *arXiv preprint arXiv:2205.13925*, 2022.
- [107] M. M. Amiri, D. Gündüz, S. R. Kulkarni, and H. V. Poor, "Convergence of federated learning over a noisy downlink," *IEEE Trans. Wireless Commun.*, vol. 21, no. 3, pp. 1422–1437, 2022.
- [108] F. Ang, L. Chen, N. Zhao, Y. Chen, W. Wang, and F. R. Yu, "Robust federated learning with noisy communication," *IEEE Trans. Commun.*, vol. 68, no. 6, pp. 3452–3464, 2020.
- [109] N. Yan, K. Wang, C. Pan, and K. K. Chai, "Performance analysis for channel-weighted federated learning in OMA wireless networks," *IEEE Signal Process. Lett.*, vol. 29, pp. 772–776, 2022.
- [110] S. Xia, J. Zhu, Y. Yang, Y. Zhou, Y. Shi, and W. Chen, "Fast convergence algorithm for analog federated learning," in *Proc. IEEE Int. Conf. Commun. (ICC)*, 2021, pp. 1–6.
- [111] R. Pathak and M. J. Wainwright, "FedSplit: an algorithmic framework for fast federated optimization," in *Proc. Adv. Neural Inf. Process. Syst. (NeurIPS)*, 2020.
- [112] A. Khaled, K. Mishchenko, and P. Richtárik, "First analysis of local gd on heterogeneous data," *arXiv preprint arXiv:1909.04715*, 2019.
- [113] S. Kar, J. M. F. Moura, and K. Ramanan, "Distributed parameter estimation in sensor networks: Nonlinear observation models and imperfect communication," *IEEE Trans. Inf. Theory*, vol. 58, no. 6, pp. 3575–3605, 2012.
- [114] B. Xiao, X. Yu, W. Ni, X. Wang, and H. V. Poor, "Over-the-Air federated learning: Status quo, open challenges, and future directions," *arXiv preprint arXiv:2307.00974*, 2023.
- [115] L. Chen, X. Qin, and G. Wei, "A uniform-forcing transceiver design for over-the-air function computation," *IEEE Wireless Commun. Lett.*, vol. 7, no. 6, pp. 942–945, 2018.
- [116] Y.-S. Jeon, M. M. Amiri, J. Li, and H. V. Poor, "A compressive sensing approach for federated learning over massive mimo communication systems," *IEEE Trans. Wireless Commun.*, vol. 20, no. 3, pp. 1990–2004, 2021.
- [117] D. L. Donoho, A. Maleki, and A. Montanari, "Message-passing algorithms for compressed sensing," *Proc. Nat. Acad. Sci. USA*, vol. 106, no. 45, pp. 18914–18919, 2009.
- [118] R. Paul, Y. Friedman, and K. Cohen, "Accelerated gradient descent learning over multiple access fading channels," *IEEE J. Sel. Areas Commun.*, vol. 40, no. 2, pp. 532–547, 2022.
- [119] S. Hua, K. Yang, and Y. Shi, "On-device federated learning via second-order optimization with over-the-air computation," in *Proc. IEEE 90th Veh. Technol. Conf. (VTC)*, Sep. 2019, pp. 1–5.
- [120] P. Yang, Y. Jiang, T. Wang, Y. Zhou, Y. Shi, and C. N. Jones, "Over-the-air federated learning via second-order optimization," *IEEE Trans. Wireless Commun.*, vol. 21, no. 12, pp. 10560–10575, 2022.
- [121] W. Jiang, "Graph-based deep learning for communication networks: A survey," *Computer Commun.*, vol. 185, pp. 40–54, 2022.
- [122] L. Liu, J. Zhang, S. Song, and K. B. Letaief, "Client-edge-cloud hierarchical federated learning," in *Proc. IEEE Int. Conf. Commun. (ICC)*, 2020, pp. 1–6.
- [123] M. S. H. Abad, E. Ozfatura, D. Gunduz, and O. Ercetin, "Hierarchical federated learning across heterogeneous cellular networks," in *Proc. IEEE Int. Conf. Acoust., Speech Signal Process. (ICASSP)*. IEEE, 2020, pp. 8866–8870.
- [124] K. Yang, Y. Shi, Y. Zhou, Z. Yang, L. Fu, and W. Chen, "Federated machine learning for intelligent IoT via reconfigurable intelligent surface," *IEEE Netw.*, vol. 34, no. 5, pp. 16–22, 2020.
- [125] M. Fu, Y. Zhou, Y. Shi, W. Chen, and R. Zhang, "UAV aided over-the-air computation," *IEEE Trans. Wireless Commun.*, vol. 21, no. 7, pp. 4909–4924, 2022.
- [126] M. Fu, Y. Zhou, Y. Shi, C. Jiang, and W. Zhang, "UAV-assisted multi-cluster over-the-air computation," *arXiv preprint arXiv:2210.10963*, 2022.
- [127] M. Fu, Y. Shi, and Y. Zhou, "Federated learning via unmanned aerial vehicle," *arXiv preprint arXiv:2210.10970*, 2022.
- [128] N. Razmi, B. Matthiesen, A. Dekorsy, and P. Popovski, "Ground-assisted federated learning in leo satellite constellations," *IEEE Wireless Commun. Lett.*, vol. 11, no. 4, pp. 717–721, 2022.
- [129] Y. Zhou, Y. Shi, H. Zhou, J. Wang, L. Fu, and Y. Yang, "Towards scalable wireless federated learning: Challenges and solutions," *IEEE Internet Things Mag.*, 2023.
- [130] H. H. Yang, Z. Liu, T. Q. S. Quek, and H. V. Poor, "Scheduling policies for federated learning in wireless networks," *IEEE Trans. Commun.*, vol. 68, no. 1, pp. 317–333, 2020.
- [131] J. Ren, Y. He, D. Wen, G. Yu, K. Huang, and D. Guo, "Scheduling for cellular federated edge learning with importance and channel awareness," *IEEE Trans. Wireless Commun.*, vol. 19, no. 11, pp. 7690–7703, 2020.
- [132] A. Bereyhi, A. Vagollari, S. Asaad, R. R. Müller, W. Gerstacker, and H. V. Poor, "Device scheduling in over-the-air federated learning via matching pursuit," vol. 71, pp. 2188–2203, 2023.
- [133] Y. Ruan, X. Zhang, S.-C. Liang, and C. Joe-Wong, "Towards flexible device participation in federated learning," in *Proc. Int. Conf. Artificial Intell. Stat. (AISTATS)*, 2021, pp. 3403–3411.
- [134] X. Gu, K. Huang, J. Zhang, and L. Huang, "Fast federated learning in the presence of arbitrary device unavailability," in *Proc. Adv. Neural Inf. Process. Syst. (NeurIPS)*, vol. 34, 2021, pp. 12,052–12,064.
- [135] H. Yang, X. Zhang, P. Khanduri, and J. Liu, "Anarchic federated learning," in *Proc. Int. Conf. Mach. Learn. (ICML)*, 2022.
- [136] J. Mao, H. Yang, P. Qiu, J. Liu, and A. Yener, "CHARLES: Channel-Quality-Adaptive over-the-air federated learning over wireless networks," in *Proc. IEEE Int. Workshop. Signal Process. Adv. Wireless Commun. (SPAWC)*, 2022, pp. 1–5.
- [137] H. Yang, P. Qiu, J. Liu, and A. Yener, "Over-the-Air federated learning with joint adaptive computation and power control," in *Proc. IEEE Int. Symp. Inf. Theory (ISIT)*, 2022, pp. 1259–1264.
- [138] Y. Zhao, M. Li, L. Lai, N. Suda, D. Civin, and V. Chandra, "Federated learning with non-IID data," *arXiv preprint arXiv:1806.00582*, 2018.
- [139] T. Li, S. Hu, A. Beirami, and V. Smith, "Ditto: Fair and robust federated learning through personalization," in *Proc. Int. Conf. Mach. Learn. (ICML)*, 2021, pp. 6357–6368.
- [140] A. Fallah, A. Mokhtari, and A. Ozdaglar, "Personalized federated learning with theoretical guarantees: A model-agnostic meta-learning approach," in *Proc. Adv. Neural Inf. Process. Syst. (NeurIPS)*, 2020.
- [141] H. U. Sami and B. Güler, "Over-the-air personalized federated learning," in *Proc. IEEE Int. Conf. Acoust., Speech Signal Process. (ICASSP)*, 2022, pp. 8777–8781.
- [142] T. Li, A. K. Sahu, M. Zaheer, M. Sanjabi, A. Talwalkar, and V. Smith, "Federated optimization in heterogeneous networks," in *Proc. Mach. Learn. Syst. (MLSys)*, 2020, pp. 429–450.
- [143] Y. Lecun, L. Bottou, Y. Bengio, and P. Haffner, "Gradient-based learning applied to document recognition," *Proc. IEEE*, vol. 86, no. 11, pp. 2278–2324, 1998.
- [144] A. Krizhevsky, G. Hinton *et al.*, "Learning multiple layers of features from tiny images," Dept. Comput. Sci., Univ. Toronto, Toronto, ON, Canada, Tech. Rep., 2009.
- [145] C. Jin, R. Ge, P. Netrapalli, S. M. Kakade, and M. I. Jordan, "How to escape saddle points efficiently," in *Proc. Int. Conf. Mach. Learn. (ICML)*, vol. 70, Aug. 2017, pp. 1724–1732.
- [146] Z. Zhang, G. Zhu, R. Wang, V. K. N. Lau, and K. Huang, "Turning channel noise into an accelerator for over-the-air principal component analysis," *IEEE Trans. Wireless Commun.*, vol. 21, no. 10, pp. 7926–7941, 2022.
- [147] M. P. Friedlander and M. Schmidt, "Hybrid Deterministic-Stochastic Methods for Data Fitting," *SIAM J. Sci. Comput.*, vol. 34, no. 3, pp. A1380–A1405, Jan. 2012.